MOLECULAR AND CELLUAR ANALYSES OF PATHOGENICITY AND HOST SPECIFICITY IN RICE BLAST DISEASE

by

GUADALUPE VALDOVINOS - PONCE

B.S., Universidad Nacional Autonoma de Mexico, 1992
M.S., Colegio de Postgraduados – Mexico, 1999

AN ABSTRACT OF A DISSERTATION

submitted in partial fulfillment of the requirements for the degree

DOCTOR OF PHILOSOPHY

Department of Plant Pathology
College of Agriculture

KANSAS STATE UNIVERSITY
Manhattan, Kansas

2007

Abstract

Rice (*Oryza sativa* L.) production worldwide is constrained by rice blast disease caused by the ascomycetous fungus *Magnaporthe oryzae*. Rice blast has become a model system for the study of fungal plant diseases based on its global relevance to agriculture and on our ability to apply molecular genetic and genomic analyses to both the pathogen and the plant. We have applied molecular and cellular analyses to understand critical processes in the *M. oryzae* disease cycle. The dark melanin pigment produced by the fungus is critical for the function of its specialized appressorial cell, which punches the leaf surface by generating the highest pressure known in any biological system, estimated at 80 times the atmospheric pressure. Without melanin, the fungus can neither generate this pressure nor puncture the plant surface and disease does not occur. *M. oryzae* genome sequencing identified a cluster of melanin biosynthesis genes that included an attractive candidate for the transcription factor that regulates melanin biosynthesis in appressoria. We report the structural and functional characterization of this putative transcription factor, although its role remains elusive. Host cellular responses after appressorial penetration are equally important in determining if disease will occur. We have characterized the cellular response of one rice variety to a compatible fungal strain (causes disease), an incompatible strain (fails to cause disease due to specific triggering of rice defenses) and a non-host strain (causes disease in barley but not in rice). Distinctive fungal and rice cellular responses correlated with the outcome of each particular pathogen-strain rice interaction. We report contrasting responses in two rice leaf sheath assays that are amenable to live cell microscopy, as well as a novel cellular response of crystalline aggregations deposited inside the host cell under appressoria on the leaf surface. Our studies have important implications for future analyses of pathogenicity and host specificity in rice blast disease.

MOLECULAR AND CELLULAR ANALYSES OF PATHOGENICITY AND HOST SPECIFICITY IN RICE BLAST DISEASE

by

GUADALUPE VALDOVINOS - PONCE

B.S., Universidad Nacional Autonoma de Mexico, 1992
M.S., Colegio de Postgraduados – Mexico, 1999

A DISSERTATION

submitted in partial fulfillment of the requirements for the degree

DOCTOR OF PHILOSOPHY

Department of Plant Pathology
College of Agriculture

KANSAS STATE UNIVERSITY
Manhattan, Kansas

2007

Approved by:

Major Professor
Barbara Valent

Abstract

Rice (*Oryza sativa* L.) production worldwide is constrained by rice blast disease caused by the ascomycetous fungus *Magnaporthe oryzae*. Rice blast has become a model system for the study of fungal plant diseases based on its global relevance to agriculture and on our ability to apply molecular genetic and genomic analyses to both the pathogen and the plant. We have applied molecular and cellular analyses to understand critical processes in the *M. oryzae* disease cycle. The dark melanin pigment produced by the fungus is critical for the function of its specialized appressorial cell, which punches the leaf surface by generating the highest pressure known in any biological system, estimated at 80 times the atmospheric pressure. Without melanin, the fungus can neither generate this pressure nor puncture the plant surface and disease does not occur. *M. oryzae* genome sequencing identified a cluster of melanin biosynthesis genes that included an attractive candidate for the transcription factor that regulates melanin biosynthesis in appressoria. We report the structural and functional characterization of this putative transcription factor, although its role remains elusive. Host cellular responses after appressorial penetration are equally important in determining if disease will occur. We have characterized the cellular response of one rice variety to a compatible fungal strain (causes disease), an incompatible strain (fails to cause disease due to specific triggering of rice defenses) and a non-host strain (causes disease in barley but not in rice). Distinctive fungal and rice cellular responses correlated with the outcome of each particular pathogen-strain rice interaction. We report contrasting responses in two rice leaf sheath assays that are amenable to live cell microscopy, as well as a novel cellular response of crystalline aggregations deposited inside the host cell under appressoria on the leaf surface. Our studies have important implications for future analyses of pathogenicity and host specificity in rice blast disease.

Table of Contents

List of Figures

List of Tables

Acknowledgements

My family and all my Mexican **friends**.

The Postgraduate Collage and the SFPI. All the faculty members, research and office staff in the Plant Pathology Program.

KSU and all the Plant Pathology members.

Drs. Guillermo Fuentes Davila, Jan E. Leach, Robert L. Bowden, Mizuho Nita, and Timothy C. Todd.

Dr. Chang Hyun Khang and his family.

Dr. Jungkwan Lee and his family

Dr. Francis M. Kirigwi

Marcelo Berretta, Karina Fabrizzi, Martha Giraldo, Anita Kesler, Gabriela Pacheco, Guillermo Schroeder, Vanesa Segovia, Adelia Sousa, Susana Valdovinos, and Mario Villatoro.

All the members of my academic committee: Dr. Barbara Valent, Dr. Robert L. Bowden, Dr. William W. Bockus, and Dr. Subbaratnam Muthukrishnan.

With all my appreciation and deep respect to Dr. Barbara Valent, my major advisor, for her constant support during my studies and for being there at difficult times.

This research was supported by the National Science Foundation Grant 0446315, the Kansas National Science Foundation Experimental Program to Stimulate Competitive Research/Kansas Technology Enterprise Corporation, and the Agricultural Experiment Station at Kansas State University.

Dedication

My dear Mexico: my motherland, my root, my culture, my people.

My family: my dear parents Fidencio Valdovinos and Josefina Ponce. My brother: Martin; my sisters Maria del Mar and Maria Teresa; my nephews Luis Alejandro and Erick; and my nieces Lluvia Alejandra, Maria Fernanda, Avellaneda, and Renata.

Francis

Dr. Barbara Valent.

CHAPTER 1 - *Magnaporthe oryzae*: The rice blast pathogen

INTRODUCTION

Magnaporthe oryzae (anamorph Pyricularia oryzae)

Couch and Kohn (2002) demonstrated, based on molecular characters and host association, that there are two *Magnaporthe* species associated with blast and gray leaf spot disease in many species of the family Poaceae. One of these species, *M. grisea*, is limited to infection of *Digitaria* species (such as crabgrass, *Digitaria sanguinalis*) and the other one, *M. oryzae*, is associated with serious diseases of rice (*Oryza sativa*), wheat (*Triticum aestivum*), barley (*Hordeum vulgare*), finger millet (*Eleusine coracana*), rye grass (*Lolium* spp.), and other cultivated grasses. Individual isolates of the fungus have a limited host range, infecting one or a few grass species.

The first description of the sexual or perfect stage (teleomorph) of *Pyricularia* from rice or other grasses was done from a teleomorph, called *Ceratosphaeria grisea*, originated from a cross between fungal isolates from crabgrass (*D. sanguinalis*) (Hebert, 1971). Afterward, in 1976, 1978, and 1982, it was reported that teleomorphs produced in crosses of isolates from other grasses (*Oryza sativa* x *O. sativa*, *Eleusine indica* x *E. indica*, *E. coracana* x *E. coracana*, *O. sativa* x *E. indica*, and *O. sativa* x *E. coracana*) were not morphologically different from *C. grisea* (Couch and Kohn, 2002). Yaegashi and Udagawa (1978), produced a teleomorph originated from a cross between *Pyricularia* isolates obtained from *E. indica*. The morphology of this teleomorph was identical to the authentic sample of *C. grisea*, and its comparison with the type species of *Magnaporthe*, led them to transfer *C. grisea* to *Magnaporthe*.

Magnaporthe oryzae is a haploid and heterothallic Pyrenomycete associated with rice blast, one of the most important fungal diseases of this crop (Kang *et al*, 1994). *M. oryzae* fruiting bodies (perithecia) are dark brown to black, globular, and occur singly or in groups (Hebert, 1971). They are partially or completely embedded in the substrate and two or more of them may fuse to form a large cavity. The necks are also sometimes fused (Hebert, 1971). The asci are cylindrical to subclavate and unitunicate. The tip of an ascus has a pore surrounded by a refractive ring. Each ascus usually contains eight ascospores, which are hyaline, three-septate, fusiform, lightly to moderately curved, and without gelatinous sheath or appendages (Hebert, 1971).

The anamorph *Pyricularia oryzae* produces simple and gray conidiophores that bear three-celled pyriform conidia with a single nucleus per cell. Because all nuclei in a conidium are derived through mitotic divisions from a single nucleus, isolation of single spore cultures purifies individual nuclei. Mature conidia have a basal appendage at the point of attachment to the conidiophore (Howard and Valent, 1996), and even though it was reported that conidia are colorless (Kawamura, 1997), they are light brown when observed under a compound microscope, and gray when observed under a stereoscope.

Disease cycle

The fungal side

Inoculation, penetration and colonization stages of the *M. oryzae* disease cycle have been genetically and cytologically well characterized *in planta*, by working with rice and other grass leaves (Koga and Kobayashi, 1980; 1982a-b; Koga and Horino, 1984a-b; Peng, 1988, 1989; Heath *et al*, 1990a-b, 1992; Kankanala *et al*, 2007), and under artificial surfaces using different mylar films composed of poly-(ethylene terephthalate), cellophane squares, hydrophobic plastic membranes, glass, etc (Hamer *et al*, 1988,1989; Bourett and Howard, 1990; de Jong *et al*, 1997; Howard *et al*, 1991; Lu, 2005). The symptoms of the disease are reproducible and completely resemble those caused by the fungus in its natural environment (Heath *et al*, 1990a; Valent, 1991; Berruyer *et al*, 2006).

M. oryzae was considered as an above ground pathogen. However, in order to obtain a better understanding about the factors involved in the ability of a pathogen to infect different plant organs, it was demonstrated that the fungus is able to infect the root system of wheat, barley, and rice under *in vitro* conditions (Dufresne and Osbourn, 2001; Sesma, 2004). Root infection occurs in a process where the appressorium is not required for penetration, and that is typical of root-infecting pathogens.

M. oryzae overseasons as mycelium and conidia on rice straw and seeds (Agrios, 1997). The asexual disease cycle on aerial plant organs begins (Figure 1-1) when the conidia land on either leaf or stem surfaces that are extremely hydrophobic due to the presence of cuticle and cuticular waxes. Once the conidia are hydrated, a drop of mucilage containing proteins, carbohydrates, and lipids is released from the apical cell so they are able to attach strongly to the waxy host surface (Howard and Valent, 1996; Talbot, 2003). After a couple of hours, conidia germinate from one or both terminal cells and appressorium formation begins. Hard and hydrophobic surfaces as well as the absence of nutrients represent a combination of signals that trigger the differentiation of the germ tube apex into the appressorium (Talbot, 2003). During the initial stages of appressorium development, the germ tube tip swells and becomes flattened against the host surface (Bourett and Howard, 1990). At this host-fungus contact point, the appressorium surface will become the appressorium pore (Figure 1-4), an area where the appressorium cell does not have cell wall; therefore the fungal plasma membrane is in direct contact with the cuticle of the epidermal plant cell. A melanin layer is synthesized between the cell membrane and the cell wall of the appressorium, except at the appressorial pore region (Howard and Valent, 1996). Mature appressoria are cells with a rigid melanized cell wall. As we will mention below, the presence of melanin limits wall permeability allowing appressoria to develop a high turgor pressure (Howard *et al*, 1991; de Jong et al., 1997). At this developmental stage, a specialized hypha (penetration peg) emerges and uses the physical pressure (80 times atmospheric pressure) generated by the appressorium to enter the plant epidermal cell. Like other plant fungal pathogens, *M. oryzae* secretes enzymes (β-1,4-D-xylanases) that might be involved in a chemical penetration component (Howard and Valent, 1996).

Once inside the cell lumen, the penetration peg enlarges to form a filamentous primary hypha that subsequently differentiates into a thicker and bulbous invasive hypha that grows for 8

to 12 hours more inside this first-invaded cell. At this time, the invasive hypha partially or completely fills the host plant cell and starts moving to the adjacent ones, apparently via plasmodesmata (Kankanala *et al*, 2007). In the subsequently invaded cells, the fungus grows for 2 to 3 hours to move into the neighboring cells.

Rice blast fungal morphology and behavior have been very well characterized by Heath *et al* (1990a) and more recently by Kankanala *et al*, (2007). The former group reported an infection hypha that is much thinner than the secondary one that develops from it. The widening of the infection hypha, now referred to as invasive hypha, is correlated with successful infection because in those cases where the primary hypha did not differentiate, the invaded plant cell died rapidly and the fungus did not grow inside the epidermal cells. These thin hyphae sometimes grew straight through the epidermal cell and into mesophyll cells below.

It has been reported that *M. oryzae* synthesizes phytotoxic compounds, for example, tenuazonic acid, pyricularin, and pyrichalasin, during tissue colonization, but roles for these toxins during colonization are not yet defined (Valent, 1997; Talbot, 2003).

The fungus uses a biotrophic invasion strategy and, in about 7 to 8 days, forms typical eyespot-shaped lesions that reduce photosynthetic area. Sporulation begins in the first invaded cells days after they were filled with the invasive hypha (Talbot, 2003; Kankanala *et al*, 2007).

The plant cell side

Plant cytological studies of the early pathogenesis events between *Magnaporthe oryzae* and leaves (blades and sheaths) of compatible and incompatible rice hosts have been described since early eighties in order to determine whether host cytological responses are correlated with the expression of genes associated with race specific resistance (Heath *et al*, 1990a; Koga and Kobayashi, 1982a; Koga and Horino, 1984 a-b; Koga *et al*, 2004; Peng and Shishiyama, 1988, 1989; Tomita and Yamanaka, 1983a-b).

In a macroscopic examination of a highly compatible interaction between M201 rice plants spray inoculated with strain 0-42, Heath *et al* (1990a) reported that small chlorotic flecks were detected on young leaves at 72 hours, and that by 3 days later these lesions had grown and

coalesced, therefore most of the inoculated part of the leaf was straw colored and desiccated. The symptoms on the older leaf developed slower and by 6 days, many of them were smaller, darker, and more isolated than those on the younger leaf. Forty eight hours after inoculation, penetrated epidermal cells did not show any response associated with defense, like papilla formation, browning or wall autofluorescence, and granular cytoplasm. At the chlorotic fleck symptom (72 hours), some mesophyll cells were browning and autofluorescent; once the plant tissue was full of hyphae, all mesophyll were autofluorescent and showed minor to moderate browning.

Melanin biosynthetic pathway

Melanins are dark brown or black pigments formed by oxidative polymerization of many types of phenolic or indolic compounds. These pigments are usually associated with proteins and carbohydrates, and have stable free radicals, which is a very important criterion to define a polymer as melanin (Butler and Day, 1998; Calvo *et al*, 2002; Henson *et al*, 1999).

Plants, animals and many microorganisms synthesize melanin (Butler and Day, 1998; Calvo *et al*, 2002; Henson *et al*, 1999). In terms of biosynthesis, melanin is classified into at least four groups depending on its immediate precursor: (1) 3,4-dihydroxyphenylalanine (DOPA) melanins, (2) γ-glutaminyl-3-4-dihydroxybenzene (GDHB) melanins, (3) catechol melanins, and (4) 1,8-dihydroxynaphthalene (DHN) melanins (Bell and Wheeler, 1986; Butler and Day, 1998; Henson *et al*, 1999). We will focus on the last group because *M. oryzae* and many other species of ascomycetes and related deuteromycetes use DHN as the monomeric melanin precursor. Because DHN melanin is synthesized by joining five ketide subunits obtained from five acetate molecules, the polyketide pathway is also known as the pentaketide melanin synthesis pathway (Henson *et al*, 1999).

The DHN melanin pathway was discovered in *Verticillium dahliae* (a plant pathogen) and *Wangiella dermatitidis* (an animal pathogen) through genetic and biochemical characterizations of melanin-deficient fungal strains generated by mutations or enzyme inhibitors (Bell and Wheeler, 1986; Butler and Day, 1998; Kimura and Tsuge, 1993; Langfelder *et al*, 2003). In *M.*

oryzae as in other fungi, acetate units are assembled by a polyketide synthase (PKS) to produce 1,3,6,8-tetrahydroxynaphthalene (4HN), the first detectable intermediate in the pathway (Figure 1-2). The 4HN is reduced to scytalone by the 1,3,6,8-tetrahydroxynaphthalene reductase (4HNR). Scytalone is then dehydrated by scytalone dehydratase (SD) to 1,3,8-trihydroxynaphthalene (3HN), which is reduced by a second reductase, the 1,3,8-trihydroxynaphthalene reductase (3HNR) to vermelone. A further dehydration step, done by SD, leads to the formation of DHN.

So far, the oxidase involved in the oxidative polymerization of DHN to melanin has not been characterized for any of the DHN-melanized fungi including *M. oryzae*; however, several studies suggest that the enzyme is a wall-bound laccase (Butler and Day, 1998; Langfelder *et al*, 2003). It has been observed that cooper deficiency blocks melanin synthesis, indicating that a copper-containing laccase (*p*-diphenol: oxygen oxidoreductase) or a tyrosinase (*o*-diphenol: oxygen oxidoreductase) is involved in melanization. Tyrosinase has not been detected in some heavily melanized species of deuteromycetes, whereas laccases has been specifically associated with pigmented cells within the same fungal colony (Bell and Wheeler, 1986). A purified extracellular laccase from *Gaeumannomyces graminis* var. *tritici* polymerized DHN into melanin; however, a mutant lacking that enzyme still produced the polymer. Many fungi, including *G. graminis* have several laccase genes, so disruption of one gene will not eliminate all laccase activity and will make difficult to identify the function of individual laccases (Henson *et al,* 1999). In *Cochliobolus heterostrophus* polymerization of DHN is catalyzed by an unidentified *p*-diphenol oxidase (Eliahu *et al*, 2007).

Melanins are usually present in cell walls of yeast cells, hyphae, conidia, chlamydospores, reproductive bodies, and specialized infection structures such as appressoria and hyphopodia. They also are present as extracellular polymers formed in the medium around fungal cells. The pigment is located in the cell wall, either within the structure of the wall, as its outermost layer, or between the cell membrane and the cell wall (Bell and Wheeler, 1986; Butler and Day, 1998; Howard and Valent, 1996; Mendgen *et al,* 1996).

Melanin has not been found in fungal cytoplasm; for example, in *Gaeumannomyces graminis*, melanin precursors are expected to be synthesized in the cytoplasm and then assembled covalently in appressorial, hyphopodial, or hyphal cell walls by wall-associated oxidases. So far, exocytosis has not been observed to occur near hyphal cell walls undergoing melanogenesis, which could suggest that melanin precursors and/or melanin are not transported to the wall in vesicles. However, the pattern of melanin granules in *Verticillium dahliae* and *V. nigrescens* walls implies that melanin precursors might be synthesized in a type of cytoplasmic organelle (vacuoles or melanosome-like bodies) and secreted from the cytoplasm to the cell wall where they are oxidized to melanin (Bell and Wheeler, 1986; Butler and Day, 1998; Henson *et al*, 1999).

Extracellular melanins, those synthesized completely apart from the fungal cell walls, seem to be derived either by secretion of phenol oxidases or phenols into the external environment. Phenol oxidases will oxidize phenolic compounds of various origins, whereas phenols will be autoxidized or oxidized by enzymes later released from the fungus (often during autolysis). It has been documented that adding hydroquinone, *p*-phenylenediamine, 1-naphthol, or syringalazine to culture media allows detection of extracellular laccases or peroxidases; however, secretion of peroxidase as well as hydrogen peroxide do not occur often in fungi. *Rhizoctonia* and many wood-rotting species of basidiomycetes secrete laccases that polymerize phenols in plant tissues degraded by these fungi (Bell and Wheeler, 1986).

Melanin can account for a major fraction of the dry weight of a fungal cell, as much as 30% for the spores *of Agaricus bisporus*, for example; which represents a significant portion of material and energy resources (Butler and Day, 1998). Why would fungi invest so much energy in melanin synthesis? Because melanin is of survival value; fungi need to grow, reproduce, and protect themselves, either as parasites or saprophytes.

Melanins have been strongly associated with protection and antagonistic functions due to their stability, insolubility and resistance properties. Some fungi synthesize melanin in response to environmental stresses, such as exposure to toxic metals, desiccation, hyperosmotic conditions, high temperature, antagonistic microbes, limited nutrients, pH shock, UV or ionizing

radiation, and host defense responses (Butler and Day, 1998; Henson *et al*, 1999; Langfelder *et al*, 2003). Likewise, many studies with melanin inhibitors as well as melanin-deficient mutants have shown that *M. oryzae*, *Colletotrichum lagenarium*, and *C. lindemuthianum* require melanized appressoria in order to infect rice, cucumber, and bean, respectively. Melanin plays a very important role as a pathogenicity factor since it mediates the buildup of a high hydrostatic pressure in the appressorium that provides the essential driving force for a mechanical penetration component. In contrast, *Alternaria alternata* melanin-deficient mutants and the wild type were pathogenic on susceptible pear leaves inoculated under laboratory conditions, indicating that the ability to produce melanin is not affecting pathogenicity of this fungus (Kimura and Tsuge, 1993; Kawamura *et al*, 1997).

Mycelia and conidia of *A. alternata* are melanized, while appressoria are colorless. *M. oryzae*, like *Alternaria*, produces melanized mycelia and spores, but its appressoria are heavily melanized. Conidial melanization in *Alternaria* is considered to play an important role in longevity and survival of conidia in nature, whereas appressorial melanization in *M. oryzae* is essential for penetration of its host plant. Both genera synthesize melanin; however, the melanization sites and the function of melanin are different (Kawamura *et al*, 1997).

Melanin biosynthetic gene cluster

Fungal gene clusters are defined as the close linkage of two or more genes involved in the same metabolic pathway. Gene clusters are widespread in prokaryotic organisms, but not in eukaryotic ones. About 8 years ago, genetic evidence suggested that some metabolic pathways genes were closely linked in filamentous fungi; specifically, fungal genes involved in synthesis of secondary metabolites, such as pigments, antibiotics, and toxins, generally occur in clusters (Keller and Hohn, 1997; Yu and Keller, 2005). Unlike primary metabolism genes, secondary metabolism pathways are not essential for growth, and they are often induced by specific growth conditions. Secondary metabolism pathways are often expressed under non-optimal growth conditions to enhance fungal survival in response to nutrient deprivation or competing organisms. Like antibiotics and mycotoxins, melanins are secondary metabolites that result from

natural product pathways that involve a considerable investment of fungal genetic resources; a single natural product pathway can consist of 25 different genes and reside in up to 60 Kb of DNA (Keller, 1997). Characterized clusters include genes encoding biosynthetic enzymes, transcription factors, and transporters (Keller, 1997; Yu and Keller, 2005).

As we will see, the genes involved in melanin biosynthesis are clustered in some fungi and not in other ones. Genetic studies of the melanin synthesis pathway have been carried out not only in *M. oryzae*, but also in other pathogenic fungi such as *Alternaria alternata*, *Colletotrichum lagenarium*, *Cochliobolus miyabeanus*, and *C. heterostrophus*. Even though these fungi synthesize DHN melanin through the pentaketide pathway, the linkage relationships and arrangement of the involved genes are quite different (Kubo *et al*, 1991).

In *Magnaporthe oryzae* the melanin biosynthetic gene cluster consists of 5 genes located on the chromosome I supercontig 195 (Figure 1-3) (Broad Institute Database, version 4 (www.broad.mit.edu/annotation/genome/magnaporthe_grisea/). From these 5 genes, only *PIG1*, 4*HNR*, and *ALB1* are known to be involved in melanin biosynthesis. The remaining characterized genes, *RSY1* and *BUF1*, are located on chromosomes III and II, respectively and will be described in the next section.

The first gene in the contig is *PIG1* (pigment of *Magnaporthe*), a 3148 bp regulatory gene. The gene encodes a 973 amino-acid protein (Pig1p) that shares 68% identity with the Cmr1p protein encoded by the *CMR1* gene (*Colletotrichum* melanin regulation), a putative transcription factor present in the plant pathogenic fungus *Colletotrichum lagenarium*; and 70% similarity with the Cmr1 protein of *Cochliobolus heterostrophus*. Like the *C. lagenarium* and *C. heterostrophus* Cmr1 proteins, Pig1p has two adjacent putative DNA-binding motifs in its N-terminal region; one is a Zn (II) 2Cys6 binuclear cluster, and the other one is a Cys2his2 zinc finger motif (Tsuji, 2000). The Pig1 protein has been associated with regulation of mycelial melanization. On the other hand, analysis of pig1p mutants suggested that the expression of melanin genes during appressorium development is independent of Pig1p.

The second gene, *4HNR*, encodes the 1,3,6,8-tetrahydroxynaphthalene reductase (4HNR), also called second naphthol reductase, that catalyzes the reduction of 1,3,6,8-tetrahydroxynaphthalene to scytalone (Figure 1.1). Even though this enzyme prefers scytalone as substrate, it is capable of catalyzing the reduction of 3HN to vermelone; however its activity is not enough to support this reaction in the absence of *BUF1* (Thompson *et al*, 2000).

The third gene in the contig is *ALB1*. This gene encodes a polyketide synthase (PKS), which is the first enzyme acting in the melanin synthesis pathway by converting acetate units to 1,3,6,8-tetrahydroxynaphthalene (Langfelder *et al*, 2003). The *ALB1* gene was defined on the basis of a genetic analysis of three *M. oryzae* mutants with altered pigmentation (*buf*$^-$, *rsy*$^-$, and *alb*$^-$). The mutants were isolated from diverse parental strains, including rice and other grasses pathogens (Chumley and Valent, 1990). We will refer to the other two mutants later in this chapter. The *alb*$^-$ pigment mutants include seven that appeared spontaneously and 15 that were isolated after UV mutagenesis or diepoxyoctane treatment. *Alb*$^-$ mutants form white colonies, secrete a yellow pigment into oatmeal agar medium, and are not pathogenic when inoculated on undamaged host plants (Chumley and Valent, 1990).

Homologues of *ALB1* have been identified in several other fungi, including the *pksP* gene of *Alternaria fumigatus* (Langfelder *et al*, 1998; Tsai *et al*, 1997,1998), *wA* gene of *Aspergillus nidulans* (Mayorga and Timberlake, 1992), *ALM* of *Alternaria alternata* (Kimura and Tsuge, 1993), *PKS1* of *Colletotrichum lagenarium* (Takano *et al*, 1995), *WdPKS1* of *Wangiella dermatitidis* (Feng *et al*, 2001), *PKS18* of *Cochliobolus heterostrophus* (Eliahu *et al*, 2007), and *alm-1* of *Cochliobolus miyabeanus* (Kubo, 1989).

The last two genes in the contig are the loci MGG_07217.5, and MGG_07218.5. So far, these genes do not have any known function. However, MGG-07218.5 codes for a putative transcription factor that belongs to the fungal Zn(2)-Cys(6) binuclear cluster domain family. Due to the location of this regulatory gene in the melanin biosynthesis contig, it was predicted to be a potential regulator of melanin synthesis during appressorium development (Ebbole and Valent, unpublished data).

In *Alternaria alternata*, *C. heterostrophus*, and *C. miyabeanus* the melanin biosynthesis genes are also clustered. An *A. alternata* clone (pMBR1) restored melanin synthesis in albino (*Alm*$^-$), light brown (*Brm1*$^-$), and brown (*Brm2*$^-$) mutants. The genes that complemented each one of these mutants were designated *ALM*, *BRM1*, and *BRM2*, respectively. They are located in a 30 Kb region in the chromosome and code for the enzymes that catalyze the respective steps in the DHN melanin biosynthetic pathway [*ALM* (Polyketide synthase), *BRM1* (Scytalone dehydratase), *BRM2* (1,3,8-trihydroxynaphthalene reductase)] (Kimura and Tsuge, 1993). In *C. heterostrophus BRN1*, *CMR1*, and *PKS18* are located on a 30 kb chromosomal fragment (Eliahu *et al*, 2007). According to genetic analysis of melanin mutants of *C. miyabeanus*, the causal agent of the rice brown spot, it was indicated that *alm-1*, *alm-2*, and *brm* were linked and that *scy* segregates independently of these 3 loci (Kubo *et al*, 1989).

Colletotrichum lagenarium represents one example where the melanin biosynthetic genes are not clustered. Kubo's research group cloned the genes that encode the three major enzymes in the melanin pathway: *PKS1* (Kubo *et al*, 1991), *THR1* (Perpetua *et al*, 1996), and *SCD1* (Kubo *et al*, 1996). Subsequently, the genes were analyzed in a temporal transcription pattern using conidia incubated under artificial conditions. It was shown that the corresponding transcripts accumulated and diminished in similar time courses during appressorium differentiation, suggesting that common mechanisms regulated their transcription. However, it was assumed that factors regulating their transcription were not identical because *PKS1*, *SCD1*, and *THR1* transcripts did not appear synchronously during appressorial differentiation. The order of expression of the 3 genes (*THR1*, *PKS1*, and *SCD*1) was not consistent with their order of function in the melanin synthesis pathway (*PKS1*, *SCD1*, and *THR1*). It was presumed that posttranscriptional regulation of the melanin genes determines the time when the melanin enzymes should work and that the order of expression of the three genes should not necessarily correlate with the order of the pathway (Takano *et al*, 1997).

RSY1 and BUF1: the other melanin synthesis genes

Above we briefly described the genes located in the melanin biosynthesis gene cluster of *M. oryzae*. One of them, *PIG1*, is so far a regulatory gene whose encoded protein (Pig1p) might regulate the transcription of *ALB1*. The other two genes, *ALB1* and *HNR*, encode the structural proteins PKS and 4HNR, respectively, which are responsible for the first two reactions in the melanin synthesis pathway (Figure 1-2).

Subsequent steps in melanin biosynthesis consist of two dehydrations and one reduction reaction. The dehydrations of scytalone to 3HN, and vermelone to 1,8-DHN are carried out by the scytalone dehydratase (SD), which is encoded by *RSY1*. The reduction of 3HN to vermelone is catalyzed by the 3HNR, encoded by *BUF1* (Figure 1-2) (Chumley and Valent, 1990; Langfelder *et al*, 2003; Thompson *et al*, 2000; Tsuji, 2000).

The *RSY1* gene (MGG_05059.5) is located on the chromosome III supercontig 175 (www.broad.mit.edu/annotation/genome/magnaporthe_grisea/GeneDetails.html). As mentioned above, the gene encodes SD, which is structurally related to the Nuclear Transport Factor 2 (NTF2) domain family (www.ebi.ac.uk/ego/DisplayGoTerm). The enzyme catalyzes the conversion of scytalone to 3HN. Homologues of the gene have been identified in *Colletotrichum lagenarium* (*SCD1*), *Cochliobolus miyabeanus* (*scy*), *Alternaria alternata* (*BRM1*), *C. heterostrophus* (SCD1), and *Verticillium* (Eliahu *et al*, 2007; Bell and Wheeler, 1986; Kubo *et al*, 1989, 1996). Mutation of *RSY1* gives a rosy pigmentation phenotype in colonies that grow on oatmeal agar. Previously wounded host plants are infected by *rsy*$^-$ mutants (Chumley and Valent, 1990).

The last gene in the melanin pathway, *BUF1* (MGG_02252.5), is located on the chromosome II supercontig 186. Like *ALB1* and *RSY1*, the *BUF1* gene was associated with mutants isolated from rice pathogens and pathogens of other grasses. The *buf*$^-$ mutants lacked activity for 3HNR, produced a buff-colored (reddish-tan) pigmentation in the growth medium, and lost pathogenecity when inoculated on unwounded *Oryza sativa* (rice), *Eragrostis curvula* (weeping lovegrass) or *Eleusine indica* (goosegrass) host plants (Chumley and Valent, 1990; Thompson, 2000; www.broad.mit.edu/annotation/genome/). Trihydroxynaphthalene reductase is the biochemical target of three commercial fungicides tricyclazole, pyroquilon, and phthalide used to control rice blast disease.

There is not a linkage relationship among *ALB1*, *RSY1* and *BUF1* genes; however the genes that seem to have the same function as them are linked in *Alternaria alternata* (*ALM*, *BRM1* and *BRM2*, respectively). In *C. miyabeanus* the albino gene (*alm-1*) and the 1,3,8-trihydroxynaphthalene reductase (*brm*) gene are closely linked, while the scytalone dehydratase gene (*scy*) is independent of the other two ones. In *C. heterostrophus PKS18*, *CMR1* and *BRN1* are clustered. Finally the corresponding genes in *Colletotrichum lagenarium* do not seem to be linked. This information demonstrates that even though the DHN melanin biosynthesis pathway is almost identical among these fungi, the linkage relationships and arrangement of the melanin genes can be different (Kimura and Tsuge, 1993).

Rice blast control: inhibitors of the DHN melanin pathway

This section will be focused on those fungicides that inhibit specific structural genes in the melanin biosynthesis pathway [melanin biosynthesis inhibitors (MBI) also called antipenetrant fungicides]. These compounds prevent plant infection by interfering with melanin synthesis in appressorium formation, and some of them kill or have another toxic effect on the fungus (Butler and Day, 1998; Shigyo *et al*, 2004).

Studies involving the action of some of the major inhibitors in the melanin biosynthesis pathway have shown that reduction and dehydration are the principal reactions in melanin synthesis; therefore it has been considered that the reductases and dehydratases are critical target enzymes for developing new melanin biosynthesis inhibitors (Kurahashi, 2001). In fact, the actual melanin inhibitors are classified into 2 groups based on their target genes: reductase inhibitors and dehydratase inhibitors.

Reductase inhibitors have a planar structure of fused bicyclic or tricyclic rings that interfere with the binding of planar bicyclic substrates (Kurahashi, 2001). One of the more used reductase inhibitors in this group is the systemic fungicide Tricyclazole, which, when applied in culture media, makes it turn red-brown as a result of the accumulation of auto-oxidation products of the pathway intermediates (Figure 1-2) (Butler and Day, 1998). This fungicide inhibits

melanin synthesis not only in *M. oryzae* but also in *C. lindemuthianum* and *C. lagenarium* (Bell and Wheeler, 1986). Other inhibitors that appear to affect the same reduction reactions are Clobenthiazone, Pyroquilon (PRQ), Fthalide (FTL), 2,3,4,5,6-Pentachlorobenzyl alcohol (PCBA) (Butler and Day, 1998; Kurahashi, 2001).

It has been reported that for *Pyricularia oryzae*, Tricyclazole reduces disease incidence because it induces the formation of fungitoxic active oxygen species by the plant. On other hand, Tricyclazole treatment of *Botrytis cinerea* made them more susceptible to attack by fungal hyperparasites. Sclerotia of *Sclerotinia* spp. are dormant, but once they are treated with Tricyclazole they lose dormancy and germinate (Butler and Day, 1998). These reports indicate that Tricyclazole may enhance pathogenicity by working through different mechanisms in addition to being an antipenetrant.

Dehydratase inhibitors block scytalone dehydratase in the melanin pathway, which results in scytalone accumulation. These inhibitors were discovered after the reductase ones. Carpropamid; like Tricyclazole, Fthalide and Pyroquilon, is a principal fungicide currently used for rice blast control. Strains resistant to these inhibitors have not emerged so far; however, in 2001 insufficient efficacy of Carpropamid was reported in Japan due to a single point mutation in the coding sequence of scytalone dehydratase. This amino-acid change (valine to methionine) reduced binding activity of Carpropamid to the enzyme (Butler and Day, 1998; Kurahashi, 2001; Shigyo *et al*, 2004).

It has also been reported that Carpropamid enhances the activity of some enzymes related to defense reactions in rice. Under practical conditions in Japan, residues of this inhibitor in rice are lower than the level required for enhancing rice defense responses; however, it was mentioned that in those countries where it is sprayed at higher concentration, the enhancement of defense responses may contribute to control efficacy in the field (Shigyo *et al*, 2004).

Cerulenin, a specific inhibitor of fatty acid synthetase produced by *Cephalosporium caerulens*, blocked melanin synthesis in *Pyricularia* spp. and *C. lagenarium* appressoria. Since synthesis of fatty acids involves condensation of acetate molecules, as occurs in the synthesis of

1,3,6,8-4HN, it was suggested that *PKS1* and the fatty acid synthetase could be related and inhibited by Cerulenin (Butler and Day, 1998).

Appressorial melanization: Life or death issue

The *Magnaporthe oryzae* appressorium is a dome-shaped cell with a chitin cell wall that contains an about 100 nm thick layer of melanin on its inner side. Melanin imparts a dark pigmentation to the appressorium when observed with a bright-field light microscope. The layer is limited to the appressorium wall, and also covers the septum that separates the appressorium and the germ tube, but is absent from the region in contact with the substratum. The zone lacking melanin, the appressorium pore, is a specialized area distinguished earlier in development by lack of cell wall. A ring material, the pore ring, can be observed under light microscope at the plane of contact with the substrate, surrounding the perimeter of the appressorium pore. Howard and Ferrari (1989) have suggested that such rings might serve in tightly sealing the pore to the surface of the substrate. The pore probably exists as the only surface area through which molecules larger than water can pass from the fungus to the underlying substrate (Howard and Valent, 1996).

The presence of melanin plays a very important role in the life of this fungus because it provides an impermeable layer to prevent outflow of glycerol, which is responsible for high turgor pressure applied as a physical force to break the host cuticle (Howard *et al*, 1991; de Jong *et al*, 1997; Talbot, 2003). It has been shown genetically that non-melanized appressoria fail to generate turgor and lose pathogenicity. Appressoria from non-melanized strains carrying single gene mutations in the *ALB1* or *RSY1* genes have much lower levels of intracellular glycerol. A similar reduction in glycerol accumulation was found after treatment of *M. oryzae* with tricyclazole. Thus, melanin biosynthesis is essential for efficient accumulation of glycerol.

Non-melanized appressoria collapsed in hyperosmotic solutions of glycerol but after some seconds they recovered and became plasmolyzed. This indicated that the non-melanized wall is permeable to glycerol which diffused through the cell wall and induced plasmolysis of the

appressorium protoplast. On the other hand, melanized appressoria showed limited recovery from cytorrhysis even after 48 h incubation in hyperosmotic glycerol. Maintenance of the enormous glycerol concentrations within appressoria is likely to be a consequence of the reduced permeability of melanized cell walls to glycerol preventing rapid outflow of the solute (de Jong *et al*, 1997).

Like *M. oryzae*, *Colletotrichum* will not penetrate host plant cells if its appressoria are not melanized, either because of the use of DHN melanin synthesis inhibitors or because they are albino mutants. It was showed that less than 10% of albino mutants of *C. lagenarium* were able to penetrate nitrocellulose membranes, compared with more than 70 % of albino mutants that were melanized by treatment with L-DOPA (Butler and Day, 1998).

There are several factors that affect the establishment of disease in plants. For a plant disease to occur, the plant and the pathogen must be in contact and interact. If at the time of the contact the disease does not occur, is because the pathogen may be unable to attack or because the plant may be able to defend itself. There are several factors than account for this lack of disease. They may be because the plant phenotype, the pathogen phenotype, environmental conditions, and/or because the interaction among all of them (The disease triangle) (Agrios, 1997).

In the next chapters we will present only one out of the several variables that affect pathogenicity in *Magnaporthe oryzae*: melanization of appressoria. We do not know the regulatory genes involved in this important metabolic pathway for the blast rice pathogen. On the plant side, we will present some preliminary data about the plant and fungal cellular responses expressed in susceptible, incompatible, and in non-host systems with the objective to determine if the plant cytological responses are correlated with the expression of specific resistance or non-host resistance.

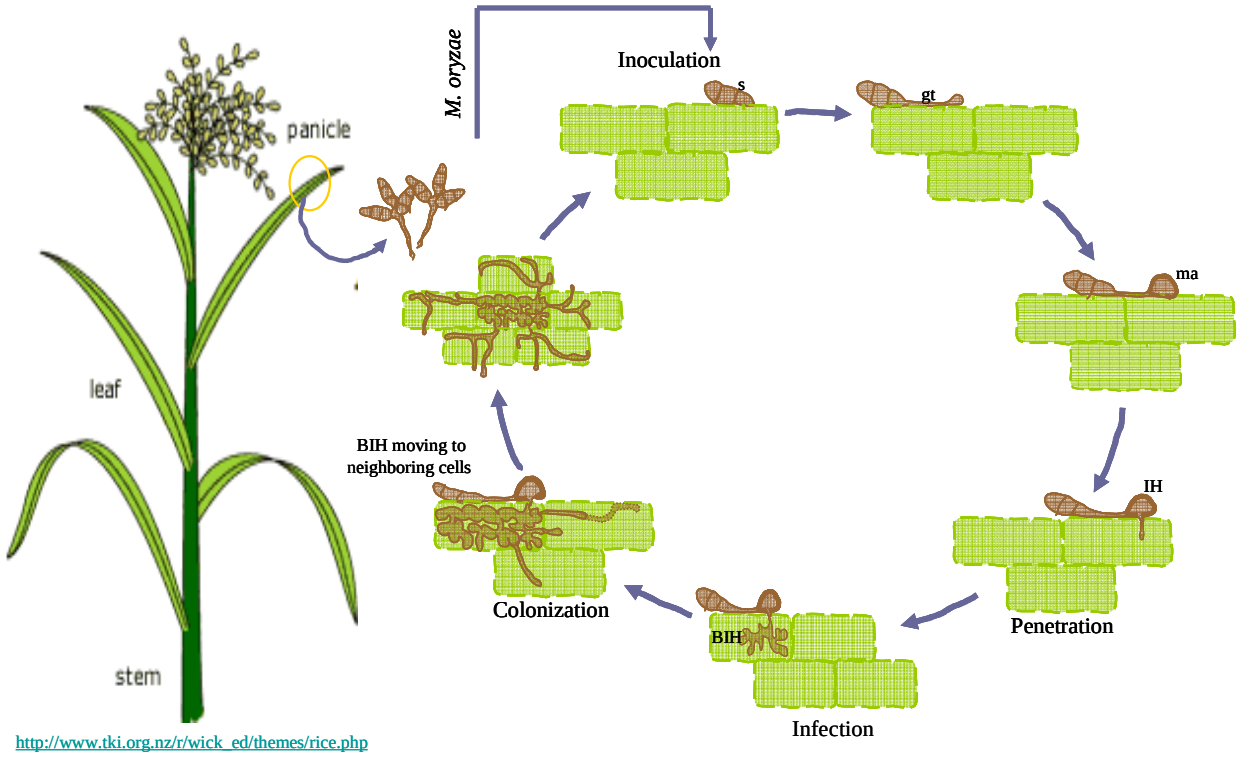

Figure 1-1. *Magnaporthe oryzae* disease cycle.

The inoculation stage of the cycle starts when spores (s) land on either leaf or stem surfaces. The spores adhere strongly to the cuticle by secreting sticky mucilage, and germinate under favorable humidity conditions. The germ tube (gt) extends and its tip differentiates into an appressorium, which melanizes as it matures. Melanized appressoria (ma) generate a high turgor pressure, so the penetration peg penetrates the plant epidermal cell wall (green squares). Invasive hyphae (IH) differentiate into bulbous invasive hypha (BIH) that fill the first infected cells and probably move to neighboring ones through plasmodesmata (dashed green lines).

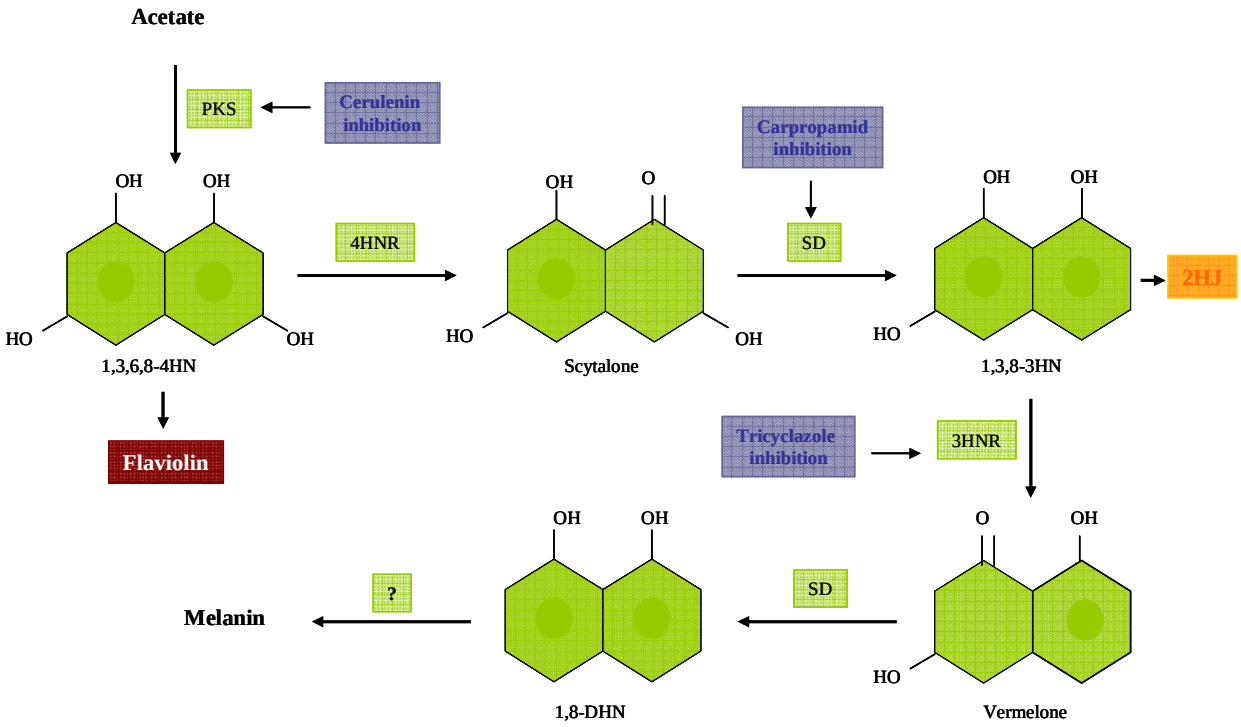

Figure 1-2. DHN melanin biosynthetic pathway.

A polyketide synthase (PKS) joins acetate units to make 1,3,6,8-tetrahydroxynaphthalene (4HN) which is converted to 1,8-dihydroxynaphthalene (DHN) through two reduction and two dehydration reactions. 4HN and 1,3,8-trihydroxynaphthalene (3HN) are reduced to scytalone and vermelone by 1,3,6,8-tetrahydroxynaphthalene reductase (4HNR) and 1,3,8 trihydroxynaphthalene (3HNR) reductase, respectively. Both dehydration reactions are catalyzed by scytalone dehydratase (SD). Specific inhibitors in the pathway are indicated by blue squares. Flaviolin and 2-hydroxyjuglone (2HJ) are the oxidation products of 4HN and 3HN, respectively. These and similar compounds account for the rosy or buff colors of strains with a reductase-deficient or Tricyclazole-inhibited pathway (Butler and Day, 1998; Chumley and Valent, 1990; Thompson *et al*, 2000).

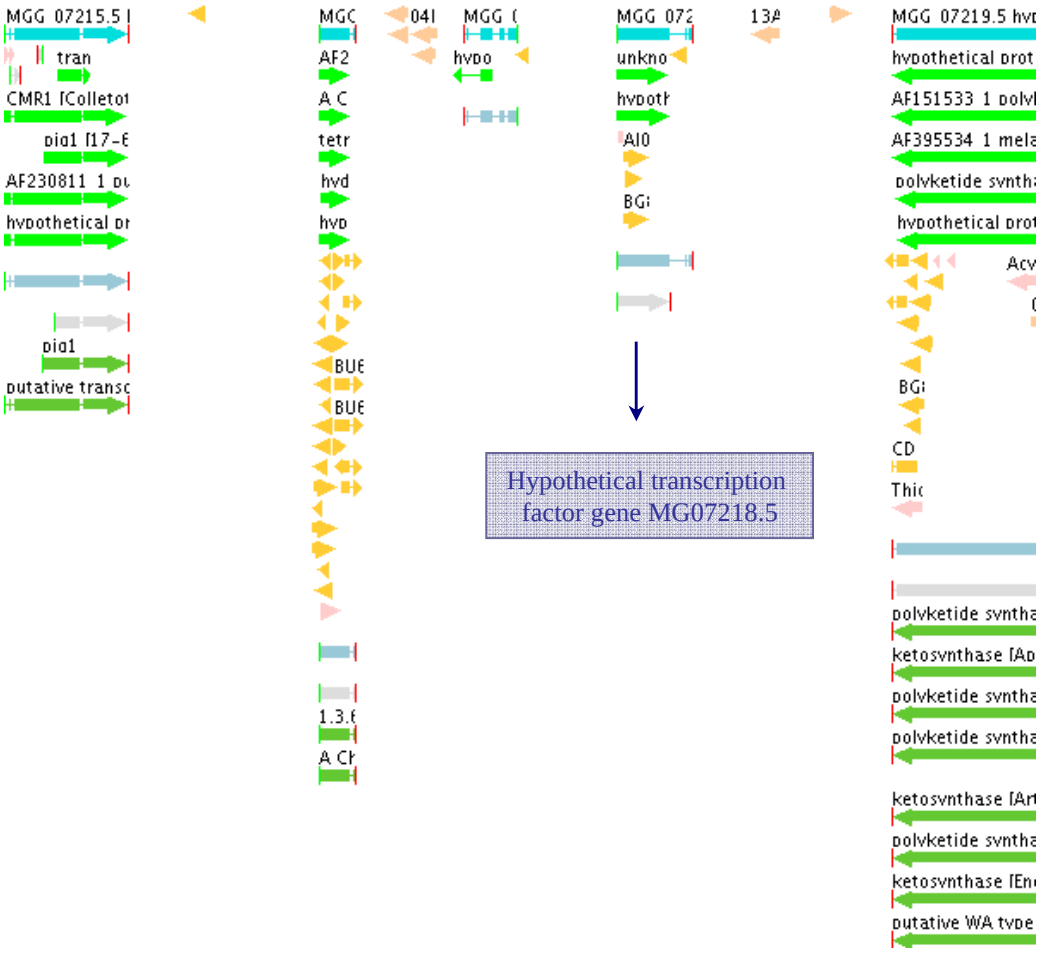

Figure 1-3. The melanin biosynthetic gene cluster of *Magnaporthe oryzae*.

The gene cluster (as depicted in the Broad Genome Database, genome assembly 5) consists of 5 genes (blue arrows) located on chromosome I supercontig 195, nucleotides 1565920-1592010. *PIG1* (first arrow on the left corner), *4HNR* (second arrow), and *ALB1* (the last arrow, the entire gene is not represented) are involved in the melanin synthesis. The hypothetical transcription factor MG07218.5 might be involved in regulating expression of the melanin structural genes during appressorium formation. The orange arrows represent EST sequences; the upper green arrows represent the regions of similarity between biological sequences; the pink arrows represent domain location; light blue arrows represent genes and structures predicted using the FGENESH program; the gray arrows also represent gene structure predicted using a GENEID program run with the *Neurospora crassa* parameter file; and the light green arrows (lower ones) represent the best local alignment with a protein assuming that introns start at GT and end at AG.

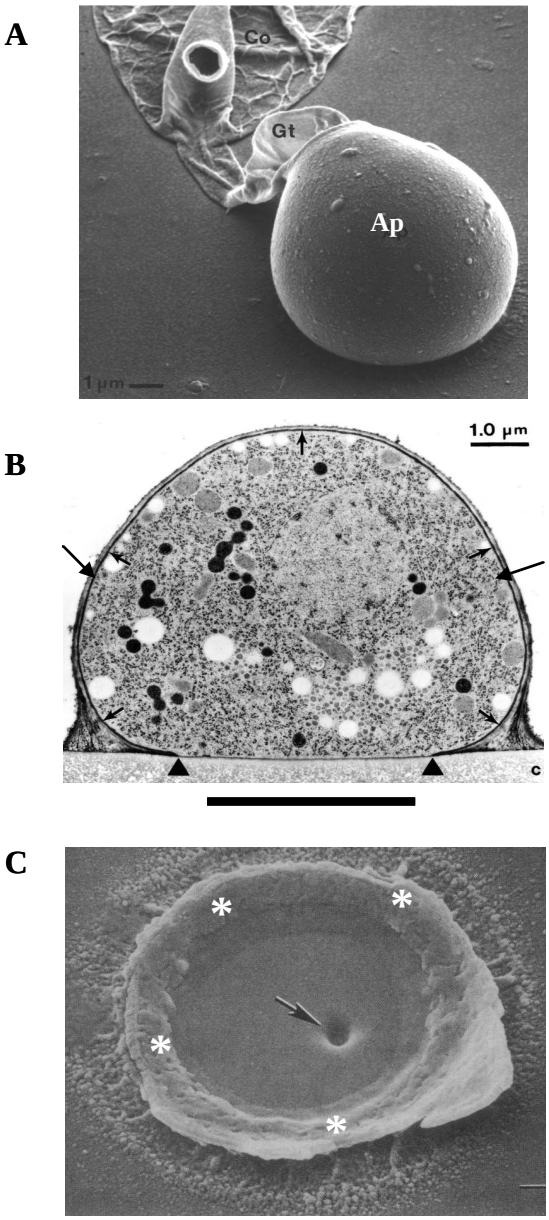

Figure 1-4. *Magnaporthe oryzae* appressorium.

(A) Scanning electron micrograph showing the characteristic dome-shape appressorium (Ap) with the germ tube (Gt) and conidium (Co). (B) Transmission electron micrograph showing the "entire wild-type appressorium cut perpendicular to the substrate". A layer of melanin is shown by arrows and the appressorial pore by the line between arrow heads. (C) Scanning electron microphotography of the remnant formed by sonication of an appressorium on a Mylar surface. Arrow shows the hole produced by the penetration peg. The pore ring (asterisks) observed at the plane of contact with the substrate surrounds the appressorial pore (lacking cell wall). [(A) and (B) Reprinted from Howard and Valent, 1996. (C) from Howard *et al*, 1991)].

CHAPTER 2 - Regulation of melanin biosynthetic gene expression in *Magnaporthe oryzae*

ABSTRACT

Magnaporthe oryzae, the causal agent of the rice blast disease, is very well known for its characteristic melanized dome-shaped appressorium. The appressorial melanin layer acts as a semipermeable barrier to solute movement; water can diffuse across it, but ions and other small molecules cannot move into or out of the cell. Glycerol is the major solute in the appressorial cell, reaching a concentration of about 3M. To maintain such a concentration, a significant amount of water is required, which can move into the appressorium through the melanin layer. However, because glycerol cannot move out, a very high turgor pressure (80 times atmospheric pressure) is generated when water is available. This turgor pressure drives the penetration peg through the plant cuticle and epidermal cell wall. Thus, the appressorial cell wall must be melanized to build up this considerable pressure and initiate infection. Melanin is derived from the 1,8-dihydroxynaphthalene (DHN) melanin pathway, in which at least four structural genes are involved. However, there is no information about the transcription factor(s) that regulate expression of these genes in appressoria. So far, only one putative factor involved in vegetative melanin biosynthesis has been characterized. The gene product, **Pig**ment of *Magnaporthe* - PIG1, carries two types of putative DNA binding motifs and probably activates the expression of *ALB1* during vegetative growth. A pigment mutant of *Magnaporthe* (*pig1*$^{-}$) produces melanized appressoria and albino mycelia. Another hypothetical transcription factor [$Zn(II)_2Cys_6$] gene (HTFG) in the melanin biosynthetic gene cluster represented a good candidate for the regulatory gene in appressorial melanization. We report expression analysis, structural analysis and functional analysis of the HTFG. The HTF coding sequence is 1353 bp in length and lacks introns. Although it is expressed constitutively, the gene appears up-regulated in appressoria. Our functional analysis failed to identify a phenotype associated with the HFTG. Further work is required to investigate the possible presence of a copy of this gene.

INTRODUCTION

As mentioned in the previous chapter, melanins are very important secondary metabolites for fungal survival. Scientists are very interested in these metabolites for many reasons; first, the DHN melanin synthesis pathway is unique in Ascomycetes and Basidiomycetes; second, as reviewed in the previous chapter, there are fungicides currently on the market that prevent direct penetration of plant tissue by inhibiting melanin biosynthesis in appressorial cells; and third, phytotoxins may result from shunt products of melanin synthesis (Bell and Wheeler, 1986; Butler and Day, 1998; Henson *et al*, 1993; Langfelder *et al*, 2003; Plonka and Grabacka, 2006). Therefore, melanins are, at least for some plant fungal pathogens, an important target for disease control.

Molecular genetic and biochemical studies have been conducted extensively in order to understand the function of the melanin biosynthetic genes; however, very few transcription factors involved in regulating their expression, or the expression of other genes important for virulence, have been identified to date (Langfelder, 2003). Transcription control is a very important mechanism for regulating gene expression; under this mechanism only the proper genes will be expressed in the proper cells during the proper development stage and environmental conditions (Lodish, *et al*, 2000).

Transcription factors, also known as regulatory genes, regulate the expression of other genes. Using precise gene regulation in different cell types (vegetative mycelia, conidia, fruiting bodies, and infection-specific cell types), in different developmental stages, or in response to specific external conditions, cells save energy and prevent the products of different genes from interfering with each other (Snyder and Champness, 2003). Synthesis of mRNA takes place in the nucleus and requires that RNA polymerase II initiates transcription, polymerizes ribonucleoside triphosphates complementary to the DNA coding strand, and terminates transcription. The initial RNA transcript is processed into a functional one by adding a poly (A) tail and removing introns; then it is transported to the cytoplasm to be translated into a protein.

The HTFG is expressed in mycelium, spore, and appressorium samples at levels that can be resolved in agarose gels (this study). However, its expression is not detectable at 24 hours after the fungus has penetrated the rice host cells (data not shown), which should indicate, in case the gene has a regulatory role, that the expression of the melanin biosynthetic pathway genes is also down regulated because the fungus does not need to be melanized to continue invading the host cells. This assumption is supported by a 36 hour post inoculated rice-*Magnaporthe* expression profile showing that the *HTF*, *4HNR*, *ALB1*, *RSY1*, and *BUF1* genes are down regulated (Appendix Table A.3) (Mosquera *et al*, submitted).

We have reviewed the role of structural genes in the melanin biosynthesis pathway of at least four different fungal species, including *M. oryzae*. However, there is not much information about the transcription factors that regulate their transcription. So far, only one putative transcription factor involved in vegetative melanin biosynthesis of *Colletotrichum lagenarium*, *Cochliobolus heterostrophus*, and *Magnaporthe oryzae* has been sequenced. The genes, **C***olletotrichum* **m**elanin **r**egulation (*CMR1*), *C. heterostrophus* (*CMR1*) and **Pig**ment of *Magnaporthe* (*PIG1*), encode for 984, 1,014, and 973 amino-acid proteins, respectively, and contain two types of putative DNA binding motifs, a Cys2His2 zinc finger motif and a Zn(II)2Cys6 binuclear cluster motif. The Cmr1 protein of *C. heterostrophus* shares 69% and 70% similarity with Cmr1p of *C. lagenarium* and Pig1p of *M. oryzae*, respectively (Eliahu *et al*, 2007).

Based on *cmr1*$^{-}$ mutant analyses, it was demonstrated that the Cmr1p protein regulates the expression of *SCD1*, *THR1*, and *PKS1* in the vegetative hyphal growth stage. Expression of *SCD1*, *BRN1*, and *BRN2* was non-detectable in *C. heterostrophus cmr1*$^{-}$ mutants (orange-pink colored mycelial phenotype), while the expression of a polyketide synthase (*PKS18*) was moderately reduced. The target genes of Pig1p are unknown, but it was presumed that it activates the expression of *ALB1* only during vegetative growth (Eliahu *et al*, 2007; Tsuji, 2000).

Where might a second gene involved in regulation of melanin biosynthesis regulation in *M. oryzae* appressoria be located? There is a hypothetical gene (MGG_07218.5 – GenBank accession number XM_367293.2) in the melanin gene cluster whose function has not been

determined yet (Figure 1.2). It is common that fungal genes involved in the same secondary metabolism pathway are clustered; since a gene, named the **h**ypothetical **t**ranscription **f**actor **g**ene (HTFG), is clustered with *PIG1*, *4HNR* and *ALB1*, there is a high probability that it could be regulating the expression of the melanin structural genes during appressorium formation. The HTFG has three exons (1343, 43, and 84 bp length) and two introns (408 and 57 bp length) that were predicted by automatic annotation (Figure 2-1). It is not common to find introns of 408 bp length. Fungal introns are small; for example, *Neurospora* introns average 134 bases, *Sordaria macrospora* 106, and *Cryptococcus neoformans* 67 bases (Spieth and Lawson, 2006).

The presence of three ESTs (GenBank accession numbers AI069001.1, AI069000.1 and BG810360.1) within the first predicted exon of the HTFG confirmed that the gene was expressed (Figure 2.1). These ESTs were obtained from the appressorium formation-specific cDNA library constructed from strain 70-15 conidia germinated for 5-8 hours on appressorium-inductive surfaces. The identification of those ESTs from the developing appressorium library is also consistent with a predicted role for HTFG in regulation of appressorial melanization.

The HTFG encodes a 486 amino acid protein whose N-terminal region contains a Cys-rich motif involved in zinc-dependent binding of DNA (Pfam accession number PF00172) (Figure 2-1). The region forms a binuclear zinc cluster in which six conserved cysteines bind two zinc atoms. The spacing of the cysteines is C-x(2)-C-x(6)-C-x(5-12)-C-x(2)-C-x(6 to 8)-C. There are also other conserved residues in the loop regions between the cysteines that can be used to define a specific pattern for this domain. The $Zn(II)_2Cys_6$ binuclear cluster DNA-binding domain is generally located at the N-terminal region of the protein, but in the UME6 protein of *Saccharomyces cerevisiae* it is found at the C-terminal region (www.expasy.org/cgi-bin). Many fungal transcriptional activator proteins contain this domain; for example, *Saccharomyces cerevisiae* has 65 including the well-studied Gal4p, involved in the regulation of galactose metabolism, *Neurospora crassa* has 107, *Aspergillus fumigatus* 195, and *Magnaporthe grisea* strain 70-15 has 71 (www.broad. mit.edu/annotation/genome/).

The HTFG represented a good candidate as a potential regulator of appressorial melanization for many reasons: first of all, this gene is a transcription factor located in the

melanin biosynthetic gene cluster of *Magnaporthe* together with the other key melanin genes (*PIG1*, *4HNR*, and *ALB1*); second, *M. oryzae* and *C. lagenarium* have *pig1*$^{-}$ and *cmr1*$^{-}$ mutants, respectively, that produce melanin in appressoria but not in vegetative mycelia. These observations suggest that Pig1p and Cmr1p are not the only transcription factors that regulate the expression of the melanin structural genes. Third, three out of four EST sequences for the HTFG in the genome database were from a library constructed from developing appressoria; and fourth, the HTFG is down-regulated along with all the structural melanin biosynthetic genes after penetration has occurred and the fungus has colonized rice cells at 36 hours after inoculation. Based on the information presented above, we proposed to confirm the structure of the HTFG, to determine if the HTFG is specifically expressed during appressorium development, and to determine whether or not the HTF protein regulates transcription of the melanin biosynthetic genes.

RESULTS

Hypothetical transcription factor gene (HTFG) structure

At the time we initiated this project, the HTFG was predicted by automated annotation to consist of 1343-, 34- and 84- bp exons separated by two introns of 408 and 57 bp (Figure 2-1). To confirm its structure, we isolated DNA from mycelia of the sequenced laboratory strain 70-15, and the pathogen field isolates O-137 and Guy11 all grown in 3-3-3 liquid medium. PCR products obtained by using a set of primers covering 741 bp bases of the annotated sequence (Appendix A, Table A.1) were purified, cloned into pGEM®-T vector, and sequenced. Sequences were compared using the multiple sequence alignment program ClustalW (version 1.8) (www.ebi.ac.uk/clustalw/). Alignment results showed that the strain 70-15 genomic annotated sequence is 100, 99, and 97% similar to the O-137, the 70-15, and the Guy11 sequences, respectively (Figure 2-2). The only differences among the sequences were numbers of residues in 3 thymine nucleotide repeat regions. Therefore, the sequence of the HTFG is relatively well conserved in different strains of the blast fungus.

To verify the structure of the HTFG transcript, reverse transcription-polymerase chain reaction (RT-PCR) products from Guy11 and KV1 mycelia were purified from an agarose gel, cloned into the pGEM®-T vector, and sequenced. Reverse transcription -PCR products obtained from two additional independent Guy11 cDNAs were also cloned and sequenced. One of the three Guy11 cDNA sequences, the KV1 cDNA, and the sequence from the genomic database were compared with ClustalW version 1.83. The alignment evaluation between the amplified cDNAs and the genomic sequence indicated that the first predicted intron was not spliced out. The second intron was spliced in these cDNAs and the splice sites matched with the consensus 5' GT(G/G/G/T) and 3' (C)AG splicing signals conserved in eukaryotes including *M. oryzae*. However, the sliced intron was 66 bp long instead of the predicted 57-bp (Figure 2-3 A). With these sequences it was not possible to determine the size of the last exon since the first round of Guy11 and KV1 RT-PCR products were obtained using a 24-bp reverse primer (Appendix A, Table A-1) whose first base was located at 23 bases before the stop codon (A of TAG as 1). However, the reverse sequence of a second independent Guy11 cDNA points it out that the last exon is a fragment of 75 bp length, at least in Guy 11 samples (Figure 2-3B).

To support the lack of the first predicted intron, the 3' end of HTFG transcript was determined by Rapid Amplification of the cDNA Ends (3'-RACE PCR). Mycelium from the Guy11 strain was grown in 3-3-3 medium under constant rotation at 26°C, filtered, dried, and frozen in liquid nitrogen for RNA isolation. First strand cDNA synthesis and amplification of the 3'cDNA ends were done following the CLONTECH protocol. Complementary DNA synthesis was done with a 10 μM 3'-RACE CDS primer A (Appendix A, Table A-1) and amplified using a specific gene primer with a 69.7°C Tm and a GC content of 75%. Reverse transcribed products were analyzed on an agarose gel, purified, and cloned into the pGEM®-T vector. Sequence analyses from the 3'-RACE PCR products confirm that the predicted first intron was not spliced out (Figure 2-4). However, the poly-A sequence in the cDNA suggested that the transcript ended before the second predicted intron, which we showed to be spliced out in our separate cDNA analyses.

In conclusion, both the RT-PCR, and the 3'-RACE PCR analyses showed that the first intron predicted by genome annotation is not real. However, if this intron is not spliced from the

mRNA, a stop codon occurs at position 1351 relative to the translation start site (A of ATG = +1), which was recognized by using the ExPASy proteomics server www.ca.expaxy.org/tools/dna.html). The 3'-RACE PCR showed that the coding sequence ends at position 1351, relative to the start site; and the RT-PCR analyses showed a spliced mRNA sequence with a 66-bp intron beginning at nucleotide 433 beyond the end of the mRNA predicted by RACE-PCR. Our results suggest that HTFG is expressed as an mRNA with a 1353 bp coding sequence, and that this gene may be subject to alternative splicing.

Hypothetical transcription factor gene (HTFG) expression

Three out of four EST sequences available for the HTFG in the public databases (Figure 2-1) were obtained from fungal cultures developing appressoria. We performed RT-PCR using RNAs purified from spores, mycelium, and germ tubes forming appressoria in order to determine the expression pattern of HTFG in these different fungal cell types. Unlike RNA isolation from spores and mycelium, RNA isolation from germlings differentiating appressoria was non-trivial because appressorium development only occurs when the germlings are attached to the natural plant cuticle or certain artificial surfaces that mimic the host surface. We first assessed efficiency of appressorium formation on artificial surfaces used in other studies (Bourett and Howard, 1990; de Jong *et al*, 1997; Hamer *et al*, 1988, 1989; Howard *et al*, 1991; Kankanala *et al*, 2007). However, in our laboratory, appressorium formation on green glass lacked reproducibility and synchrony reported previously, and recovery of RNA from cultures developing on cover slips was problematic. We therefore developed the following procedure for recovering appressorial RNA from infected leaf sheaths. Leaf sheath segments of rice variety YT16 were inoculated with a conidial suspension at $1x10^5$ spores/mL and maintained inside a humid chamber at room temperature. Appressorial development was verified by dissecting the epidermal leaf sheaths for microscopic observation at 4, 6, 8, and 10 hours post inoculation (hpi). Leaf sheath sections with developing appressoria were frozen in liquid nitrogen for RNA isolation. RNA samples were tested for fungal RNA content by RT-PCR with actin primers (Appendix A, Table A-1). Although most of the RNA in these infected leaf sheath samples was derived from host plant

cells, we reproducibly detected fungal actin mRNA expression (the actin primers spanned an intron differentiating the genomic and mRNA fragments) in these samples (Figure 2-5 C).

The RT- PCR results showed that the HTFG was expressed in spores (data not shown), mycelium and in appressoria. However, the relative intensities of the amplification products for actin and the HTFG suggested that the HTFG was expressed at higher levels in appressoria than in mycelia (Figure 2-5 A-B). The relative intensities of the actin fragment amplified from appressoria (Figure 2-5 C) and mycelia (Figure 2-5 D) were consistent with the relative purity of the fungal RNA in each sample. That is, the mycelial sample was prepared from pure fungal RNA and the appressorial sample was prepared from infected tissue RNA mixtures of low levels of appressorial RNA and abundant plant RNA. In spite of this major difference in fungal RNA content, the HTFG was much easier to detect in the appressorial samples than in the mycelial samples using the same number of RT-PCR cycles for each. These data suggested that the HTFG is up-regulated in developing appressoria, which was consistent with our hypothesis that the HTFG is involved in regulation of appressorial melanization.

Hypothetical transcription factor gene (HTFG) replacement

In order to know whether the second HTFG encodes a protein required for the expression of the enzymes involved in melanin biosynthesis during appressorium development, a gene replacement experiment was done by using protoplast transformation. Transformation of the Guy11 (0-391) strain was performed with a vector carrying a selectable marker, the hygromycin B resistance gene, flanked by 1.2 kb of the 5’ and 3‘ flanking regions of the target gene coding sequence. The target sequence for replacement was within the first exon of the gene covering a size of 900 bp length from the start codon (Figure 2-6). Sixty-four independent transformants were obtained after a second selection on hygromycin-TB3 agar plates. After 4 to 6 days, transformants were transferred onto oatmeal agar plates and grown until sporulation. Single spore cultures were isolated from each transformant to ensure that each one was generated from a single nucleus.

PCR, RT-PCR, and Southern hybridization analyzes were done to determine if the HTF coding sequence had been replaced by the hygromycin resistance gene (double homologous recombination between the HTFG and the vector carrying the hygromycin B marker-*hyg*) (Figure 2-7). PCR results suggested that 18 out of a total of 64 independent transformants had double homologous recombination with the engineering construct. In other words, recombination took place since the upstream (5') and downstream (3') flanking DNA sequences were identical between the target gene and the engineering construct (Figures 2-7 and 2-8 A). The fact the HTF primers did not amplify the expected band (957 bp) in samples 6-17, 21, 27-36, and 40-43 suggested the HTF coding region was not present in those samples and that it could have been replaced by the hygromycin resistance gene. To support this assumption, DNAs from the same transformants were amplified using the hygromycin primers, resulting in an about 1377 bp band. So far, PCR analysis using the hygromycin primers demonstrated that the coding region of the HFTG was replaced by hygromycin in samples 6-13, 15-17, 21, 27-31, 36, and 40-43 (Figure 2-8 B). Even though the other 46 transformants conserved the HTF coding region, all of them integrated the hygromycin gene (Figure 2-8 and data not shown). For example, transformants loaded in lines 3-5 show both the HTFG and the hygromycin band. However, the hygromycin marker was integrated into a different region by non-homologous recombination (ectopic recombination); the 5' and 3' flanking regions of the engineering construct were not complementary to the site where the recombination occurred.

Total RNA from four of the putative gene replacement mutants was isolated and reverse transcribed to prove they do not transcribe the HTF mRNA. Previously, the RNA samples were amplified by actin primers, to ensure the mRNA was not degraded. In all the samples the actin primers (the same ones used for PCR) amplified the expected ~258 bp band (Figure 2-9 A). Subsequently, we demonstrated that the HTF mRNA was synthesized only by the wild type and the ectopic transformant. In both samples, the primers amplified an approximately 957 bp fragment (Figure 2-9 B).

To conclude whether or not the coding sequence of the HTFG had been replaced by the hygromycin resistance gene, transformants KV43, KV46, KV50, and KV53 were tested by Southern hybridization analyzes. Hybridization with the HTF coding region probe (Figure 2-10

A) resulted in a 1.5 Kb band in the wild type Guy11 and in the ectopic transformants. As expected, the band was not present in the knock out transformants, which means the coding region of the target gene was not present in their genomic DNA. Hybridization of the hygromycin probe in the ectopic, KV43, KV46, KV50, and KV53 transformants (Figure 2-10 B) resulted in an about 2.4 Kb band which indicated that the coding region of the HTFG was replaced by the hygromycin gene. In all the evaluated *htf::hyg* transformants, there is an about 2.3 Kb band that corresponded to the hybridization between the HTF probe and an about 400 bp fragment still present in the genomic DNA digested with the enzyme *PpuMI* (Figures 2-6 and 2-10). The presence of an approximately 8.0 Kb band in all the samples, including the ectopic and wild type, suggests that the Guy 11 strain has an additional sequence with homology to the HTFG probe (Figure 2.10 A).

With our approach for gene replacement, the possibility to have multiple ectopic integrations, ectopic integration at different positions, and/or gene truncation is much higher by protoplast mediated transformation than by *Agrobacterium tumefaciens* mediated transformation (ATMT). In Southern hybridization blots, it was apparent, after taking into account the intensity and the number of the bands, that in the KV43 and KV46 *htf::hyg* mutants the hygromycin gene was integrated several times. However, these events deleted the HTFG coding sequence from the genome.

HTFG mutants showed no evident differences in appressorial melanization

The *pig1*$^{-}$ mutant Bc1317 produces melanin in appressoria but not in vegetative mycelia, suggesting that the second HTFG could regulate the expression of the structural melanin genes. To investigate this hypothesis, appressoria from 8 *htf::hyg* knockout mutants (KV38, KV39, KV41, KV42, KV43, KV46, KV50, and KV53), one ectopic transformant and the wild type strain were induced on YT16 rice leaf sheaths and on glass cover slides. Samples were evaluated at 5, 12, 16, and 24 hpi under a compound microscope. No differences were observed in the timing of appressorial melanization; all appressoria were completely melanized after 12, 16, and 24 hpi (Figure 2-11).

HTFG knockout mutation showed wild type levels of pathogenicity

Three independent replicas of a whole plant rice blast assay were done to see whether the knockout mutation affected pathogenicity of Guy 11. Each *htf::hyg* knockout mutant (KV43, KV46, KV50, KV53), the ectopic transformant, and the wild type strain were inoculated onto separate susceptible YT16 rice plants. Under the evaluated conditions, all the mutants caused blast disease, inducing the typical eyespot lesions characterized by tan centers surrounded by brown margins (Figure 2-12 A-B and 2-13 A-B). Similar results were observed in the ectopic and wild type combinations. Mock inoculated plants showed no symptoms. In each interaction and even in the same leaf we observed symptoms that ranged from lesion type 1 to type 5, which corresponds to avirulent and virulent interactions, respectively (Valent *et al*, 1991).

DISCUSSION

The disease cycle in *Magnaporthe oryzae* absolutely depends on appressorial melanization; once these structures are melanized, the penetration peg has the physical power to penetrate the host surface layers and enter the epidermal cells to establish the infection. After this, the fungus does not need to synthesize melanin anymore. Strains with mutations at any of the melanin structural genes develop non-melanized appressoria, so they are not able to penetrate host plants. However, if the plant surface is artificially wounded, the mutant fungus produces an invasive hypha, colonizes the first invaded cell, and moves into the neighboring ones like a wild type strain (Chumley and Valent, 1990; Kankanala *et al* 2007). These observations are very well supported by a microarray analysis showing that three out of five melanin structural genes (*4THNR*, *BUF1*, and *RSY1*), as well as our target gene, the HTF, were down regulated at 36 hours after YT16 leaf sheaths were inoculated with KV1 strain (Mosquera *et al*, submitted). When the fungus had completely colonized the first cell, its *4HNR* gene was repressed 28-fold compared with mycelium growing in liquid medium, and *ALB1* was repressed eight-fold. *PIG1* was expressed at similar levels in both conditions (Appendix A, Table A-3). On the other hand, the expression of the HTFG was repressed five-fold in rice cells relative to the fungus growing in

liquid culture. The p-values for both transcription factors point out that the variability observed in the three biological and four technical replicas was much higher for PIG1 (0.85) than for the HTF (1.39^{E-12}) (Mosquera *et al*, submitted).

PIG1 could be regulating the expression of *ALB1*, at least to synthesize PKS as the first enzyme involved in the DHN-melanin biosynthesis pathway during vegetative growth (Tsuji *et al*, 2000). However, we do not know which gene encodes the transcription factor that regulates the expression of the melanin genes during appressorial development. In this study we hypothesized that the transcription factor gene locus MGG07218.5, the HTFG, might be involved in this metabolic pathway because it encodes a regulatory protein belonging to the Zn(II)2Cys6 binuclear cluster domain family. The HTFG is located in the melanin biosynthetic gene cluster together with *PIG1*, the tetrahydroxynaphthalene reductase, and the albino gene. The PIG1p has been associated with the regulation of melanin biosynthesis during vegetative growth because a *pig1*$^{-}$ mutant produces albino mycelia and melanized appressoria (Tsuji *et al*, 2000). The HTFG appeared highly expressed in appressoria and more repressed than the *PIG1* gene when the fungus invaded the first epidermal plant cell.

To address our hypothesis, we investigated the structure of the HTFG, its expression in appressorial samples, and its role in the regulation of melanin synthesis during development of appressoria. We demonstrated that the most likely structure for the HTF is a 1353 bp length ORF (open reading frame) that lacks introns. The translated nucleotide sequence shows a 451 amino acid protein that has a $Zn(II)_2Cys_6$ binuclear cluster DNA-binding domain in its N-terminal region (SCDGCFLAKVKCSKARPICSSRCLACGIECRY). Interestingly, this result agrees with a 1215-bp gene present at 2716 bp downstream from the *PKS1* stop codon of the fungus *Glarea lozoyensis*. That gene lacked introns and encoded a putative protein (GenePept accession version AAN59954.1) of 405 amino acids with a high degree of similarity with the Zn(II)2Cys6 binuclear cluster DNA-binding protein, and is 34% identical to our target HTFp (Zhang *et al*, 2003). The protein blast alignment also showed that the HTFp is 53% identical to a *Colletotrichum lagenarium* transcription factor (GenePept accession version BAE98094.1). Additionally, this transcription factor has recently been shown to function in melanin biosynthesis. Mutants in the *C. lagenarium* gene show decreased appressorial melanization and

fail to infect cucumber plants (Yasuyuki Kubo, Kyoto Prefectural University, personal communication). Even though these results were observed in a different system, they support our original hypothesis that the HTFG may still play some role in melanin biosynthesis.

Questions remain about the structure of the HTF transcript, specifically relating to potential alternative splicing of this gene. All of our experiments suggest that the very large intron predicted in the original automated annotation of this gene in the genome database is not real. If this intron is not removed from the transcript, the stop codon after 1351 nucleotides limits the resulting predicted protein to 450 amino acids. Consistent with this, the 3'-RACE PCR experiments produced mRNA clones that end with a polyA sequence before the second intron predicted in the genome database. However, our RT-PCR experiments with two independent strains of the fungus identified transcripts with the second predicted intron spliced out. To see if this second predicted intron was due to a sequencing error in the genome database, we re-sequenced the HTFG in the sequenced strain 70-15 and we also sequenced the gene in the rice pathogen field isolates Guy 11 and O-137. This gene contained the putative second intron in all three genomes, suggesting that this intron was indeed spliced in transcripts obtained in our RT-PCR experiments. Therefore, these data suggest that some HTFG transcripts contain an intron that occurs at 432 bp downstream from an in-frame stop codon. Further studies are needed to explain these results and to determine if the HTFG undergoes alternative splicing.

According to RT-PCR results obtained with Guy11 mycelium, spore, and appressorium samples, we demonstrated that the HTFG is expressed constitutively. However, relative to the expression of the fungal actin gene, the HTF transcript was much easier to detect in appressorial samples than in mycelial ones. This was true in spite of the fact that our infected sheath appressorial RNAs contained mostly rice RNA. This result suggested that the expression of the HFTG was upregulated in developing appressoria, which was consistent with our hypothesis that the second HTFG is actively regulating the appressorial expression of *ALB1*, *4THNR*, *BUF1* and *RSY1* structural melanin biosynthesis genes.

In order to determine the role of the HTFG in melanin biosynthesis during appressorial development, we did protoplast mediated fungal transformation with a vector carrying the

hygromycin resistance gene flanked by fungal genomic sequences surrounding the HTFG coding sequence. PCR, RT-PCR and Southern blot analysis indicated that the coding sequence of the target gene was replaced by the hygromycin gene through a double homologous recombination event. However, the gene replacement did not affect melanin synthesis either in appressoria or vegetative mycelia. All the appressoria were melanized under the experimental conditions evaluated.

Since no visible differences were observed among the wild type, the ectopic transformant, and the *htf*⁻ mutants, we maintained inoculated leaf sheaths under humid conditions to evaluate whether or not the gene replacement had affected other aspects of pathogenicity. Results revealed that the ectopic and 2 *htf*⁻ mutants were able to infect and invade the rice cells in the same manner that the wild type was. Based on these results, we did whole plant rice blast assays to confirm pathogenicity in these mutants and additional ones. Even though the blast symptoms were not totally reproducible in each replica, the plants developed the typical symptoms of the disease, ranging from lesion type 1 to type 5. We did not detect differences in lesion numbers in the mutants, as would be expected from a defect in penetration.

Is the HTFG really involved in appressorial melanization? The appressorium phenotypes of the ectopic transformant and the *htf*⁻ mutants indicate that the gene is not involved; however, Southern hybridization blots (Figure 2-10) showed a homologous 8.0 Kb band in the wild type strain Guy11 and all transformants. These data raise the possibility that there is an extra copy of the HTFG that hybridized with the HFT probe. This copy is not present in the genomic database sequence of *M. oryzae* strain 70-15. Nor was this putative second copy detected by the PCR and RT-PCR screens for gene replacement transformants (Figures 2-8 and 2-9). This putative second copy of the target gene could explain why the *htf*⁻ mutants produce melanized appressoria. As mentioned, biosynthesis of melanin has a critical role in the life cycle of *M. oryzae*; therefore, it makes sense to suggest that the rice blast fungus has the mechanisms that assure its pathogenicity (copies of transcription factors involved in melanin biosynthesis). The HTFG may still play some role in melanin biosynthesis, but there may be functional redundancy that makes this hard to prove. As a result, the homologous sequence seen in our Southern analysis needs further investigation.

MATERIAL AND METHODS

Gene structure and expression

Fungal strains and growth media

Four strains of *Magnaporthe oryzae* were used in this study: Guy11 (0-391), O-137, KV1, and 70-15. Guy 11 is a hermaphroditic isolate [bears both functional male and female fruiting bodies – perithecia (Agrios, 1997)] pathogenic to rice (*Oryza sativa*) and barley (*Hordeum vulgare*) (Yaegashi, 1988) obtained from rice plants in French Guiana (Valent *et al*, 1991). 0-137 is also a field isolate collected from rice plants in China (Sweigard *et al*, 1995). Strain KV1 was obtained by transformation of 0-137 with a constitutively expressed enhanced yellow fluorescent protein (eYFP) for easy microscopic visualization in infected rice tissue (Kankanala *et al*, 2007). 70-15 is a laboratory strain that was used for genomic sequencing (Dean *et al*, 2005). All fungal strains were stored in desiccated, frozen filter papers according to Valent *et al*. (1991). Sections from the stored filter papers were removed from frozen storage and the fungus was grown on oatmeal agar plates at 24°C under continuous illumination in a Percival Scientific incubator Model CU-36L4.

For DNA or RNA isolation from mycelium, an ~6 cm^2 section (by 2-3 mm deep) was cut from mycelium grown for ~ 2 weeks on an oatmeal agar plate and blended in 50 mL of 3-3-3 medium (3.0 g of yeast extract, casamino acids, and glucose dissolved in 1000 mL of water). The fragmented mycelium was transferred into a 1.0 L flask with 200 mL of the same medium and cultured under constant rotation (150 rpm) at 26°C. After 24 hours, the mycelium was filtered and blended with 50 mL of 3-3-3 medium. The sample was transferred to a 1.0 L flask with 200 – 250 ml of the medium and cultured for 5 hours under the conditions described above. Finally, the mycelium was harvested by filtration through a Whatman No.1 filter paper and blotted dry with paper towels. The mycelium was then frozen in liquid nitrogen and stored at -80°C.

Genomic DNA isolation

Mycelium samples were ground in liquid nitrogen, transferred into 1.5 mL eppendorf tubes, and suspended in 700 µL of CTAB buffer. Samples were mixed by inverting the tubes and incubated at 65°C for 1 hour. Then, 700 µL of chloroform: isoamyl alcohol (24:1 vol/vol) were added; the samples were mixed and incubated at room temperature for 1 hour in constant movement. Samples were centrifuged at 13,200 rpm for 10 minutes and the upper phases (~0.5 mL) were transferred into 1.5 mL eppendorf tubes. DNA was precipitated by adding 500 µL of isopropanol; each sample was centrifuged for 5 min at 13,200 rpm and the aqueous phase was removed. The DNA pellets were washed twice with 50 µL of 70% ethanol and dried at room temperature. After 20 min, DNA pellets were re-suspended in 100 µL of an RNase A containing buffer (10 mM Tris-Cl pH 8.5). DNA was quantified with a nanoDrop spectrophotometer version 3.1.2 (NanoDrop Technologies, Inc. Wilmington, DE. USA) and the working concentration was adjusted to 50 ng/µL.

Total RNA isolation

RNA isolation was done following the TRIzol® reagent protocol (Invitrogen™, catalog number 15596-018). Fungal samples (mycelia grown in liquid culture, spores from mycelia grown on oatmeal agar, and appressoria grown on rice leaf sheaths) were ground in liquid nitrogen and the powder transferred into 1.5 mL eppendorf tubes. One mL aliquots of cold trizol were added to the samples, which were then incubated at room temperature. After 5 minutes, 200 µL of chloroform were added; samples were shaken by hand for 15 seconds, incubated at room temperature for 3 minutes and centrifuged at 11,000 rpm for 15 minutes at cold temperature (~4.0°C). The aqueous phase was transferred into fresh 1.5 mL eppendorf tubes; 250 µL of sodium acetate and 250 µL of isopropyl alcohol were added. Samples were mixed by inverting the tubes, incubated at room temperature for 10 minutes, and centrifuged at 11,000 rpm for 10 minutes at ~4.0°C. The supernatants were removed and the RNA pellets were washed twice by

adding 1000 µL of 75% ethanol, mixed by hand and centrifuged at 6,500 rpm for 5 minutes at ~4.0°C. RNA pellets were dried at room temperature for 20 minutes, dissolved with 20 µL of DEPC water, and stored at -80ºC. Total RNA was quantified with a nanoDrop spectrophotometer (version 3.1.2. NanoDrop Technologies, Inc. Wilmington, DE. USA).

Complementary DNA synthesis

Complementary DNA (cDNA) synthesis was done according to the Invitrogen™ protocol (catalog number 11904-018). For RNA/primer mixture preparation, each RNA sample was mixed with the dNTP mix and the random hexamers in a total volume of 10 µL. Samples were incubated at 65°C for 5 minutes and chilled on ice for at least 1 minute. Nine micro-liters of a reaction mix composed of RT buffer, $MgCl_2$, DTT, and RNaseOUT recombinant ribonuclease inhibitor were added to each RNA/primer mixture. Samples were mixed, centrifuged, and incubated at 25°C for 2 minutes. One micro-liter of the SuperScript™ II reverse transcriptase was added to each tube except the negative controls. Samples were incubated at 25°C and after 10 minutes, they were incubated at 42°C for 50 minutes, chilled on ice, and centrifuged. One micro-liter of RNase H was added to each sample. Finally, they were incubated at 37°C for 20 minutes and stored at -20°C for later amplification.

Polymerase Chain Reaction (PCR) and Reverse Transcription-PCR

PCR primers were designed to amplify specific regions of the HTFG (Appendix A, Table A-1). PC / RT-PC reactions were performed in a 25 µL reaction mixture with DNA *Taq* polymerase (Promega) and genomic DNA or cDNA from the fungus. The reaction mixture consisted of 0.5 µL of DNA Taq polymerase, 2.0 µL of 10x buffer, 1.5 µL of 25 mM MgCl2, 1.0 µL of 10 mM dNTP, 0.5 µL of each 10 mM primer, and 2µL of the template in a total volume of 25 µL.

The PCR program consisted of an initial denaturation of 1 min at 94 (95)°C followed by 35 (25) cycles of 30 seconds of denaturation at 94 (95)°C, 30 (45) seconds of annealing at 55°C, and 45 seconds of extension at 72°C, with a final elongation step at 72°C for 1 minute. The amplified products were electrophoresed on a 0.8% agarose gel. DNA bands were staining by immersing the gel in 150 mL of double distilled water containing 15 μL of ethidium bromide. After 20 minutes, the gel was distaining in double distilled water for 10-15 minutes. DNA bands were visualized with a UV transiluminator.

Rapid Amplification of 3'cDNA End (3'- RACE PCR)

The 3' end of the HTFG was identified according to the manufacturer's protocol using total RNA isolated from mycelium grown in liquid culture (BD SMART™ RACE cDNA amplification kit from Clontech Takara BIOCompany - catalogue number 634914). The 3'-RACE cDNA was synthesized by mixing (in separate 0.5 mL tubes) 1.0 μg of total RNA from Guy11 or KV1 mycelium and the oligo dT primer (Appendix A, Table A-1) in a final volume of 5 μL for each reaction. The samples were mixed, spun briefly and incubated at 70°C for 2 minutes. After cooling on ice and spinning them, a 5 μL mix containing 5x first-strand buffer, 20 mM DTT, 10 mM dNTP mix and reverse transcriptase was added to each tube. The samples were mixed by pipetting, spun briefly, and incubated at 42°C. After 1.5 hours, the reaction products were diluted with Tricine-EDTA buffer, heated at 72°C for 7 minutes and stored at -20°C. Amplification of the 3'-RACE cDNA was done by preparing a PCR master mix for all of the PCR reactions. For each 50 μL of reaction, PCR-grade water, advantage 2 PCR buffer, dNTPs, and the advantage 2 polymerase were mixed. The 3'-RACE cDNA, UPM (universal primer mix), GSP (gene specific primer- Appendix A, Table A-1) and the master mix were mixed in a final volume of 50 μL. The cDNA was amplified using the following program:

5 cycles:	94°C – 30 seconds
	72°C – 3 minutes
5 cycles:	94°C – 30 seconds
	70 °C – 30 seconds

72°C – 3 minutes

25 cycles: 94°C – 30 seconds

68°C – 30 seconds

72°C – 3 minutes

The amplified products were electrophoresed on a 0.8% agarose gel at 50 volts. DNA bands were visualized with a UV transiluminator.

Gene replacement

Guy 11 strain protoplast preparation

Protoplasts were produced by blending 6.0 to 8.0 cm^2 sections of an 18–20 day mycelium culture with 50 mL of complete medium. The macerated mycelium was transferred to a 1.0 L flask with 250 mL of complete medium and cultured for 48 hours at 26°C and 100 rpm. One more blender maceration was done after 24 hours of growth. The resulting mycelium was filtered, washed with 5-10 mL of a $Na_3C_6H_5O_7$-$2H_20$/EGTA/NaCl (7M NaCl) buffer, and weighed. For digestion, 1 mL of Novozym 234 solution was added per 1.0 g of mycelia. The digestion mixture was incubated for 2.5 hours at 100 rpm and 30°C. Protoplasts were filtered through cheesecloth, washed with $Na_3C_6H_5O_7$-$2H_20$/EGTA/NaCl (7M NaCl) buffer, and filtered again through nitex (Sefar Nitex Inc., catalog number 3A03-0025-102-14. NY, United States. The protoplast suspension was centrifuged at 2173 RCF (4500 rpm) for 8 minutes at 24°C. The protoplasts were washed with STC [20% (w/v) sucrose, 50mM Tris-HCl Ph8.0, 50 mM $CaCl_2$] and centrifuged twice under the conditions mentioned above. The pellet was resuspended in STC and the largest protoplasts were counted using a hemacytometer. Aliquots of $6.4x10^5$ protoplast/mL were frozen by placing them directly in a -80°C freezer.

Knockout vector construction by fusion PCR

The fusion PCR method involves the selection of primers that amplify each of the 5' and 3' flanking regions of the target gene (HTF) as well as the hygromycin selection marker fragment.

In the first PCR round, the 5', 3' flanking regions and the hygromycin cassette from the pCNS43 plasmid were amplified by using three set of primers (Appendix A, Table A-1). First fusion PCR products (5' flanking-1.2 Kb, HYG-1.4 Kb, and 3'flanking-1.2 Kb) were electrophoresed on a 1% agarose gel at 100 volts, purified by following the QIAGEN PCR purification protocol, and used as templates for the second PCR. In this PCR round, the three products from the first PCR were mixed in a 1:1:2 (5'flanking:3'flanking:HYG) ratio, ligated and partially amplified by using a PCR parameter of 94°C for 2 minutes followed by 10 cycles of 94°C for 30 seconds, 56°C for 20 minutes, and 72°C for 5 minutes. The PCR was finished with a single cycle of 10 minutes at 72°C.

Finally, the knockout fragment was obtained by a third fusion PCR round. The second PCR product was amplified using nested primers located near the edge of the flanking fragments [Nested 5'F (Appendix A, Table A-1) and Nested 3'R (Appendix A, Table A-1)] in a PCR program of 1 cycle of 2 minutes at 94°C; 30 cycles of 94°C for 30 seconds, 65°C for 1 minute, and 72°C for 3 minutes, and 1 cycle of 10 minutes at 72°C. Because the expected band (3.8 Kb) was obtained along with other non-specific ones, the PCR fragments were separated by electrophoresis on a 10 cm long 0.8% agarose gel run at 35 volts for 5.5 hours. The expected DNA fragment was purified from the gel following the QIAGEN gel extraction protocol. The knockout DNA fragment was stored at -20°C to be used in the protoplast transformation.

Chemical protoplast transformation

One protoplast suspension tube was placed on ice until the cells thawed. A 200 µL aliquot was placed into a 1.5 mL micro-centrifuge tube and mixed with 2.5 µg of the fusion PCR DNA fragment. The tube was incubated at room temperature for 15 minutes and then 1 mL of PTC solution (40% Polyethylene glycol 8000 in STC) was added. After 20 minutes of incubation at room temperature, the protoplast-DNA mixture was transferred into a 15 mL falcon tube,

mixed with 5.0 mL of TB3 liquid medium, and incubated at 26°C and 100 rpm for 19 hours. The tube was centrifuged at 4100 rpm for 10 minutes and the supernatant discarded. The protoplast pellet was resuspended in 100 μL of STC and mixed well. Protoplasts were poured onto TB3 agar plates containing 100 μg hygromycin/mL and incubated at 24°C for 5-7 days. After a second selection in TB3-Hyg agar plates, the transformants were transferred onto oatmeal agar plates for sporulation. Single conidium cultures from each transformant were isolated to ensure that each new strain had originated from a single nucleus.

Transformant confirmation

PCR and RT-PCR Experiments

See protocol above.

Southern blot hybridization

Genomic DNAs from Guy11 wild type, one ectopic transformant, and 4 *htf::hyg* transformants (KV43, KV46, KV50, and KV53) were digested with the restriction enzyme *PpuMI* (Figure 2-6) overnight at 37°C. Digested DNA was electrophoresed in 0.8% agarose gels at 35 volts in 0.5x TAE buffer. Nucleic acids were transferred into a positively charged nylon membrane according to the manufacturer recommendations (Hybond™-N+; Amersham Biosciences Corp, USA). Following electrophoresis, DNA samples were observed on a UV transiluminator and photographed.

HTF and hygromycin labeled probes were prepared according to the GE Healthcare Amershan AlkPhos protocol. Previously, Guy11 mycelial DNA and the hygromycin cassette from the plasmid pCNS43 were amplified with the HTF specific primers and the hygromycin primers, respectively (Appendix A, Table A-1). PCR products were electrophoresed in a 0.8% agarose gel at 50 volts, purified, and quantified with a nanoDrop spectrophotometer. Ten nano-grams of the HTF and hygromycin DNA were denatured by heating for 5 minutes in a vigorously boiling water bath. Samples were cooled on ice for 5 minutes and centrifuged briefly. The reaction buffer, the labeling reagent, and a cross-linker working solution were added to the

cooled DNA samples, which were then incubated for 30 minutes at 37°C and maintained on ice while the hybridization conditions were set up. The HTF and hygromycin blots were pre-hybridized in a hybridization oven at 58°C for 15 minutes. To avoid placing the probe directly on the blot, the hybridization buffer was mixed with the corresponding probe. Later, the buffer-probe mix was added to the blot. Hybridization was carried out at 60°C for 14.5 hours.

Gene function

Rice plant variety

The rice cultivar used in this study (YT16) is a double haploid line derived from a cross between Yashiro-mochi and Tsuyuake (Jia *et al*, 2000). The cultivar is susceptible to strains 0-137 and Guy 11 (Berruyer *et al*, 2006). Five YT16 seeds per pot were sown in Sungro Metromix 200 potting soil and incubated in a Conviron BDW120 growth chamber programmed to water the plants with a 0.14% (wt/vol) solution of Jack's fertilizer 20-10-20. Plants were grown at 80% relative humidity under a daily cycle of 12 hours light (Appendix A, Table A-2).

Appressorium induction (leaf sheath and cover slide assays)

Appressoria from Guy11 strain, 1 ectopic transformant, and 8 *htf::hyg* knockout mutants (KV38, KV39, KV41, KV42, KV43, KV46, KV50, and KV53) were induced on 28 - 30 day old YT16 leaf sheaths and on glass cover slides (Fisher Finest-Premium cover glass 22 x 22-1, Fisher Scientific).

For appressorium induction on leaf sheaths, each strain was inoculated by injection onto separated leaf sheath segments (three replications of each strain were done). Leaf sheaths were removed from the plants and cut into about 5.0 cm segments; four to five segments were placed horizontally into plastic Petri dishes with wet filter paper and inoculated with ~ 5.0 mL of a

$1x10^5$ spore/mL suspension prepared in 0.25% gelatin. Petri dishes were maintained under laboratory conditions. At 5, 12, 16 and 24 hours after inoculation, leaf sheaths were dissected to obtain the adaxial epidermis with 3 or 4 underlying mesophyll cell layers. Appressorium growth and melanization were observed with a Carl Zeiss Axioplan 2 microscope. Images were acquired using an Axiocam HRc camera. Dissected samples at the evaluated point times were frozen in liquid nitrogen and stored at -80°C for RNA isolation.

For appressorium induction on artificial surfaces, three glass cover slides were placed on one precleaned microscope slide and inoculated with a 40 μL drop of a $1x10^5$ spore/mL suspension in double distilled water. For each strain three microscope slides were placed into a sterile 150 x 15mm plate. Paper towels moistened with sterile water were placed into each plate to maintain high humidity. The fungal samples were grown under laboratory conditions and evaluated at the same time that inoculated leaf sheaths were done. The experiment was repeated three times for each strain.

Rice blast assay

Each *htf::hyg* knockout mutant (KV43, KV46, KV50, and KV53), one ectopic transformant and the wild type strain was inoculated onto separate three week-old YT16 plants. One rice pot was placed inside a plastic bag and the youngest, most susceptible leaf (about half emerged) of each plant was marked with a permanent marker. Four 1.0 mL disposable plastic pipettes were driven into the soil in each pot in order to hold the bag off of the plants. Plants were placed in a particle containment hood (Microvoid model 5300 tabletop laminar flow workstation from Air Control, Inc. NC, Unated States.) and inoculated with 5.0 mL of a $1x10^5$ spore suspension in sterile 0.25% gelatin solution by using an artist's air brush (Paasche H No. 1) connected to compressed air at 20 psi. As a control, one rice pot was also sprayed with 5 mL of a sterile 0.25% gelatin solution.

After inoculation, the bags were sealed in order to maintain the humidity required for spore germination and penetration. The plants were kept in low light laboratory conditions for 24

hours and then removed from the bags and returned to the growth chamber. Finally, the marked youngest leaves were scored 7 days after inoculation according to a scale of 5 lesion types established by Valent *et al* (1991). The experiment was repeated three times for mutants KV43 and KV53, and 4 times for mutants KV46 and KV50.

Figure 2-1. Feature map (Broad genome database) of the hypothetical transcription factor gene locus MGGO7218.5.
The gene MGGO7218.5 (upper blue arrow) is located in supercontig 195 together with three of the five melanin structural genes. According to the automated annotation, this gene has three exons (*) separated by two introns (◂). Orange arrows represent ESTs obtained from the *M. oryzae* strain 70-15. The presence of a Zn(II)2Cys6 binding domain is indicated by the pink arrow. The light blue arrow represents genes and structures predicted using the FGENESH program. Recently, the gene annotation program GENEID predicted that the gene ends without the introns (gray arrow).

Figure 2-2. Alignment of the strain 70-15 HTF genomic sequence (from the BROAD genome database) with its homologue in strains O-137 and Guy11, and with the sequence we determined experimentally from strain 70-15 (E70-15).

The HTF genomic sequences were aligned against the automatically annotated sequence of 70-15 (AA70-15) using the default parameters of ClustalW (starting from the last 123 bp of the first predicted exon). Exons and introns are shaded green and yellow, respectively. The AA70-15 sequence is 100, 99, and 99% similar to the O-137, experimental 70-15, and Guy11 FHT sequences respectively. The differences observed among the sequences are explained by a variable amount of thymine in 3 thymine nucleotide repeated regions (indicated by red arrows).

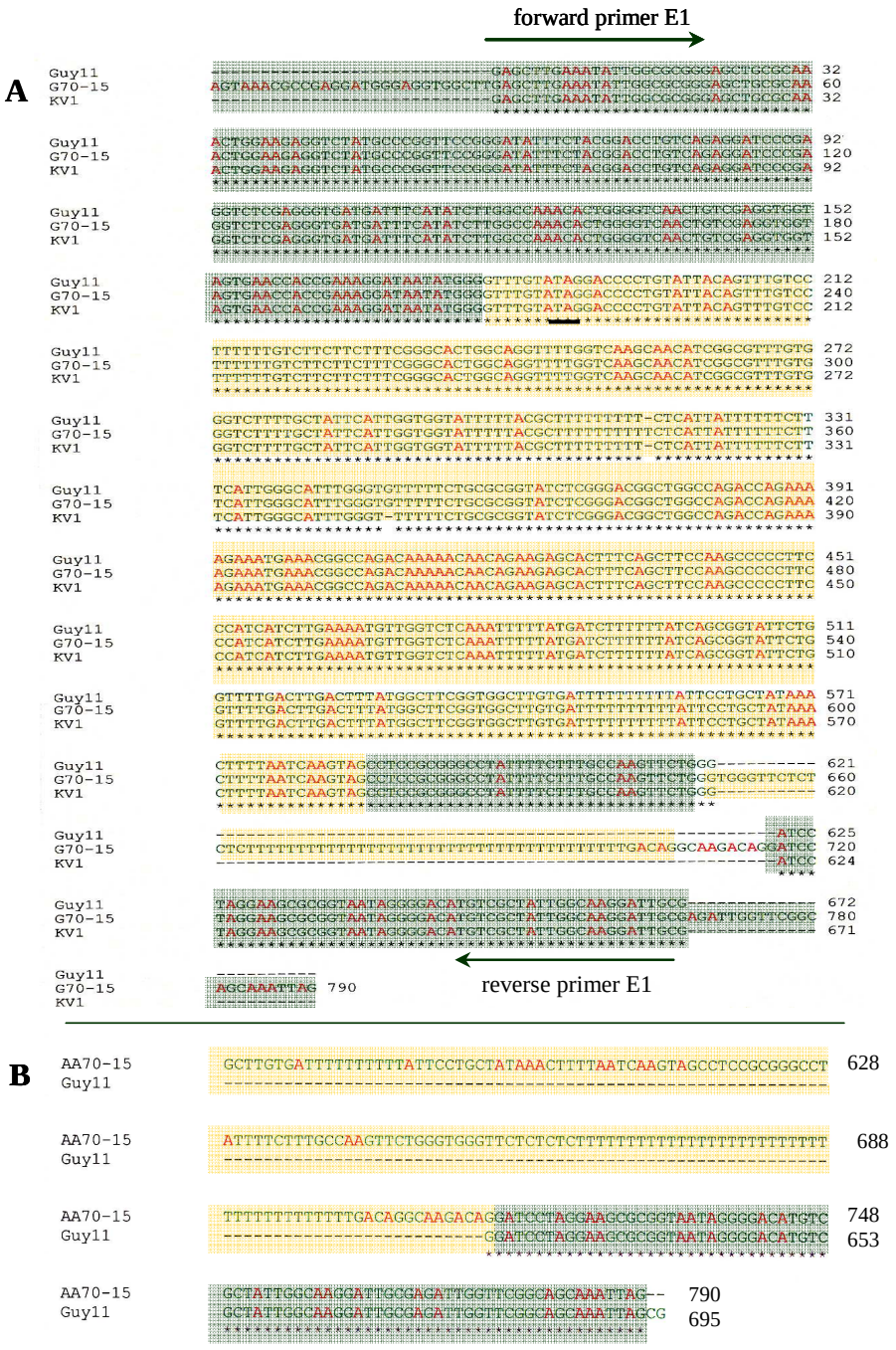

Figure 2-3. Alignment of the HTFG with reverse transcribed sequences of Guy11 and KV1. (A) The HTF genomic sequence of the 70-15 strain was aligned against reverse transcribed DNA sequences of Guy11 (top line) and KV1 (bottom line) strains. Predicted exons and introns are shaded green and yellow, respectively. The predicted first intron is not spliced out, since identical nucleotides (*) are present in the cDNA clones. We confirmed the presence of a stop codon (underlined), suggesting that the HTFG lacks introns. (B) The 70-15 genomic annotated sequence (top line) aligned against a Guy11 cDNA (bottom line). Both sequences are 100% similar and Guy11 cDNA indicates another 75-bp exon.

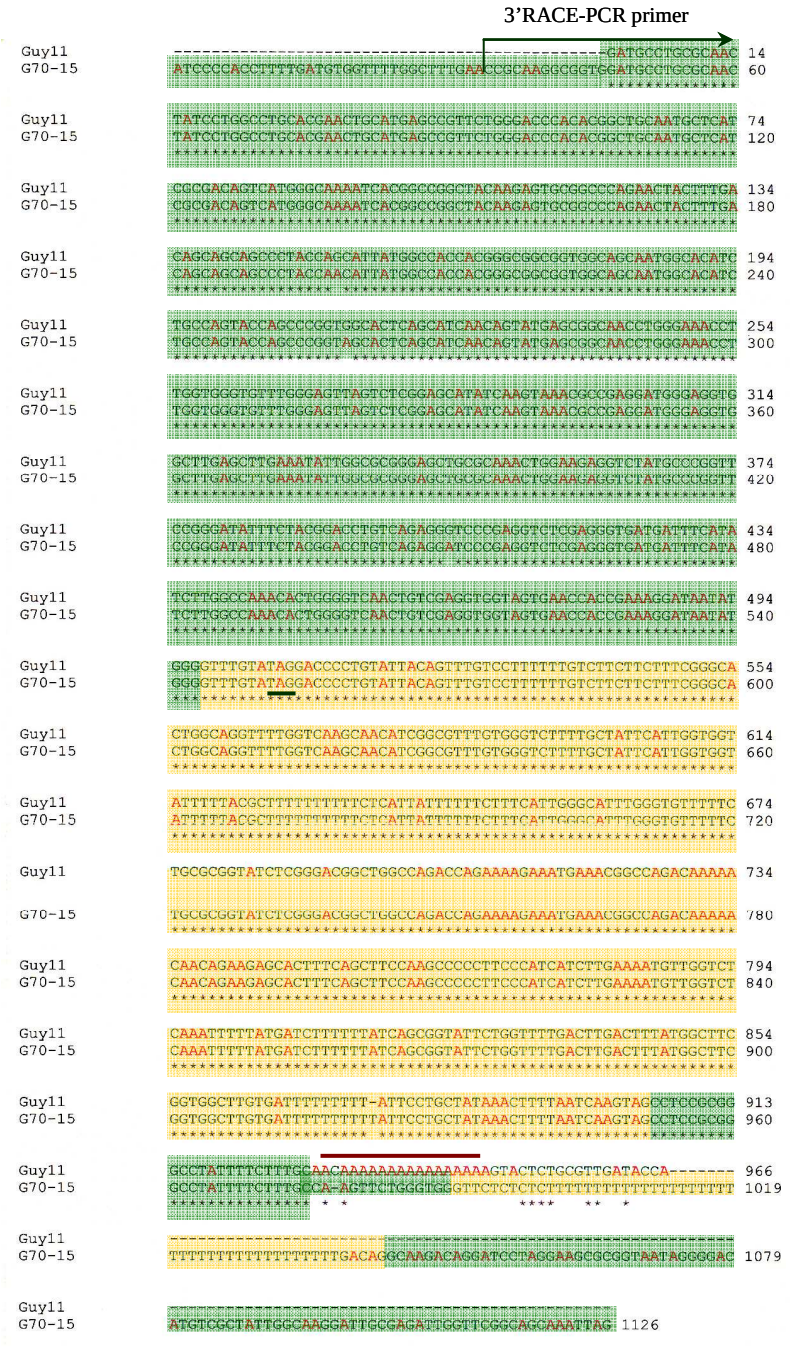

Figure 2-4. ClustalW alignment of the strain 70-15 genomic HTF sequence with its homologous cDNA sequence obtained from a 3'-RACE PCR from strain Guy11.
Exons and introns are shaded green and yellow, respectively. Identical nucleotides are showed by asterisks. Identical nucleotides are shared in the first predicted intron. These results support our previous data indicating the first predicted intron is not spliced out, and that the HTF is a gene that lacks introns.

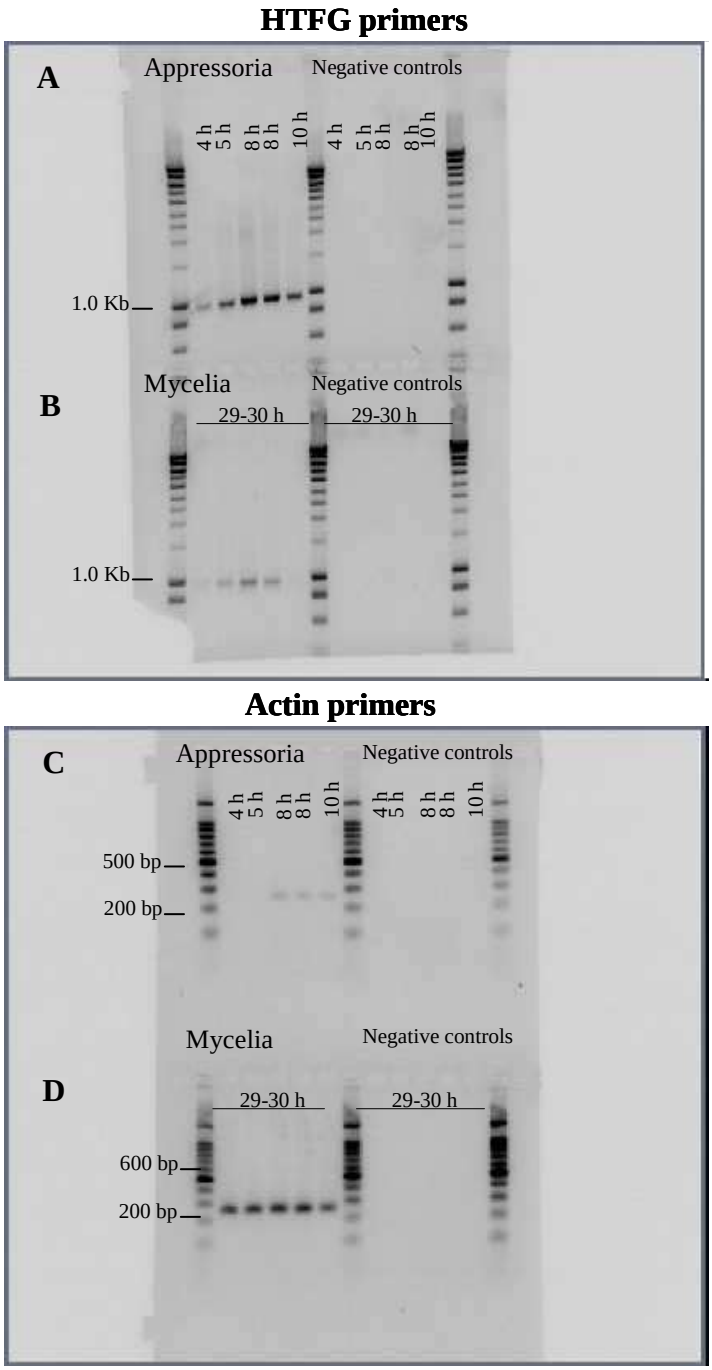

Figure 2-5. RT-PCR results from the HTFG expression in appressorial and mycelial samples of Guy11.

The same amounts of appressorium (A) and mycelium (B) RNAs were reverse transcribed in the same experiment under identical conditions; therefore, the band intensities indicate that the expression level of the gene is higher in appressoria. Wells 1, 2, 3, 4, and 5 (between the standards) were loaded with appressoria induced at 4, 5, 8, 8, and 10 hours post inoculation, respectively. Actin was amplified in appressoria (C) and in mycelia (D) samples. Mycelial RNA was obtained from mycelia grown in liquid culture for 24-29 hours. Actin primers amplified weak bands in appressoria induced at 8 and 10 hpi (C), while all the mycelia samples (D)

transcribed the actin gene. Wells 6, 7, 8, 9, and 10 in the 4 panels represent the negative controls of samples 1, 2, 3, 4, and 5, respectively. For these, complementary DNA in these samples was synthesized without adding the reverse transcriptase, so the absence of bands in these wells indicated that those bands in panels A to D were amplified only from cDNA.

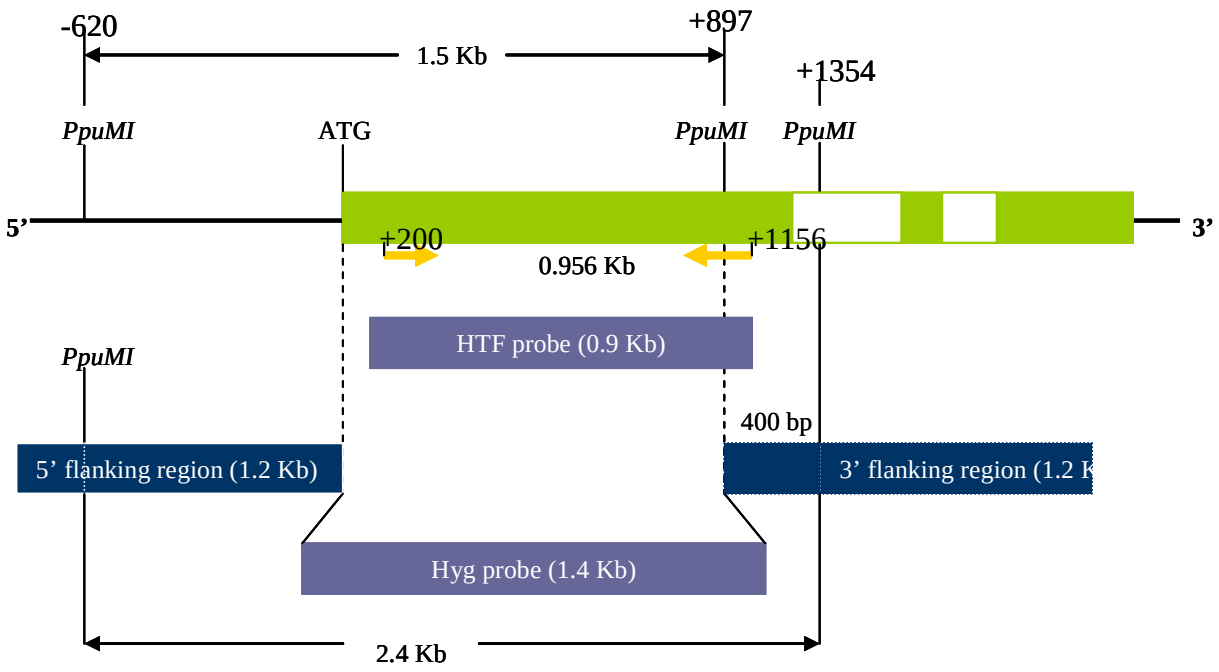

Figure 2-6. Graphic representation of the *Magnaporthe oryzae* MGG_07218.5 locus based on the automated gene sequence.
Green and white boxes represent exons and introns, respectively. Numbers indicate the genomic position of the *PpuMI* restriction sites relative to the translation start codon (A of ATG as +1). Yellow arrows indicate the position of the primers used to amplify the HTF probe.

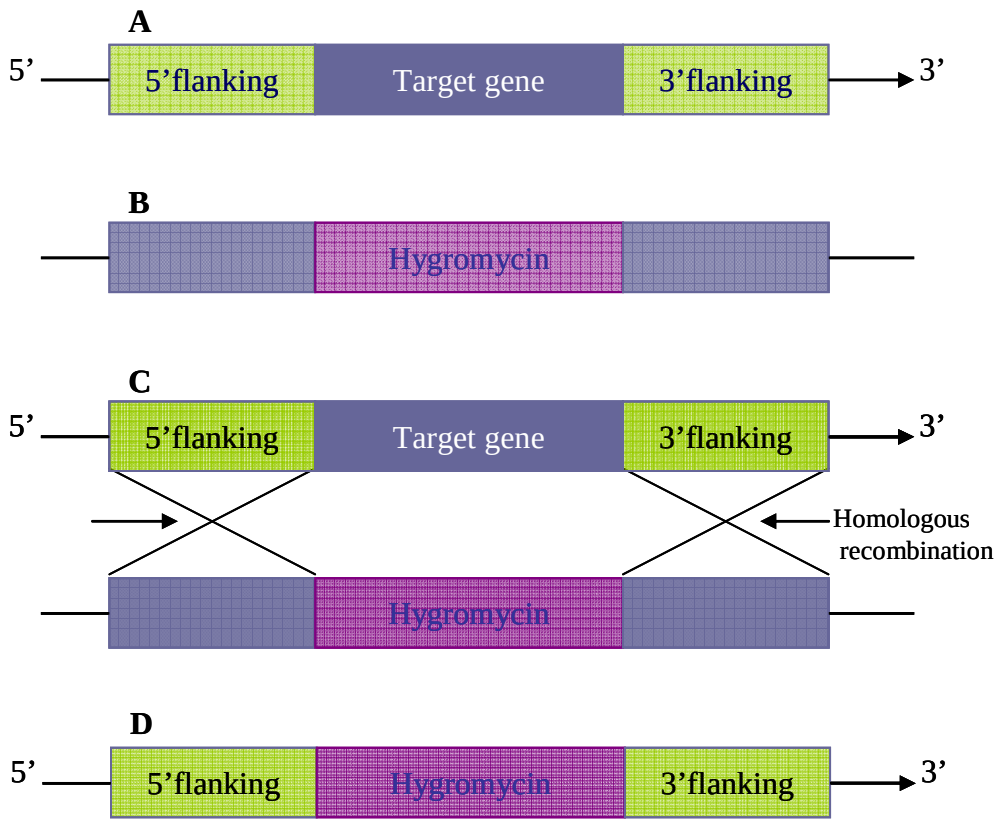

Figure 2-7. Homologous recombination for replacing the HTFG.
(A) The coding sequence is represented by the dark blue box flanked by the 5’ and 3’ flanking DNA sequences. (B) represents the engineered construct used to replace the HTFG. The selectable marker, violet box, is flanked by DNA sequences identical to those ones flanking the HTFG. Guy11 protoplasts, transformed with the engineered construct, grew on oat meal agar; during cellular division the engineered construct and the HTFG recombined at the regions that have identical sequences (Homologous recombination-arrows). The final result is a new fragment of DNA (hygromycin) inserted in place of the target gene (D). The original engineering construct took the coding sequence of the HTFG (E); however it is not able to replicate, so it is lost in dividing Guy11 cells.

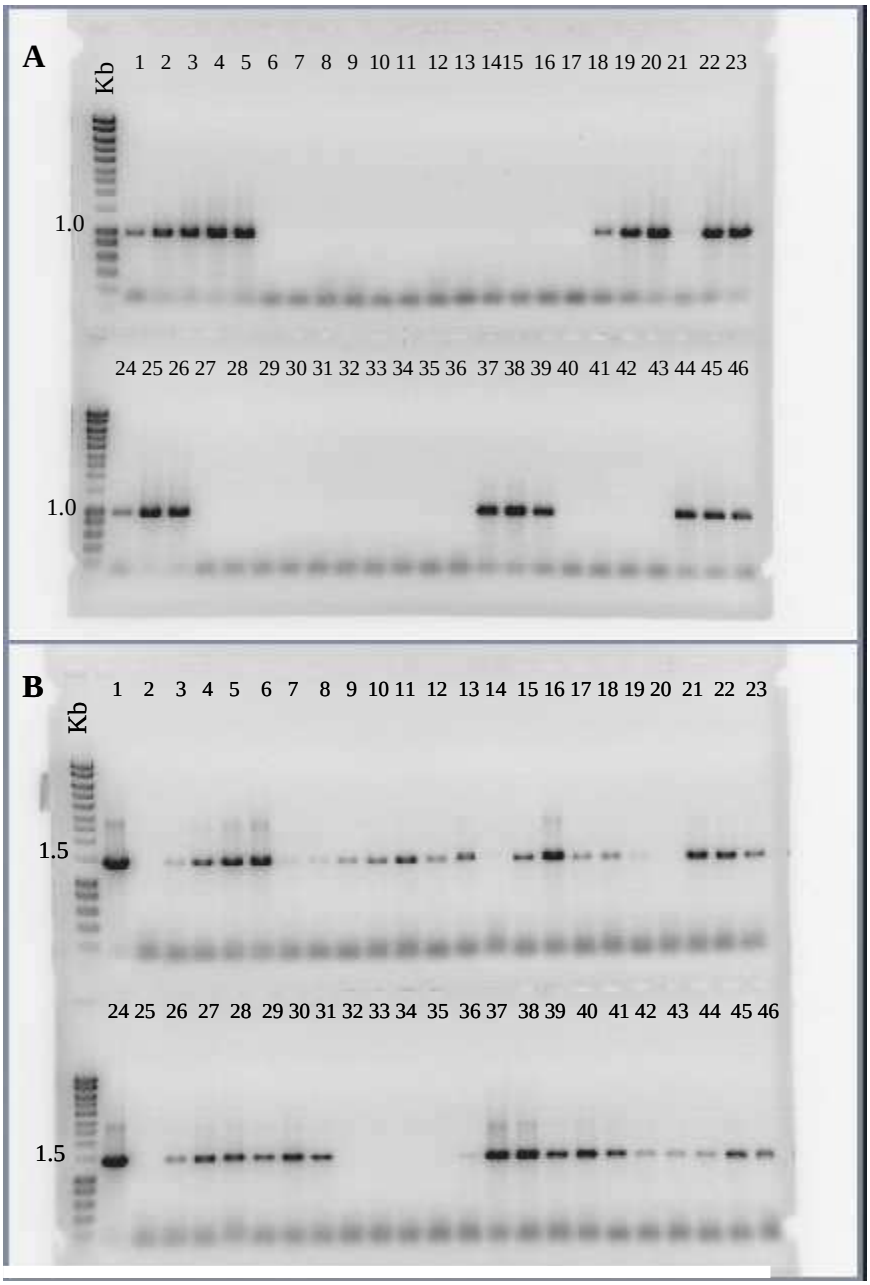

Figure 2-8. PCR screening of the *htf::hyg* mutants.
(A) The HTF primers did not amplify the target gene in samples loaded in lines 6-17, 21, 27-36, and 40-43; so this should indicate the target gene was replaced by the hygromycin resistance gene. A second PCR analysis using hygromycin specific primers (B) demonstrated that the hygromycin gene replaced the HTF coding region in samples 6-13, 15-17, 21, 27-31, 36, and 40-43. Lines 1 and 24 in panel A correspond to wild type DNA. Lines 1-2 and 24-25 in panel B correspond to positive (pCNS43 plasmid with hygromycin cassette) and negative (wild type) control DNA samples, respectively.

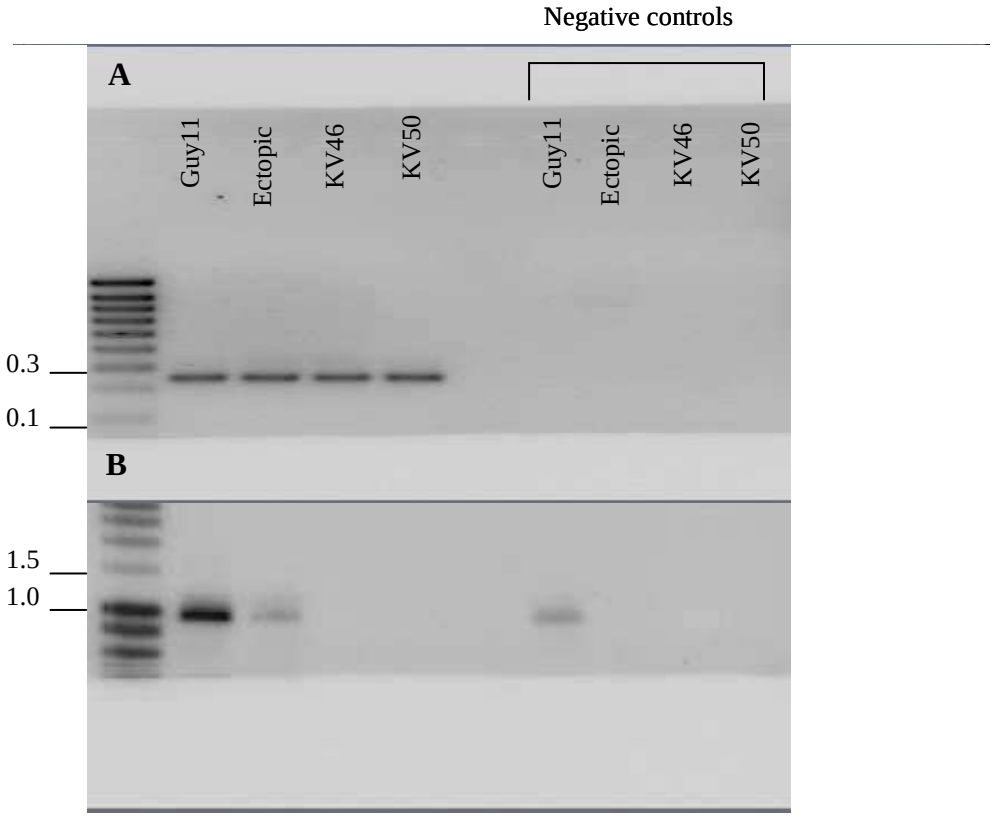

Figure 2-9. RT-PCR screening of *htf::hyg* mutants.

Total RNA from Guy11 wild type, one ectopic transformant as well as the KV46 and KV50 mutants was reverse transcribed to prove they do not synthesize the HTFG mRNA. These samples were amplified with actin primers (panel A) in order to verify that RNA was not degraded. As expected, the actin primers amplified an approximately 258 bp band in all the samples, except in the negative control ones. Samples in panel B show an approximately 1.0 Kb band amplified by the HTF primers in the Guy11 and ectopic samples. The ectopic transformant transcribed the target gene because it is still in the chromosome. However, because KV46 and KV50 had lost the HTFG, there was not a template to be amplified by the corresponding primers. The presence of a band in the wild type sample well (negative control) indicate that this RNA had some genomic DNA contamination.

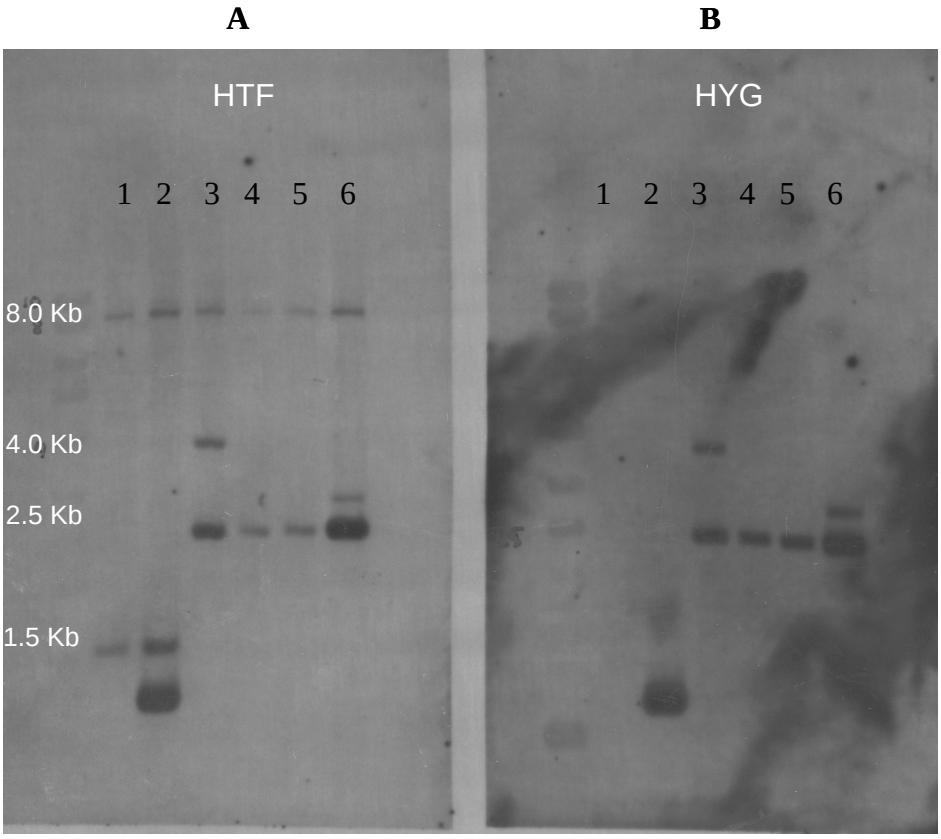

Figure 2-10. Southern hybridization analysis.
Genomic DNA from the wild type strain (lane 1), ectopic (lane 2), KV43 (lane 3), KV46 (lane 4), KV50 (lane 5), and KV53 (lane 6) was isolated and digested with *PpuMI*. Digested DNAs were electrophoresed on 0.8% agarose gels and transferred onto a nylon membrane. The blot membrane in panel A was probed with a 0.9 Kb genomic fragment of the HTF coding region. A duplicate blot membrane in panel B was probed with a 1.4 Kb fragment containing the hygromycin resistance gene.

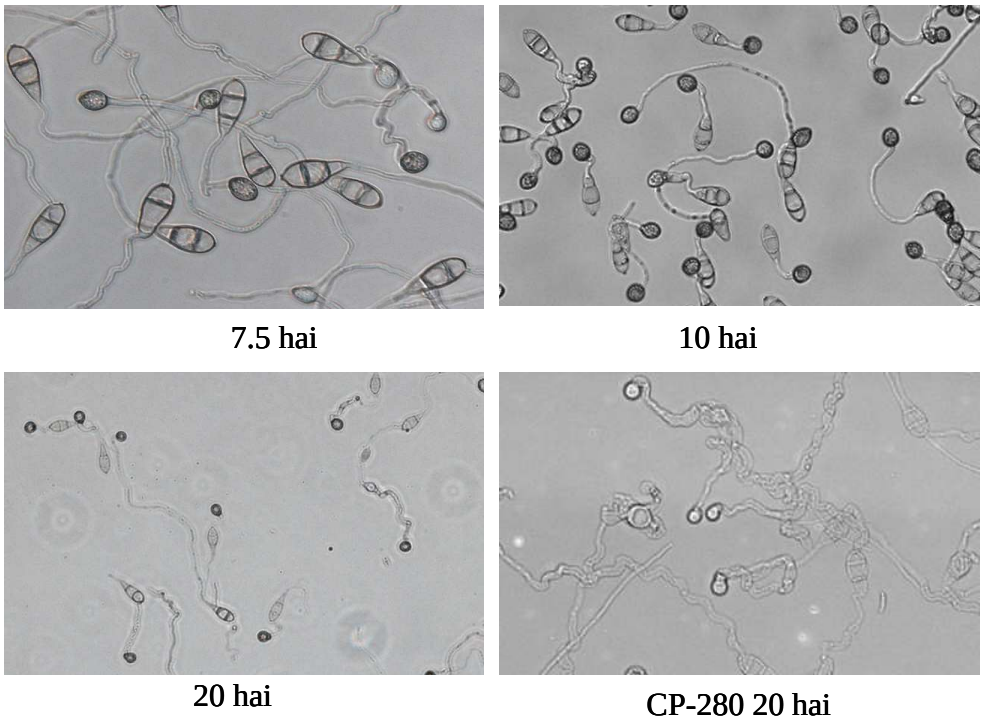

Figure 2-11. Induction of appressoria on artificial surfaces
To determine whether the HTFG regulates the expression of the melanin synthesis genes, appressoria from 8 knockout mutants as well as the wild type and the ectopic strains were induced on glass cover slides and on rice cultivar YT16 leaf sheaths (data not shown). Appressorial melanization started between 5 and 7 hai; however, appressoria were completely melanized after 12 hai. CP-280 is a 4091-5-8 *alb1* mutant that produces non-melanized appressoria.

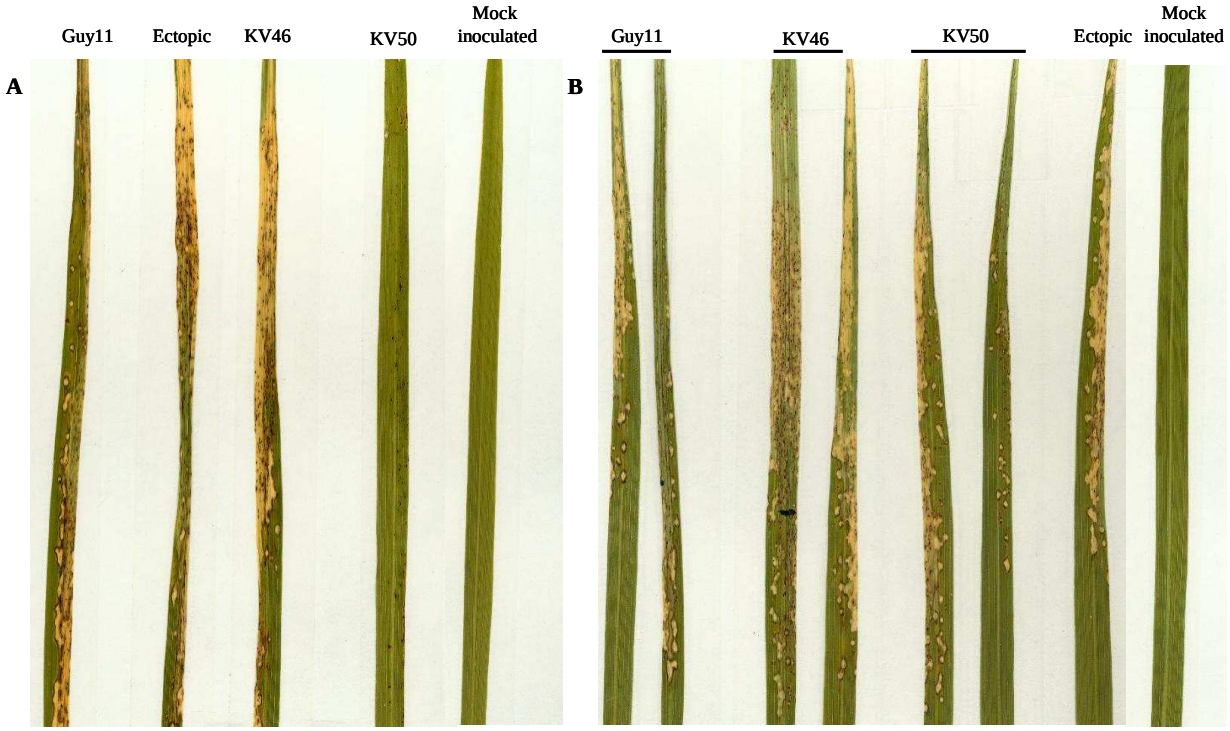

Figure 2-12 A-B. Rice blast infection assay.
Inoculation was done using a $1x10^5$ spore/mL suspension. HTFG replacement does not reduce pathogenicity on YT16 plants. Induced lesions are the typical ones that have been documented in the *Magnaporthe oryzae–Oryza sativa* interaction. Panels A and B show YT16 plants inoculated with KV46, KV50, Guy11 strain and an ectopic transformant in two independent assays.

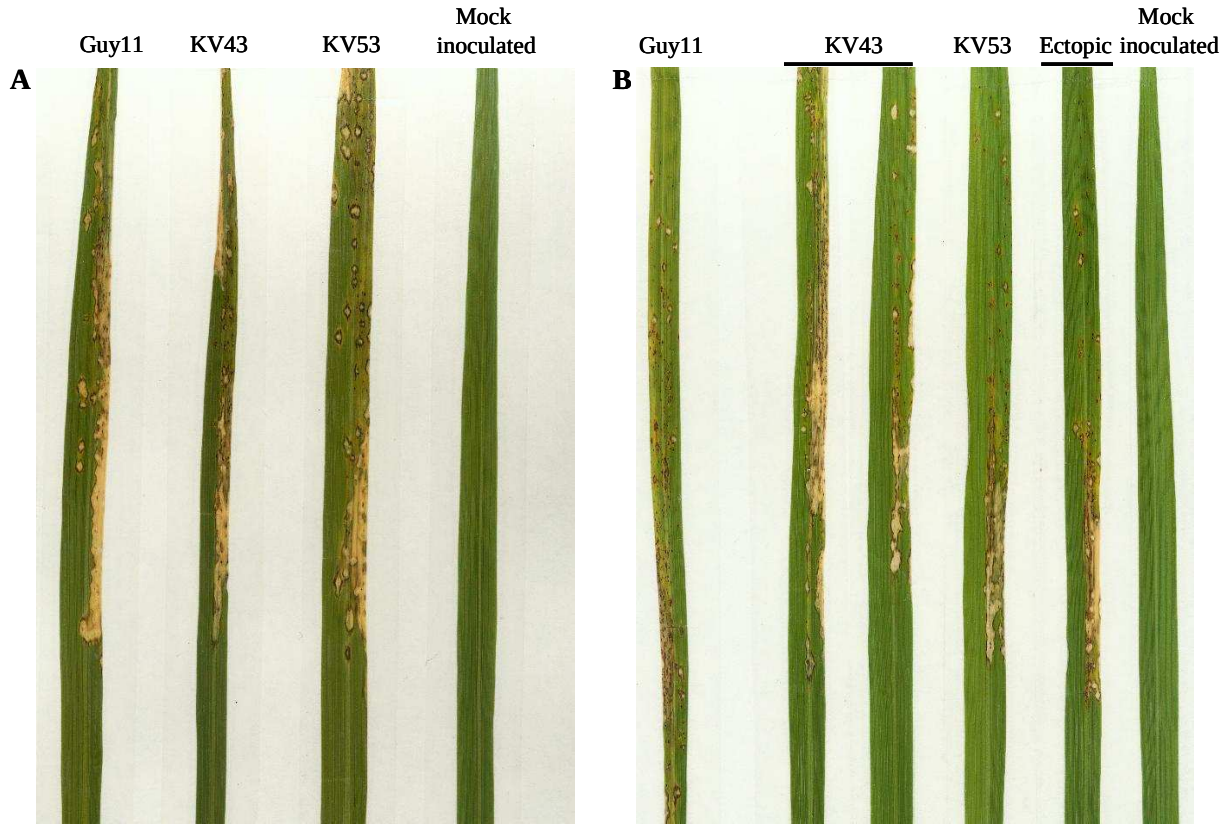

Figure 2-13. Rice blast infection assay.
Inoculation was done by using a $1x10^5$ spore/mL suspension. Panels A and B show YT16 plants inoculated with KV43, KV53, Guy11 and ectopic strains in two independent assays. Induced lesions are the typical ones that have been documented in the *M. grisea-Oryza sativa* interaction. The *htf::hyg* knockout mutants are pathogenic to rice and neither showed any detectable differences between them and the wild type or ectopic strains.

CHAPTER 3 - *Magnaporthe oryzae* strain 4091-5-8 and the *Oryza sativa* cultivar Yashiro-mochi: a non-host system?

ABSTRACT

Even though non-host resistance is highly effective and durable, and should be exploited to improve rice breeding programs, its molecular bases are not completely understood. The first data to understand pathogenicity of *Magnaporthe* spp. and the mechanisms of race-specific resistance were generated by detailed cytological analyses. However, these studies involved fungal development on artificial surfaces and plant cellular responses from fixed or clarified infected tissue, which are not the best experimental conditions to investigate fungal growth and the physiological reactions of host cells. Currently, the objective is to utilize conditions allowing *in planta* artificial infections of living tissues under conditions similar to those occurring under natural environments.

We proposed to study the relationship between fungal penetration and cytological responses of living leaf sheath epidermal cells by comparing responses in a susceptible, a resistant, and a non-host interaction. All three interactions were compared in excised and in intact sheath tissue. We report here that the cytological basis for the non-host interaction differs from those mediated by the *Pi-ta* resistance gene. Results from the excised method suggested that the occurrence of aggregations around the appressoria (AA), not reported previously, correlated with the expression of non-host resistance. However, data from intact leaf sheaths indicated that mixed reactions, including some occurrences of AA, account for the non-host resistance. Further studies are needed to understand and define the cytological responses associated with non-host interactions in rice-*Magnaporthe* interactions.

We also showed that excision of leaf sheath segments from the intact plant alters the cytological responses of the host to pathogen invasion, especially in the resistant and non-host interactions. These results have major implications for future studies using live cell imaging of sheath tissue to investigate race-specific and non-host resistance mechanisms.

INTRODUCTION

All plant species, including those with agricultural value, establish symbiotic associations with microbes; these associations have coevolved in a diverse and complicated exchange of signals and responses that can result in a "friendly" acceptance of the microbe (mutualism – mycorrhizal relationship); in slow recognition and moderately effective defenses against the microbe (compatible association); or in strong and rapid defense responses that block further infection (incompatible association) (Bent, 1996). Interestingly, a compatible association (disease) is the exception rather than the rule since plants are exposed to a diverse group of potential pathogens, but only a few of them will cause disease (Huitema, 2003).

Mechanisms of plant defense

The first line of defense against a pathogen is the plant surface, which must be penetrated by the pathogen to cause the infection. However, plants have preformed physical (amount and quality of wax and cuticle that cover the epidermal cells; the structure of epidermal cell walls; the size, location, and shape of stomata and lenticels; and the presence of tissue with thick-walled cells), and/or chemical barriers (fungi-toxic exudates; antifungal compounds such as phenolic, tannins or some fatty acid-like compounds) that block successful infection to specialized pathogens (Agrios, 1997; Dangl and Jones, 2001; Nürnberger *et al*, 2004).

In addition to this preformed or passive defense mechanism, plants also have sophisticated induced responses that restrict pathogen invasion (Hammond-Kosack and Jones, 1996). Unlike mammals, plants do not have mobile defender cells or a somatic adaptive immune system; instead, their immune system depends on the innate immunity of each cell and on systemic signals coming from the infection sites. Plant immunity occurs through transmembrane

pattern recognition receptors (PRRs) that respond to pathogen-associated molecular patterns (PAMPs), or protein products encoded by resistance genes (Jones and Dangl, 2006).

PAMPS (Pathogen-associated molecular patterns)

The pathogen-associated molecular patterns are elicitors of diverse chemical composition and from different plant pathogenic microbes (exogenous elicitors) (Nürnberger *et al*, 2004). The first exogenous elicitors characterized were oligosaccharides, but there are also glycoproteins, lipids, and many polypeptides of viral, bacterial or fungal origin that are able to trigger initiation of plant defense responses against pathogens. A well known example is flg22, a highly conserved N-terminal fragment of flagellin and the main building block of eubacterial flagellae, which triggers defense-associated reactions in plants as diverse as *Arabidopsis* and tomato. The ability to recognize PAMPs varies considerably between monocotyledonous and dicotyledonous plants; for instance, rice cells appear to possess the capacity to recognize bacterial flagellins, but the structural properties of the defense-eliciting "epitope" is presumably different from flg22 (Jones and Dangl, 2006). In another example, a partial enzymatic hydrolysis from the cell walls of *Magnaporthe oryzae* triggered phytoalexin biosynthesis in suspension-cultures of rice cells, but not in soybean cotyledon cells, suggesting differences in the recognition of gluco-oligosaccharide elicitor signals in these plants (Yamaguchi, 2000). Products released during plant cell wall degradation by microbe-associated hydrolytic enzymes are also recognized by PRRs and trigger defense responses (endogenous elicitors) (Nürnberger *et al*, 2004).

Race or cultivar-specific resistance

In genetic terms, plant cultivar-specific disease resistance is determined by specific interactions between pathogen avirulence (*AVR*) gene loci and alleles of the corresponding plant disease resistance (*R*) locus (Bent, 1996; Hammond-Kosack, 1996; Nürnberger *et al*, 2004). According to the gene-for-gene hypothesis proposed by Flor (1971), when the corresponding dominant plant *R* gene and the dominant *AVR* gene are present in both host and pathogen, the resulting interaction will be incompatible, in other words, the plants will be resistant to the pathogen. The biochemical model that accounts for this genetic interaction establishes that the *R* products (receptors) recognize *AVR*-dependent signals (elicitors) and trigger a chain of signal-

transduction events that result in the activation of defense mechanisms that block pathogen growth (Bent, 1996; Dangl and Jones, 2006; Laugé *et al*, 2000).

It has been considered that a typical response of most gene-for-gene interactions is the activation of a hypersensitive response (HR) that includes apoptotic cell death within a few hours of pathogen contact. Other features of specific resistance include the production of reactive oxygen species (ROS), cell wall fortification (papilla formation and cell wall thickness), accumulation of benzoic acid (BA) and salicylic acid (SA), defense-related proteins (PR proteins) and phytoalexins (low molecular weight anti-microbial compounds), among others (Agrios, 1997; Bent, 1996; Hammond-Kosack and Jones, 1996).

There are some incompatible plant-microbe interactions whose resistance, conferred by the classic gene-for-gene relationship, has been well characterized at the cytological and molecular levels (Hammond-Kosack and Jones, 1996). One example is the interaction between the fungus *Cladosporium fulvum*, the causal agent of leaf mold, and tomato plants. The genes isolated from the plant include the *Cf-2*, *Cf-4*, *Cf-5*, and *Cf- 9* resistance genes (membrane proteins with extracellular leucine-rich repeats-LRRs), which confer resistance to the races 2, 4, 5, and 9 carrying the avirulence genes *Avr2*, *Avr4*, *Avr5*, and *Avr9*, respectively. *Cladosporium fulvum* grows and secretes the *AVR* proteins in the apoplast of the host leaves and, since the resistance proteins are assembled within the plant plasma membrane, the *AVR-R* interaction occurs in the apoplast. Consequently fungal growth is blocked either within the substomatal cavity or in the mesophyll tissue (Agrios, 1997; Hammond-Kosack and Jones, 1996). The activation of defense responses has been studied under artificial conditions by working with intact leaf and cotyledon tissues and with cell suspension cultures. In an *in vivo* cotyledon assay, *Cf-2* and *Cf-9* tomato seedlings were infiltrated with *AVR2* and *AVR9* gene products, respectively. After 2, 4, and 6 hours, both plant-pathogen interactions activated very similar host responses, including cell death. On the other hand, *Cf-5* expressing cell cultures treated with AVR5 protein activated a much faster defense response (10 minutes) relative to the *Cf-2*/*AVR2* and *Cf-9*/*AVR9* interactions, and cell death was not induced (Hammond-Kosack and Jones, 1996). In general, it is noticed that many of the tomato defense responses are similar, but the time of the expression is different. A successful *R-Avr* gene-mediated resistance response

involves a rapid pathogen perception resulting in the coordinate induction of a diverse array of defense mechanisms within the initially infected cell as well as in the surrounding cells.

Plant nuclear migration has been observed in susceptible (Heath *et al*, 1997; Pappelis *et al*, 1974), gene-for-gene resistance (Heath *et al*, 1997), non-host systems (See below) (Huitema *et al*, 2003), and in plant cellular activity such as the formation of infection threads during root nodule development (Heath *et al*, 1997). Earlier studies have reported that one of the first signs of cell death in cowpea epidermal cells infected with the rust fungus is a modification in the appearance of the plant nucleus. Heath *et al* (1997) observed that in resistant and susceptible cowpea epidermal cells, the plant nucleus migrated to penetration sites during plant wall penetration. Later, the nucleus migrated away from successful infection sites when the fungal penetration peg established contact with the host plant plasma membrane. However, in the susceptible cowpea cells the nucleus migrated back to the fungus when it started hyphal tip growth. It was hypothesized that the return of the plant nucleus to its normal position after the fungus established contact with the plant plasma membrane raises the possibility that the fungus blocks penetration-related signals that would trigger a variety of plant defense responses, including callose deposition.

Non-host resistance

Non-host resistance, also named species-specific resistance, is a type of interaction in which the entire plant species is resistant to all strains of a pathogen that is able to infect other plants (Heath, 2001; Thordal-Christensen, 2003). This plant-microbe interaction system, where the plant is a non-host plant and the microbe is a non-host pathogen, is the most common and durable form of plant resistance to disease; however it is still not well understood (Mellersh and Heath, 2003; Neu *et al*, 2003; van Wees and Glazebrook, 2003).

Non-host resistance is believed to occur through diverse mechanisms. Holub and Cooper (2004), classified non-host resistance mechanisms into two groups: non-specific defenses and inaccessible defenses. The non-specific defense mechanism is constitutive or passive and applies when the pathogen lacks the necessary pathogenicity factors. The second type of non-host

resistance applies when the pathogen cannot overcome either preformed antimicrobial compounds or active defenses (Zellerhoff *et al*, 2006). Mysore and Ryu (2004), proposed a Type I non-host resistance, which does not result in a visible cell death, and a Type II, which renders a hypersensitive response characterized by cell death at the penetration site (Oh *et al*, 2006).

There are data suggesting non-host resistance includes constitutive physical and/or chemical plant barriers that block fungal growth; however, these barriers rarely can completely account for the lack of successful pathogen infection. Inducible defense responses are also involved; these responses are probably elicited nonspecifically similar to recognition of PAMPs. Current models suggest that a complex integration between specific resistance, based on gene-for-gene interactions, and nonspecific defense responses can contribute to non-host resistance. Heath *et al* (2002), showed that nonspecific wall-associated defense responses were associated with the failure of *Uromyces vignae* to penetrate into cowpea plants. Other studies suggest that single pathogen proteins can induce defenses in a gene-for-gene manner. Genetic analyses of the powdery mildew-wheat interaction have led to the identification of major genes conditioning the resistance of wheat to the *Erysiphe graminis* f. sp. *agropyri* (causes powdery mildew on *Agropyron* spp.) pathogen based on the gene-for-gene interaction (Neu *et al*, 2003). Therefore, lack of disease in a non-host system could be explained by a non-host plant having several resistance proteins that match the proteins encoded by avirulence genes in the non-host pathogen and/or by a basic lack of pathogen compatibility due to the absence of appropriate signals from the plant. The importance of one or the other resistance mechanisms in a non-host interaction may differ from one pathosystem to the next and will probably depend on the history of coevolution of the particular plant and pathogen (Ayliffe and Lagudah, 2004; Heath, 2001; Huitema *et al*, 2003; Mellersh and Heath, 2003; Neu *et al*, 2003).

Even though the advances in molecular biology and biochemistry have provided several tools to investigate non-host resistance, its molecular mechanisms and signal components are poorly understood. Some studies compared host and non-host resistance in order to know whether or not defense-related genes are expressed only in non-host interactions. A microarray experiment was used to compare a host pathogen (*Pseudomonas syringae* pv. *tomato-AvrRpt2* - *Pst*) and a non-host pathogen (*P. syringae* pv. *phaseolicola* NPS3121 - *Psp*) in *Arabidopsis* carrying the resistance gene *RPS2* (Tao *et al*, 2003). Interestingly, the microarray data did not

indicate a significant difference between the genes expressed during host and non-host resistance. The transcription profile of *Psp*-infected plants at 6 hours was similar to those of *Pst*-infected plants at 3 and 6 hours; however, gene expression was delayed following infection by the non-host pathogen relative to the host resistance response (Tao *et al*, 2003). In contrast, Oh *et al* (2006) reported that defense-related gene expression in tobacco plants (*Nicotiana tabacum*) inoculated with the *Tobacco mosaic virus*-TMV (*R-Avr* gene interaction) was delayed compared to tobacco plants challenged with the non-host bacterial pathogens *P. syringae* pv. *syringae* 61 (*Pss*61), *P. syringae* pv. *phaseolicola* NPS3121 (*Psp*NP3121), and *Xanthomonas axonopodis* pv. *glycines* 8ra (*Xag*8ra). Expression of most defense-related genes induced during *R*-gene mediated resistance was activated at 48 hai with TMV; the same genes were upregulated as early as 9 hai with *Pss*61, *Psp*NP3121, and *Xag*8ra. In this study, Oh and co-workers also characterized Type I (no visible cell death) and Type II (hypersensitive response) non-host resistances by determining expression profiles of previously reported pathogenesis-related protein genes (*PR protein-1a, acidic β-1,3-glucanase, acidic chitinase, PR protein-4b* or *hevein like protein, Osmotin-like protein* and *SAR8.2*) and nonhost-related or cell death-related genes [*N. glutinosa*-cell death marker1 (*Ng-CDM1*), *N. tabacum*-harpin induced 1 (*Nt-hin1*), and *N. tabacum*-hypersensitive response related 203J (*Nt-hsr203J*)]. According to an earlier hypothesis, incompatible pathogens must induce a hypersensitive response (HR) in a non-host plant; however, it has been shown that some non-pathogenic bacteria fail to induce such a response in a non-host plant. Inoculation of tobacco with *Psp*NPS3121 and *Pss*61 induced strong HR at 24 hai; in contrast, *Xag*8ra induced no visible response at all. Both *Psp*NPS3121 and *Pss*61, as well as *Xag*8ra induced the expression of defense related genes. There was a high degree of similarity in expression of *PR protein-1a* and *acidic chitinase* between tissues inoculated with *Psp*NPS3121 and *Xag*8ra, suggesting that the plants inoculated with *Xag*8ra are responding to the pathogens without producing HR. It was proposed that Type I non-host resistance is an evolutionarily older defense mechanism than Type II non-host resistance, or gene-for-gene resistance.

Plants expressing the Type II non-host resistance (hypersensitive response) require a more coordinated group of proteins for recognition of specific bacterial effectors; once the pathogen has been recognized, the plant initiates several downstream signaling pathways that result in a HR phenotype. The expression of *Nt-hsr203J* and *Nt-hin1* might be considered as

indicators for differentiating between host and non-host resistance. These genes were highly induced from 48 to 72 hai with TMV. In contrast, inoculation with Pss61, *Psp*NPS3121, or *Xag*8ra induced their expression at 3 to 6 hai. On the other hand, *Nt-hsr203J* expression was reduced by 12 hai in *Pss*61 and *Kag*8ra-inoculated plants, but remained at high levels with *Psp*NPS3121 (24-48 hai). The expression pattern of *Ng-CDM1* was originally identified as an important indicator of HR-induced cell death, because only the Type II non-host resistance pathogens (*Pss*61 and *Psp*NPS3121) induced its expression.

So far, we presented two non-host interaction examples where bacteria are the microorganisms involved; obviously, if we do an extensive literature review we will find several other examples. What about fungi? How much do we know about non-host interactions with these microorganisms, specifically with biotrophic ones? Since biotrophic fungal pathogens keep plant cells alive and minimize tissue damage in susceptible hosts (compatible interaction), they are considered good microbes for studying non-host resistance (Mellersh and Heath, 2003). Non-host resistance to biotrophic fungal pathogens that penetrate the host cells directly is expressed as a penetration failure (Mellersh *et al*, 2002). The uredial stage of many rust fungi is established by penetrating the epidermal tissue through stomata; therefore, it has been suggested that compatibility with the host species requires the ability to avoid prehaustorial defenses within the substomatal cavity, breach the mesophyll cell walls to form the first haustorium, and establish a biotrophic relationship with the living plant cells to obtain nutrition and maintain growth (Heath, 1981 in Mellersh *et al*, 2002). Certainly, studies comparing host and non-host resistance to rust fungi showed that non-host resistance is expressed before the formation of the first haustorium. This resistance may involve a poor ability to locate and recognize stomata; but if the fungus reached the substomatal cavity, its growth is invariably restricted. In this case, fungal growth may be inhibited before the formation of a haustorial mother cell, or the haustorial mother cell may fail to penetrate the host cell. As in a gene-for-gene interaction, the common response of a non-host plant after the fungus formed the first haustorium is a hypersensitive reaction (HR) of the invaded cell, as was observed in tobacco and tomato plants inoculated with *Uromyces vignae*.

Magnaporthe oryzae and its non-host plants

Isolates of the *Magnaporthe grisea* sp. complex include pathogens of rice (*Oryza sativa*), barley (*Hordeum vulgare*), wheat (*Triticum aestivum*), maize (*Zea mays*), ryegrass (*Lolium* spp.), finger millet (*Eleusine coracana*), goosegrass (*Eleusine indica*), weeping lovegrass (*Eragrostis curvula*) and some non-typical hosts such as *Commelina* spp (Heath *et al*, 1990a, 1992; Jarosch *et al*, 1999; Zellerhoff *et al*, 2006). Like in many other plant-microbe systems, only some of these *Magnaporthe*-host interactions will result in disease; however, when disease occurs it becomes a serious problem to world agriculture. Like wheat and maize, rice is one of the most important food crops of the world; therefore rice blast disease has been the subject of extensive studies in order to identify novel strategies to achieve durable resistance. Significant advances have been made in order to understand the molecular bases of disease resistance in rice and in many other cereals. The majority of these studies have focused on single dominant genes with easily determined resistance phenotypes due to the relative simplicity in doing experiments, although there are still many questions that need to be answered. On the other hand, the molecular bases of non-host resistance remain unknown. Non-host resistance is highly effective and durable; therefore, genes involved in this phenomenon should be exploited to improve rice breeding programs (Heath, 2001; Neu *et al*, 2003; Thordal-Christensen, 2003; Zellerhoff *et al*, 2006).

Fungal invasion of resistant or susceptible rice plants is commonly associated with different growth patterns and plant responses that can be detected at the cytological level. In fact, cytological studies have been done since the 1930s in order to observe and understand the plant-fungus interface as well as to determine whether host cytological responses are correlated with the expression of genes associated with race-specific resistance. These cytological studies have been carried out by inoculating leaf blades (Koga and Kobayashi, 1980; Koga and Kobayashi, 1982 a-b; Peng and Shishiyama, 1988, 1989; Heath, *et al*, 1990) and leaf sheaths (Tomita and Yamanaka, 1983; Koga and Horino, 1984 a-b; Koga *et al*, 1994) of highly resistant, resistant, moderately resistant and susceptible rice plants (Table 3.1). Many of the cytological evaluations focused on identifying correlations between the expression of race-specific resistance and both the inhibition of specific stages of fungal development and plant cellular reactions at infection

sites, such as fine cytoplasmic granulation, coarse cytoplasmic granulation, and cell necrosis (Koga and Kobayashi, 1982 a-b; Tomita and Yamanaka, 1983). Cytological analysis results obtained from leaf blade and leaf sheath samples from susceptible and resistant rice plants indicated that the plant cell may have no reaction at all, or it may express cell wall discoloration (deep or light browning), granulation of cytoplasm (fine and coarse granulation), and/or necrosis. However, the cellular reactions that were most frequently correlated with race-specific resistance were fine cytoplasmic granulation or light brown cytoplasm together with callose deposition in the cell walls (Koga and Kobayashi, 1982 a-b; Koga, 1994; Tomita and Yamanaka, 1983).

As mentioned above, the first data to understand pathogenicity of *Magnaporthe* spp. and the basis of race-specific resistance were generated by detailed cytological analyses. However, these studies involved fungal development on artificial surfaces and plant cellular responses from fixed or clarified infected tissue, which are not the best experimental conditions to investigate fungal growth and the physiological reactions of host cells. Nowadays, the objective is to utilize conditions allowing *in planta* artificial infections of living tissues under conditions similar to those occurring under natural environments. One method to observe and study the infection process of *Magnaporthe* spp. in un-fixed tissues is inoculating the rice leaf sheaths. This method, which was first reported in 1949 (Sakamoto, 1949 in Koga *et al*, 2004), uses excised leaf sheaths and allows observing restriction of the invading hyphae by hypersensitive cell death in a blast resistant rice plant. This reaction corresponded to the symptoms induced on leaf blades inoculated with the fungus. However, it was observed that in an excised susceptible rice leaf sheath the invading hyphae develop rapidly and the host shows little reaction. This highly susceptible plant response did not correspond to symptoms observed in leaf blades, suggesting than an artificial effect is occurring in excised leaf sheaths of a susceptible plant. Moreover, excised leaf sheaths become yellowish by 3 days preventing the observation of the slow developing host cell reactions (Koga *et al*, 2004). Tomita and Yamanaka (1983a) reported a sliced-sheath inoculation method for continuous observation of 4 *M. oryzae* isolates (Ken 62-89, Ken 60-19, Ken 54-04, and F 67-54) inoculated individually on 3 rice cultivars (Shimokita, Kusabue, and Fukuyuki). The sliced-sheath inoculation method, unlike the leaf sheath one, uses the inner epidermal (adaxial epidermis) tissue of the leaf sheaths. Lysigenous aerenchyma and vascular bundles are completely removed from the sheath, and the fungal suspension is

inoculated directly on the "naked" epidermal layer. However, fungal growth in all the rice-fungus combinations was slower and less biomass accumulated relative to the non-sliced leaf sheaths; and no plant cellular responses were reported. It was suggested the fungal growth pattern observed in this experiment could be due to physiological changes in sheath cells resulting from their dissection from the plant. Recently, Koga and co-workers (2004) published a novel inoculation method of *M. oryzae* that utilizes sheaths of leaves that have been removed intact from the rice plants (Intact Method). By using this method, both the fungal growth and epidermal cell responses were successfully observed in susceptible and resistant rice plants over a period of 5 days.

To this point, we have presented data associated with resistance responses expressed in an incompatible interaction where the rice plant is the host for the rice blast pathogen. However, there are not many cytological studies about the defense mechanisms involved in non-host interactions between rice and a non-host microbe. So far, Heath *et al* (1990a) reported a microscopical analysis of a non-host interaction between rice (cultivar M201) and the *M. grisea* strain 4091-5-8, which, in contrast, establishes a highly compatible interaction with weeping lovegrass and a low to moderately compatible interaction with goosegrass. According to this study, the fungus never spread from the initially penetrated leaf epidermal cells, and as reported previously in the major gene resistance interactions, the epidermal cells also responded rapidly by developing a granular cytoplasm, and discoloration or autofluorescence of cell walls. This response reported by Heath *et al,* (1990a) resembles a classical gene-for-gene type of HR response. The strain 4091-5-8 appears to carry the major avirulence gene *AVR1-M201*, which determines specific avirulence on the rice cultivar M201 (Valent *et al,* 1991). If this statement is correct, the data by Heath and co-workers did not explain whether the incompatibility of 4091-5-8 on rice M201 is due to the action of a gene-for-gene interaction, the action of minor pathogenicity genes, or to the combination of both mechanisms.

Previous studies in our laboratory focused on the excised leaf sheath assay for cellular and molecular analyses of fully susceptible biotrophic interactions (Kankanala *et al,* 2007; Mosquera *et al*, submitted). For this chapter, we proposed to study the relationship between fungal penetration and cytological responses of living leaf sheath epidermal cells by comparing

responses in a susceptible, a resistant, and a non-host interaction (Table 3.2). All three interactions were compared in excised and in intact sheath tissue. For the non-host interaction, we focused on *M. oryzae* strain 4091-5-8 on rice cultivar Yashiro-mochi (Ya-mo), which showed a unique cytological response in invaded rice cells from excised sheaths in our preliminary experiments. Yashiro-mochi has the dominant *Pi-ta* resistance gene, and 4091-5-8 does not have its corresponding avirulence gene (*AVR-Pita*). For susceptible and resistant interactions, we chose rice pathogen strains KV11 (*avr-pita*$^{-}$) and KV1 (*AVR-Pita*), respectively. We report here that the cytological basis for the non-host interaction differs from the cytological basis for the resistance response mediated by the *Pi-ta* resistance gene. We also showed that excision of leaf sheath segments from the intact plant alters the cytological responses of the host to pathogen invasion, especially in the resistant and non-host interactions. These results have major implications for future studies using live cell imaging of sheath tissue to investigate race-specific and non-host resistance mechanisms.

RESULTS

Magnaporthe oryzae laboratory strain 4091-5-8 infects weeping lovegrass, goosegrass, and barley, but not rice (Valent et al. 1991). Our objective was to identify the host cellular responses that could be correlated with host species specificity in the 4091-5-8 strain. In order to facilitate observation of fungal growth in living rice epidermal cells, we transformed the 4091-5-8 strain with enhanced yellow fluorescent protein (eYFP), which was expressed constitutively in the fungal cytoplasm. Subsequently, we spray-inoculated barley plants in order to corroborate pathogenicity of the transformed 4091-5-8 strain, which will be referred to from now on as KV33. Barley plants were inoculated independently as described by Valent *et al* (1991) by using a $1x10^5$ spore/mL suspension. Ya-mo plants were also inoculated individually with spore suspensions containing $1x10^5$, $1x10^4$, and $5x10^3$ spores/mL. As expected, strain KV33 infected barley, but not Yashiro-mochi plants (Figure 3-1). Barley leaf blades showed small eye-spot lesions with gray centers surrounded by dark margins, resembling lesions types 3 and 4 according to the scale established by Valent *et al*, (1991). Thus, our transformed strain maintained the expected host specificity.

In a preliminary assay, we independently inoculated excised Yashiro-mochi leaf sheaths with KV1, KV11, and KV33 strains to evaluate percentage of spore germination and percentage of appressorial formation. According to the conditions under which the assay was carried out, the highest percentage of spore germination occurred at 6 hai (Figure 3-2); at this time some of the germ tubes had developed melanized appressoria as well, but the highest percentage of appressorium formation was observed between 12 and 14 hai (Figure 3-2).

Excised leaf sheath inoculation

Fungal development

At 24-27 hai (Figure 3-3A), strain KV11 (compatible interaction) had developed appressoria (A) at 20% of the infection sites, primary hyphae (PH) at 20% of infection sites, and bulbous invasive hyphae (BIH) at 59% of infection sites. Strain KV1 (incompatible interaction) had developed appressoria (A) at 1% of the infection sites, primary hyphae (PH) at 6% of infection sites, and filamentous invasive hyphae (FIH) at 92% of infection sites. Strain KV33 (non-host interaction) had developed appressoria (A) at 65% of the infection sites, primary hyphae (PH) at 32% of infection sites, and filamentous invasive hyphae (FIH) at 3% of infection sites. Already, a major difference was apparent between the compatible and the incompatible interactions. KV11 had formed the beaded bulbous invasive hyphae that characterize the fully susceptible interaction, but KV1 was growing poorly as thin filamentous hyphae that never differentiated into BIH. Major differences also had occurred between the incompatible and non-host interactions. Whereas KV33 grew at the filamentous invasive stage in 3% of the host cells, KV1 did in 92% of the infection sites.

At 37 to 38 hai (Figure 3-3B), 87% of the first-invaded cells from leaf sheaths inoculated with compatible KV11 contained bulbous invasive hyphae that had begun moving into neighboring cells. On the other hand, in 85% of the cells, the incompatible KV1 thin filamentous hyphae had developed a few branches that moved into a second cell. At 39 hai, non-host KV33 fungal growth had practically stopped; the fungus still appeared as appressoria in 48% of the

infection sites, and as primary hyphae in 52% of the invaded cells (Figure 3-3B). Clearly, KV33 growth was blocked at an earlier stage than KV1, which could grow as FIH before stopping.

Leaf sheath epidermal cell reactions

As reported previously in other studies (Peng and Shishiyama, 1988; Heath *et al*, 1990), some invaded epidermal cells did not show any visible response at 24 hai, which correlates with our data. We observed that at 24 hai the highest percentage of non-visible responses was shown in leaf sheaths inoculated with KV11 (compatible interaction) (Figure 3-5A). On the other hand, epidermal cells from leaf sheaths inoculated with KV1 (incompatible interaction) or KV33 (non-host interaction), responded with cytoplasmic disorganization and aggregations around the appressoria, which were maintained at a high percentage, even during late infection periods (Figure 3-5B). These data agree with results obtained from microscopical studies of compatible and incompatible interactions in rice leaf blades (Peng and Shishiyama, 1988; Heath *et al*, 1990), rice leaf sheaths (Koga and Kobayashi, 1982 a-b; Koga, 1994), and sliced leaf sheaths (Tomita and Yamanaka, 1983) challenged with *Magnaporthe* spp.

The cytoplasmic disorganization response was divided into three groups (Figure 3-4): the first one (CR1) was characterized by the presence of fine and irregular granular material; the second (CR2) by coarse cytoplasmic granulation and the presence of spherical or globular brown bodies (globules) suggesting a polyphenolic composition; and the last one (CR3) by disorganization and/or fragmentation of the plant plasma membrane. In order to facilitate quantification of these responses, we referred to them as CR alone.

At 24 and 36 hai (Figure 3-5A-B), the CR response was observed in 63 and 93% of the epidermal cells inoculated with KV1, respectively. In contrast, the CR response was delayed for about 12-14 hours in the compatible (KV11) and non-host interactions, which agrees with studies done with leaf blades and leaf sheaths of susceptible and resistant interactions (Koga and Kobayashi, 1982 a-b; Tomita and Yamanaka, 1983; Peng and Shishiyama, 1988).

Aggregations around appressoria are, so far, structures of unknown chemical composition that look like fine spherical or irregular granules, or like needle-shaped crystals (Figures 3-4 and 3-6). Such an impressive cell response has not been reported previously and appeared to completely block fungal growth (Figure 3-8). At 24 and 36 hai, the percentage of cells showing AA was much higher in leaf sheaths inoculated with KV33 relative to those inoculated with KV11 or KV1 (Figure 3-5A-B). Initially we speculated that the aggregations were formed by the plant plasma membrane; so, to investigate this assumption we plasmolyzed previously infected epidermal tissue using a 0.75 M sucrose solution. If the plasma membrane was involved in the AA organization, we would not expect to see AA after challenging the cells with the sucrose solution; however, after plasmolysis some appressoria were enclosed by those aggregates and the protoplast moved away from the plant cell wall (Figure 3-6).

Relationship between fungal growth and type of epidermal cell reaction

At 24 hai, 84% of the epidermal leaf sheath cells invaded with KV11 did not show any visible response, which allowed KV11 to grow as bulbous invasive hypha (BIH) in 59% of the infected cells (Figures 3-3A and 3-5A). In the incompatible interaction (KV1), 37% of the epidermal cells remained without any visible reaction, but 63% of them showed the CR response. KV1 was growing inside more than 90% of the invaded epidermal cells; however its growth was reduced to thin filamentous invasive hypha (FIH), which might be correlated with the high frequency of cytoplasmic reactions. As mentioned, KV33 appressoria co-localized with plant-cell aggregations at 65% of the infection sites, which probably explains why appressoria failed to maintain further growth.

At 36 hai, KV11 was growing as bulbous invasive hyphae that moved to neighboring epidermal cells at 87% of the invaded sites. (Figures 3-3B and 3-5B). KV11 could clearly continue growing and invading neighboring cells even though the first infected cells had responded with CR. The KV1 strain continued to grow as FIH and to move to neighbor cells, even in those ones that had previously showed the CR response.

The maximum stage of development reached by KV1 was filamentous invasive hyphae that moved to the neighboring cells (85%). The percentage of epidermal cells that showed the CR type reaction was similar between the compatible (KV11) and incompatible (KV1) interactions; however, the response occurred at least 12 hours earlier in the incompatible interaction, so KV1 failed to thrive.

At 24 hai, KV33 (non-host interaction) had developed appressoria at 65% of the infection sites and primary hypha at 32% of these sites (Figure 3-3A). This fungus-leaf sheath interaction resulted in the induction of aggregations of unknown composition around the appressoria. This response was maintained for about 12 hours more together with the CR (Figure 3-5 A-B), which was probably associated with the poor growth of KV33, which was practically blocked at the appressorial and primary hyphal stages.

Intact leaf sheath inoculation

Fungal development

At 24 hai, KV11 (compatible interaction), KV1 (incompatible interaction), and KV33 (non-host interaction) grew to the appressorial stage in 84, 44, and 68% of the epidermal cells, respectively (Figure 3-7A). In all the plant-fungus interactions, none of the epidermal cells showed much fungal growth beyond the appressorial stage. Strains KV11, KV1, and KV33 had developed primary hyphae at 15, 18 and 31% of the infection sites, respectively; and only KV1 had grown to the filamentous invasive hyphal stage at 37% of the sites.

At 36 hai, the highest percentage of epidermal cells with fungal growth still at the appressorial stage was observed in leaf sheaths inoculated with KV33 (Figure 3-7B). Only 22% of the cells showed appressoria with a short primary hypha and 10% showed filamentous invasive hypha. At this stage of development, fungal growth appeared completely stopped; the fungus did not move into the next cell and did not differentiate into a bulbous invasive hypha. In contrast, in 70% of the epidermal cells infected with KV11, the fungus grew bulbously, filled the cells, and began moving into the neighboring ones.

Leaf sheath epidermal cell reactions

In this experiment, the plant cellular responses observed more frequently were cytoplasmic responses (CR) and mixed reactions (MR). The MR response was characterized by the expression, in the same cell, of cell wall and/or cytoplasmic discoloration with cytoplasmic reactions and/or aggregations around the appressoria (Figure 3-4)

At 24 hai (Figure 3-8A), 97, 69, and 78% of the cells inoculated individually with KV11 (compatible interaction), KV1 (incompatible interaction), or KV33 (non-host interaction) had not developed any visible response. However, the CR was the highest response induced in leaf sheaths challenged with KV1 and KV33.

At 36 hai (Figure 3-8B), 71% of the leaf sheath cells inoculated with KV1 responded with the CR reaction; in contrast, only 2.5 % of the cells did in plants inoculated with KV11 ($Pr > 0.05$), and 15% in plants inoculated with KV33 ($Pr > 0.05$). A high percentage of epidermal cells (60%) from plants inoculated with KV33 showed the MR reaction. In contrast, CR response was significantly different in plants challenged with KV1 (17%) ($Pr > 0.05$) and completely blocked in plants inoculated with KV11 (0%) ($Pr > 0.05$).

Aggregations around the appressoria (AA) were observed in 2% of the cells in intact leaf sheaths inoculated with KV1 and in 1% in those inoculated with KV33. This rare occurrence of the AA response in the intact leaf sheaths inoculated with KV33 contrasts with the results in excised sheaths, in which more than 60 % of the invaded cells showed AA (Figure 3-5A-B).

Relationship between fungal growth and type of epidermal cell reaction

At 24 hai (Figures 3-7A and 3-8A), 97% of the epidermal leaf sheath cells inoculated with KV11 did not show any visible response, and in about 84% of the cells KV11 had developed to the appressorial stage. However, the fungus grew slowly compared to the other two interactions: only 15% of the cells had developed to the primary invasive hyphal stage. At 36 hai, most invaded cells still showed no visible defense mechanisms, but still the fungus grew slowly. Even though the fungus had developed bulbous invasive hyphae in 70% of the epidermal cells, only a few cells displayed bulbous invasive hyphae that had moved to the neighboring cells. These data showed a high delay in KV11 fungal growth in intact leaf sheaths compared to the excised ones.

Between 24 and 36 hai (Figures 3-7A-B and 3-8A-B), KV1 (incompatible interaction) had grown slowly. The fungus displayed a continuous array of developmental stages with the exception of the bulbous invasive hypha, which is associated with the highly susceptible interaction. At 36 hai, no more than 40% of the cells displayed the filamentous invasive hyphal stage, and only in 15% had KV1 started invading new cells. This could be partially correlated with the CR response that was expressed at 24 hai in 29% of the cells and increased until 71% at 36 hai.

At 24 hai (Figures 3-7A-B and 3-8A-B), KV33 (non-host system) reached the appressorial stage in more than 60% of the epidermal cells, and it reached the filamentous invasive hyphal stage in only 31% of them. At 36 hai, no further growth was observed; the fungus stopped growing practically at the appressorial stage. We assume that this earlier blockage in the fungal growth was partially associated with the CR response and with the presence of mixed responses that were expressed in 60% of the plant cells.

Together, these data indicate that the KV11 (compatible interaction) and KV1 (incompatible interaction) grew more slowly and less extensively compared to fungal behavior in the leaf sheaths inoculated by the excised leaf sheath method. The visible plant cellular reactions associated with non-host resistance were quite different in the intact and excised sheath assays.

Other epidermal cell responses

Additional plant cell responses observed in this study were the induction of crystal-like bodies within the plant cytoplasm, nuclear migration toward penetration sites, papilla formation, browning of the plant cell wall, and cytoplasmic discoloration (Figures 3-4 and 3-6).

Occurrence of the crystal-like bodies was an infrequently induced response in all the interactions evaluated, but was more commonly observed in leaf sheaths inoculated with KV1. We did not quantify the proportion of cells expressing this reaction, so we do not have statistical data to support that its induction was much higher in the rice-KV1 resistant interaction.

Nuclear migration toward penetration sites and papilla formation were other types of responses observed in this study. At 24 hai, nuclear migration toward penetration sites was not noticed either in epidermal cells from leaf sheaths inoculated with KV11 (compatible interaction) or in those inoculated with KV33 (non-host interaction). At 36 hai, only 1.5, 1.7, and 2% of the epidermal cells from plants inoculated with KV11, KV1, and KV33, respectively, had a visible nucleus associated with the penetration site (Figure 3-6). To further investigate if the nucleus was associated with appressoria, dissected epidermal leaf sheaths were stained with coomassie brilliant blue. Nuclei stained blue; however, because coomassie blue is not a specific dye for DNA, we partially confirmed that plant nuclei moved toward penetration sites.

As mentioned before, formation of papilla is a defense response associated with the reinforcement of plant cell walls once the pathogen and the host epidermal cell have been in contact (Agrios, 1997; Hückelhoven, 2007). In our study, we rarely observed this reaction in leaf sheaths inoculated with KV33 (Figure 3-9), which agrees with data reported by Heath *et al* (1990 a) where papilla formation was induced at a low frequency in rice plants inoculated with the 4091-5-8 strain (non-host interaction).

Plant cell walls from compatible interactions (weeping lovegrass + 4091-5-8 and rice + 0-42) did not form papillae. These data did not agree with the Koga (1994) study which showed papilla formation in living cells of susceptible interactions.

Browning of the plant cell wall and cytoplasmic discolorations are epidermal cell responses that have been commonly observed in rice-*Magnaporthe* interactions. In this study we observed that at 24 hai (Figure 3-5A-B), browning of the epidermal cell walls occurred in 15% of the leaf sheath cells from excised tissue inoculated with KV11 (compatible interaction), at 1% in those inoculated with KV1 (incompatible interaction) and at 5% in leaf sheaths inoculated with KV33 (non-host interaction). Twelve hours later (Figure 3-7A), only 7% of the epidermal cells challenged with KV1 displayed the browning cell wall response. On the other hand, at 24 hai, only 4% of the epidermal cells inoculated with KV33 by the intact leaf sheath method showed the browning cell wall response. Additionally, at 36 hai, 6% of the epidermal cells challenged with KV11 and 4% challenged with KV33 showed a light brown cytoplasmic response.

DISCUSSION

The present study was set up to provide data regarding the cytological relationship between fungal penetration and cellular reactions of epidermal leaf sheaths by comparing responses in susceptible (Ya-mo+KV11), resistant (Ya-mo+KV1), and non-host (Ya-mo+KV33) interactions. Additionally, we looked for any correlation between plant cell responses and species specific resistance.

Spore germination and development of appressoria

Plant epidermal tissue is the first surface that the pathogen has to confront to initiate the disease cycle; therefore preformed structural and/or chemical defenses play an important role in protecting the plant from pathogen infection. In this study we observed that the percentage of spore germination in the compatible strain KV11 was lower than in the other two interactions (incompatible KV1 and non-host KV33). We did not observe any visible response during this stage of the fungal development that could account for this difference.

With respect to appressorium formation, we did not observe any significant difference among the interactions evaluated. Based on these data, we infer that the recognition phase involved in the differentiation of the germ tube tip into an appressorium occurred under optimal conditions. We also speculate that at this time of the disease cycle it is improbable that the expression of any defense mechanism can inhibit the pre-penetration development of *M. oryzae*. This result agrees with data reported by Peng and Shishiyama (Peng, 1988) studying appressorium formation in highly resistant, resistant, and susceptible interactions.

Penetration

Penetration pegs were not observed in this study due to the resolution of the light microscope; but in an electron microscopic study, Koga (1994), inoculating leaf sheaths of compatible and incompatible lines of rice, reported that microfibrils of the compatible host cell wall around penetration pegs were disorganized and electron dense compared to the regular pattern observed in non-penetrated ones. Host cell cytoplasm did not show any change while the penetration pegs were passing through the cuticle, but when they reached the cell wall, appositions or papillae were formed between the host cell wall and the plasma membrane. In contrast, epidermal cells from inoculated resistant plants did not show papilla formation at the penetration site. These results differed with data reported by Heath *et al*, (1990a), where they did not observe papilla formation in highly susceptible rice leaf blades inoculated with the strain O-42, but did in the non-host interaction between rice (M201) and the strain 4091-5-8. Our data did not allow us to establish any conclusion about the induction of papilla in the interactions evaluated. We observed spherical structures associated with the epidermal cell wall, but we did not see any sign of the fungus at these locations. In addition, some times it was not possible to distinguish the papilla from the plant cell nucleus, even though the samples were stained with coomassie blue.

Comparison of epidermal plant cell responses and fungal development between excised and intact rice leaf sheaths inoculated with KV11 strain (compatible interaction)

At 24 hai, a high ratio of epidermal cells from excised leaf sheaths inoculated with the compatible strain KV11 (compatible interaction) showed bulbous invasive hyphae as the most advanced stage of the fungal development. Since at this time 80% of the host epidermal cells did not show any visible defense response, it appeared that KV11 had time enough to grow well and begin invade the neighboring epidermal cells, which was confirmed in leaf sheaths evaluated at 36 hai. At this time and even though 90% of the cells responded with the cytoplasmic reaction, more than 80% showed healthy bulbous invasive hyphae moving to the neighboring cells. Cytoplasmic reactions were delayed for at least 12 hours; so the presence of granular material did not have any effect in KV11 fungal development. These observations are in agreement with previous studies in our laboratory, which focused on the excised leaf sheath assay for cellular and molecular analyses of fully susceptible biotrophic interactions (Kankanala *et al,* 2007; Mosquera *et al*, submitted).

Epidermal cells from the intact leaf sheath assay showed all the spectrum of fungal development stages as well as some of the plant cell responses described in the excised leaf sheath assay. However, fungal growth was slower in the epidermal cells from intact leaf sheath assay than in those from the excised leaf sheath experiment; and a much higher percentage of cells from the intact leaf sheath experiment showed no-visible responses compared to the cells from the excised leaf sheath assay.

Excised leaf sheaths were subject to double damage. The first one was generated mechanically by cutting the leaf sheaths into about 6.5 cm fragments, and the second one by inoculating the pathogenic KV11 fungal strain. On the other hand, intact leaf sheaths were apparently subject to a single mechanical damage that was generated during its dissection from the rice plant. We assume the mechanical damage caused in the excised leaf sheaths pre-induced plant cell defense mechanisms that were highly magnified by the presence of the biotic stress, the KV11 fungus. It is important to point it out that the defense responses induced by the fungus were not observed in epidermal leaf sheath cells mock inoculated by the excised or the intact method.

Comparison of epidermal plant cell responses and fungal development between excised and intact rice leaf sheaths inoculated with KV1 strain (incompatible interaction)

We did not have enough data to establish a statistical analysis in KV1 growth and plant cell responses between the excised and the intact leaf sheath methodologies; however, remarkable differences were observed, principally at the filamentous invasive hyphal stage. At 24 hai, the incompatible strain KV1 stopped at the appressorial stage in 44% of the cells inoculated using the intact method, but it did so in only 1% of the cells inoculated using the excised one. These results differ from data reported by Koga *et al* (2004). In this study Koga and co-workers observed no significant differences at the appressorial stage in an incompatible interaction evaluated with intact and excised leaf sheath assays. At this same time, KV1 showed the filamentous invasive hypha as the more advanced stage of development in about 90% of the epidermal cells from excised leaf sheath assays. In contrast, the fungus reached the same stage in only 37% of the cells from intact leaf sheaths.

At 36 hai, KV1 grew in excised leaf sheath epidermal cells as thin filamentous invasive hyphae that never differentiated into a bulbous stage; instead, the hyphae branched rarely and moved into the next cells. The fungus grew faster and invaded several cells, but its hyphae did not appear healthy and were not able differentiate into the bulbous invasive hypha that characterize the highly susceptible interaction. These observations correlate with Heath *et al*, (1990 a), where it was observed that lack of invasive hypha differentiation into a bulbous one is inversely correlated with successful infection. On the other hand, in intact leaf sheath cells, KV1 started moving to neighboring epidermal cells as thin filamentous hyphae in 28% of host cells, and it formed apparently healthy bulbous invasive hyphae that moved to neighboring cells in 18% of host cells.

The low level of differentiation into a healthy bulbous invasive hypha might be associated to the extensive CR reaction exhibited by the invaded epidermal cells. As mentioned, the CR reaction observed in this study was characterized by the presence of fine and/or coarse granular material, globular particles that resemble tannins, and fragmentation or disorganization of the plant cytoplasm. This cytoplasmic granulation has been considered a typical response that

precedes the hypersensitive reaction (HR) in incompatible rice-*Magnaporthe* interactions. In cells showing the HR, the host plasma membrane is broken, the host nucleus is degraded, and cell organelles collapse. Debris and vesicles derived from these responses appear as granular material under light microscopy (Koga, 1994). In a highly resistant interaction (based on the major gene-for-gene model) between rice and *M. oryzae*, it was reported that fine particles were rapidly observed after penetration of the epidermal leaf sheath cells. The infection hyphae did not grow further and the finely granulated cells became pale yellow or slightly brown throughout the cell. Generally these cells did not become deeply brown. It was suggested that the appearance of cytoplasmic granulation was associated with suppression of fungal growth and the infection hyphae extended very slowly into the surrounding cells (Tomita, 1983b).

According to our microscopic observations, the CR response induced in the interactions evaluated resembled the cytoplasmic granulations reported by Koga and Kobayashi (1982a-b), Tomita and Yamanaka (1983a-b), and Koga (1994). The CR response occurred at a high percentage of the infection sites at 24 hai, so at 36 hai the host cells had displayed a much more severe reaction.

Kankanala *et al*, (2007) reported that the bulbous invasive hyphae of KV1 infecting epidermal cells of YT16 leaf sheaths (compatible interaction) are enclosed by a plant membrane [extra-invasive hyphal membrane (EIHM)], which could be required to obtain the nutrients from the plant. If the granular material observed in our study resulted from plant and nucleus membrane disruption, and the EIHM has its origin in a plant membrane, we assume that the absence of the EIHM could account for the thin invasive hyphal growth. We did not observe clearly whether or not the invasive hypha grew to the mesophyll cells, but Heath *et al*, (1990a) observed that when the primary hypha grew without differentiating into a bulbous one, the invaded cell died rapidly and the hypha moved to the mesophyll rather than to the other epidermal cells.

In another study, Koga and Kobayashi (1982a-b), suggested that cytoplasmic granulation of plant epidermal cells correlates with the expression of specific resistance resulting in the inhibition of fungal penetration and growth of the infection hypha. In contrast, Peng and

Shishiyama (1988) inferred that the expression of race specific resistance of rice plants is associated with light browning and callose deposition in the epidermal cell wall that blocked infection hyphal development. Our data did not correlate with this assumption because the browning cell response was observed in a very low percentage of the epidermal cells at 24 and 36 hai. Our results correlate with those reported by Tomita and Yamanaka (1983); cell browning was observed in few cells and late in the disease cycle. Based on these data, we suggest that Ya-mo resistance might be explained by the presence of *AVR-Pita* in KV1 and the presence of *Pi-ta* resistance gene in the rice plant. Possibly this gene-for-gene interaction, together with other unknown defense mechanisms, and/or the expression of a basic immunity accelerate the cytoplasmic granulation response that result in inhibition of fungal growth.

Summarizing, the incompatible strain KV1 grew faster but appeared unhealthy in excised leaf sheaths. In contrast, it grew slowly and appeared healthier in intact leaf sheaths. These results do not agree at all with those reported by Koga *et al* (2004). They observed that in an incompatible interaction (rice *Pi-z*^{t} + Kita 1) the hyphal growth after 24 hours was restricted to invaded cells. In their study, cells that displayed the hypersensitive response increased from 70-76% at 24 hai to 86-90% in infections sites at 36 hai, regardless of the excision treatment. The rest of the infection sites had no hyphae, hyphal index 0 and no-host reactions. The differences between our study and theirs might be explained by the different *R* genes involved (*Pi-ta* versus *Pi-z*^{t}) or by differences in the physiological state of the plant tissue and the assay conditions.

Comparison of epidermal plant cell responses and fungal development between excised and intact rice leaf sheaths inoculated with KV33 strain (non-host interaction)

At 24 hai, the non-host strain KV33 differentiated into appressoria at about 60% of the excised and intact inoculated epidermal cells, and in about 30% of those treated with both inoculation methods, the fungus reached the primary hyphal stage. At 36 hai, KV33 had not shown further differentiation. In 48 and 52% of the excised inoculated cells, the fungus had stopped growing at the appressorium and primary hypha stages, respectively. In contrast, 67% of the intact leaf sheath cells displayed appressorial growth, 22% primary hyphae, and 10% filamentous invasive hyphae.

As mentioned previously, KV33 induced a remarkable response in the excised epidermal leaf sheath cells. This response was described as aggregations around the appressorium (AA) and, so far, it had not been described in previous cytological studies with the rice-*Magnaporthe* spp. system. We observed the AA reaction in 65 and 66% of the epidermal cells at 24 and 36 hai, respectively. In contrast, it was practically zero in cells inoculated by the intact method. Under the intact leaf sheath inoculation method, 60% of the cells responded with a mixed reaction at 36hai. This mixed reaction was characterized by the presence of granular material and/or fragmentation of the cytoplasm and plant membrane, together with the presence of aggregations around the appressoria.

Taking into account that the AA response was induced in more than 60% of the cells from excised leaf sheaths inoculated with the non-host pathogen KV33, we hypothesize that this response might be associated with non-host resistance. The KV33 strain has the *AVR1-YAMO* avirulence gene and the cultivar Ya-mo has the *Pi-ta* resistance gene. It is not known whether these two genes correspond to each other or whether *AVR1-YAMO* corresponds to another resistance gene in Ya-mo. If *AVR1-YAMO* interacts with *Pi-ta* and the interaction results in an AA response extensively displayed in the incompatible interaction (KV1) compared to the compatible one, we could assume that AA correlates with the expression of specific resistance in the KV33 + Ya-mo interaction. However, AA is not the classical HR response induced in a gene-for-gene interaction; in addition, we did not observe AA induction in the incompatible interaction between KV1 and Ya-mo; instead, the interaction between *AVR-Pita* and *Pi-ta* gene resulted in a rapid and extensive cytoplasmic granulation response that appeared to be more characteristic of the gene-for-gene interaction.

If we compared defense mechanisms induced in compatible (KV11) and incompatible (KV1) interactions, we could assume that independently of the inoculation method, the CR reactions are correlated with specific resistance because its expression was observed in both excised and intact leaf sheath cells inoculated with KV1 and KV11. Timing and extent of this defense response could account for the difference observed between the 2 interactions. CR was delayed and less extensive in the compatible interaction relative to the incompatible one. It is

important to point it out that we did not observe CR or AA responses in mock excised or intact inoculated leaf sheaths.

Based on our studies, we do not recommend the excised sheath inoculation procedure to compare the cytological and/or molecular bases of compatible, incompatible, and non-host interactions in the rice-*Magnaporthe* system. The intact leaf sheath inoculated method offers better conditions to study fungal growth in living host cells. In addition, the intact method maintains the leaf sheath tissue alive for longer periods, which allows studying reactions induced by the fungal pathogen and not by those induced by mechanical damage.

At this point, we observed major differences between the excised and the intact leaf sheath cells when inoculated with the non-host strain KV33. The excised method results suggest that the occurrence of AA could correlate with the expression of non-host resistance. However, data from intact leaf sheaths indicated that mixed reactions, including the presence of AA, account for the non-host resistance observed in 60% of the epidermal cells. Further studies are needed to understand and define the cytological responses associated with non-host interactions in rice-*Magnaporthe* interactions.

Future work

Rice is one of the most important crops together with maize and wheat, so any abiotic or biotic factor that affects their production deserves special attention. The rice blast system has been the subject of intense study, not only because of its importance as a serious disease at the world level, but also because rice and *Magnaporthe oryzae* are amenable to advanced experimental approaches including genetic analysis and genomics (Ebbole, 2007).

Knowledge of the genes that are responsible for the non-host resistance would improve the opportunities to breed resistant plants, and provide a better understanding about the cell biology and biochemical responses that are occurring at the rice cell-fungus interface. The

preliminary data presented in this study open many questions that must be addressed in future work.

KV33 is a non-host pathogen of rice that expresses the eYFP constitutively. The strain has the *AVR-M201, AVR-CO39* and the *AVR1-YAMO* genes; therefore, we might continue using this strain. However, we need to be sure the non-host rice lacks any corresponding resistance genes. A good candidate could be the YT16 cultivar, which has been recognized so far as the universal susceptible for all *M. oryzae* isolates (B. Valent, personal communication).

In future studies, we would focus on the intact assay and evaluate the epidermal tissue at least 12 hours earlier and at 48 hai. Next steps include use of highly specific fluorescent dyes for DNA (DAPI for instance) and plasma membrane localization. Results obtained from these analyses would allow understanding the origin of the aggregations around the appressoria as well as the role of the plant cell nucleus and plant plasma membrane at the infection sites. Another option would be to construct transgenic rice plants that express a reporter gene fused with a protein constitutively expressed in nuclei (histones) and plant plasma membranes (integrines). Microarray analysis of infected tissue from susceptible, resistant and non-host interactions would correlate phenotype with gene expression.

MATERIAL AND METHODS

Bacterial strain, fungal strains, and cultivar plants

The *Agrobacterium tumefaciens* strain (stored as pBV64) used in this experiment contains the binary vector SK1022 that carries the enhanced yellow fluorescent protein (eYFP) expressed with the *Cochliobolus heterostrophus* glyceraldehyde-3-phosphate dehydrogenase gene promoter. The hygromycin B resistance gene was used for fungal selection.

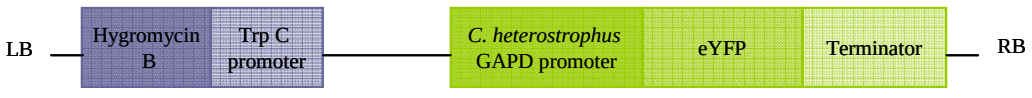

Magnaporthe grisea 4091-5-8 is a fertile laboratory strain obtained from a cross between a Japanese field isolated that infects weeping lovegrass [K76-79 (*Mat1-2*)] and a Japanese field isolate that infects finger millet and goosegrass [WGG-FA40 (*Mat1-1*)] (Valent *et al*, 1991). Strain 4091-5-8 is a pathogen of weeping lovegrass and goosegrass, but it does not produce visible symptoms on rice; it carries putative *AVR-M201*, *AVR-CO39* and *AVR1-YAMO* genes. KV1 was obtained by protoplast transformation of the *M. oryzae* field isolate 0-137 obtained from rice in China. The strain expresses the eYFP as well as the avirulence *AVR-Pita* gene (Kankanala *et al*, 2007). KV11 is also a laboratory strain obtained by *Agrobacterium tumefaciens*-mediated transformation of the *M. oryzae* field isolate Guy11 (0-391) obtained from rice in French Guiana (Mihwa Yi and B. Valent, unpublished).

Yashiro-mochi (Ya-mo) is a Japonica cultivar that carries the *Pi-ta* resistance gene. Seeds of the barley cultivar Garnet were obtained from The U. S. National Plant Germplasm System–NPGS (USDA, ARS National Small Grains Research Facility. National Small Grains Collection 1691 S 2700. W. Aberdeen, Idaho, United States, 83210).

Agrobacterium tumefaciens-mediated transformation of strain 4091-5-8

A. tumefaciens was cultured on LB-kanamycin (50 μg/mL) medium at 28°C for 2 days. INDUCTION: A single colony obtained from the culture was transferred into 5 mL of minimal medium containing kanamycin and cultured at 28°C in darkness with shaking (200 rpm) for 3 days. A 1 mL aliquot of the minimal medium culture was spun and resuspended in 1 mL of induction medium supplemented with kanamycin (50 μg/mL) and acetosyringone (100 mM). Then, the resuspended pellet was transferred into a 1.5 mL eppendorf tube with 4 mL of induction medium. The cells were cultured for 6.5 hours at 28°C under dark with shaking at 200 rpm. CO-CULTIVATION: The strain 4091-5-8 was grown on oatmeal agar plates at 24°C under continuous illumination in a Percival Scientific incubator Model CU-36L4. Conidia were harvested from 17 day old cultures using double distilled water. The concentration of the bacteria grown in induction medium was adjusted to 0.1 at OD_{600} and 1000 μL were mixed with an equal volume of a spore suspension of the strain 4091-5-8 ($1x10^6$ spores/mL). The bacteria-fungus mix

(200 and 100 μL) was plated on nitrocellulose membranes (Whatman® sterile membrane filters; 47 mm diameter and pore size 0.45 μm) on the co-cultivation medium with kanamycin (50 mg/mL) and acetosyringone (100 mM). Plates were incubated under dark conditions for 38 hours at 28°C. SELECTION: The nitrocellulose membranes were transferred onto TB3 agar medium (recipe) with hygromycin B (50 mg/mL) as the antibiotic for selecting fungal transformants, and with cefotaxime (200 mg/mL) as the agent to eliminate the *A. tumefaciens* bacterial cells. Plates were incubated under dark conditions at 24°C. After 6 days, the membranes were removed and the plates were incubated at 24°C for 2 days. Single colonies from the first selection were transferred onto TB3 medium containing hygromycin B and cefotaxime for a second selection. Plates were incubated under dark conditions at 24°C for 5 days.

Individual transformants were transferred into 24-well plates (COSTAR® Corning, Incorporated, Corning, NY) containing oatmeal agar and incubated at 24°C until conidiation. Single conidia from each transformant were isolated in order to ensure that the new strain was obtained from a single nucleus.

Intact leaf sheath inoculation method

The intact leaf sheath inoculation method was established according to Koga *et al*, (2004) with some modifications (Appendix A, Figure A-1.1). Briefly, 4 leaf sheaths from the sixth leaf of 28 to 30 day old Ya-mo rice plants were removed with the leaf blades and roots intact. Then, the leaf sheaths were laid horizontally in a 6.3 L plastic serving tray. To avoid movement of the leaf sheaths, they were held in place with 2 plastic ties placed at about 2 cm from the roots and blades. Each leaf sheath was individually inoculated from side to side by injecting ~5 mL of a $1x10^4$ spore/mL suspension of the KV1, KV11, or KV33 strains. The last complete leaf sheath was mock inoculated with double distilled water (control). Finally, the roots were covered with wet paper towels and the tray covered with clear plastic wrap to maintain high humidity. Leaf sheaths were incubated at room temperature.

For quantitative analysis of fungal development and plant cell responses, the samples were observed by DIC and fluorescent microscopy (see below) at 2 point times (24 and 36 hai). The experiment was performed three times. For each experiment one intact leaf sheath per treatment and time point was examined until at a minimum of 50 penetration sites (sites at which the fungus had developed appressoria) were found.

Each stage of fungal development (Appendix A, Figure A-1.2) [appressorium (A), penetration hypha (PH), filamentous invasive hypha (FIH), filamentous invasive hypha moving to next cells (FIH-M), bulbous invasive hypha (BIH), and bulbous invasive hypha moving to next cells (BIH-M)] and each type of epidermal leaf sheath cell response [no-visible reaction (NVR), brown cell wall (BCW), light brown cytoplasm (LBC), cytoplasmic reactions (CR), aggregation around the appressoria (AA), mixed reactions (MR), and nuclear migration toward penetration sites (NM)], was expressed as the percentage of the total number of infection sites having any fungal development stage and any of the plant cell reactions. Treatments were compared by using the Restricted Maximum Likelihood (REML) method in SAS. Data were normalized with an Arc-sine transformation.

Excised leaf sheath inoculation method

The sixth leaf sheaths from 28 to 30 day-old rice and barley plants were dissected into 6 to 7 cm length segments. Four segments from each species were laid horizontally over plastic ties adapted to hold them in Petri dishes containing wet paper towels to maintain high humidity (Appendix A, Figure A-1.1.). Leaf sheath segments were individually inoculated with each strain and incubated as described for the intact method. Quantitative analysis of fungal development and plant cell responses, were also analyzed by DIC and fluorescence microscopy at 24 and 36 hai. The experiment was performed only once. Four leaf sheaths segments per treatment and time point were examined at a minimum of 50 penetration sites.

Microscopy

Epidermal leaf sheath samples inoculated with *Magnaporthe oryzae* were dissected at 24 and 36 hours after inoculation (hai). Samples were mounted in double distilled water and examined by DIC imaging with an Axioplan 2 imaging microscope (Carl Zeiss, Germany). Cells were observed with an EC plan neofluar 20x objective and with a 63x C-Apochromat water-immersion objective. Images were acquired using a Zeiss AxioCam HRc camera and analyzed with Zeiss Axiovision digital image-processing software versions 3.1 and 4.6. Fluorescence of the EYFP protein was observed using a fluoArc lighting system and an YFP-specific filter (excitation 500 ± 20 nm, emission 535 ± 30 nm, filter set 46).

To assess the origin of the crystal-like bodies, the epidermal tissue from the infected leaf sheaths was dissected and plasmolyzed in a 0.75 M sucrose solution for 25-30 minutes. Later, the samples were mounted in the same sucrose solution and observed under the microscope. For identification of nuclei the epidermal tissue was dissected and stained with a 0.25% Coomassie brilliant blue R250 solution in 90 ml of a methanol: water (1:1 v/v) mix with 10 ml of glacial acetic acid. After 30-35 minutes, the samples were rinsed with a mix of methanol: water (1:1 v/v) and mounted in water for microscopy.

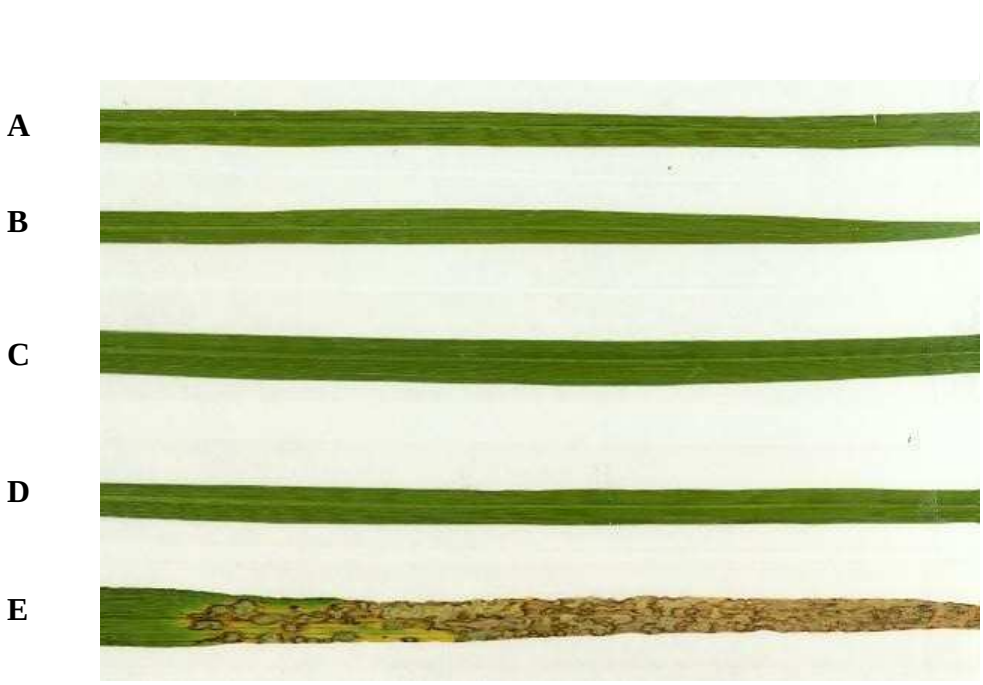

Figure 3-1. Barley and rice leaf blades inoculated with *M. oryzae* transformant KV33.
Ya-mo leaf blades were spray inoculated individually with spore suspensions at (A) $1x10^5$, (B) $1x10^4$, and (C) $5x10^3$ spores/mL. Ya-mo plants were inoculated with 0.25% gelatin solution as a control (D). Barley plants (E) were inoculated with a spore suspension at $1x10^5$ spore/mL. Symptoms resembled lesion types 3 and 4 according to the scale proposed by Valent *et al* (1991).

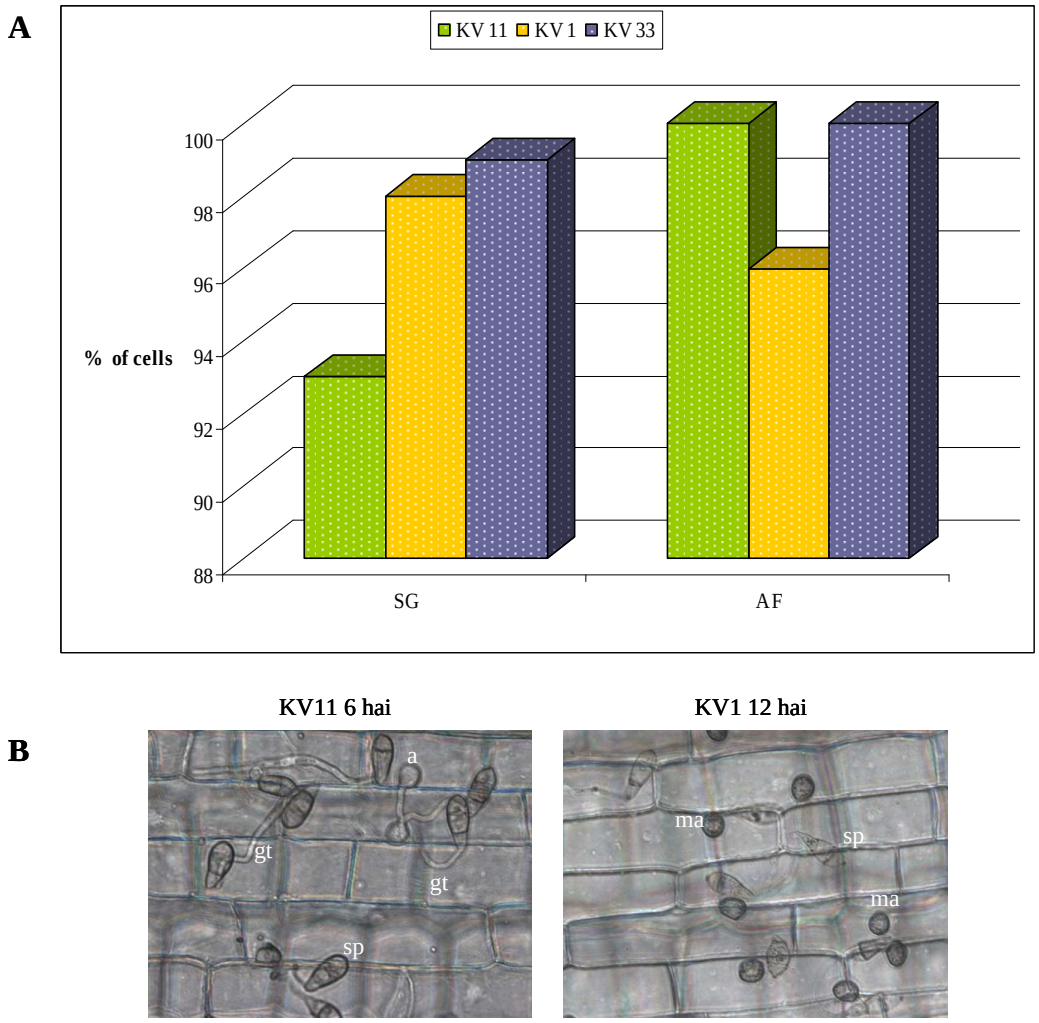

Figure 3-2. Spore germination (SG) and appressorial formation (AF) induced on Yashiro-mochi excised leaf sheaths.

Panel A shows the percentage of SG and AF on leaf sheaths inoculated with KV11, KV1, and KV33. The highest percentage of germination was observed at 6 hai together with differentiation of some appressoria (Panel B left). The highest percentage of melanized appressoria was quantified at 12 hai (Panel B right). **a**, appressoria; **ma**, melanized appressoria; **gt**, germ tube; **sp**, spore.

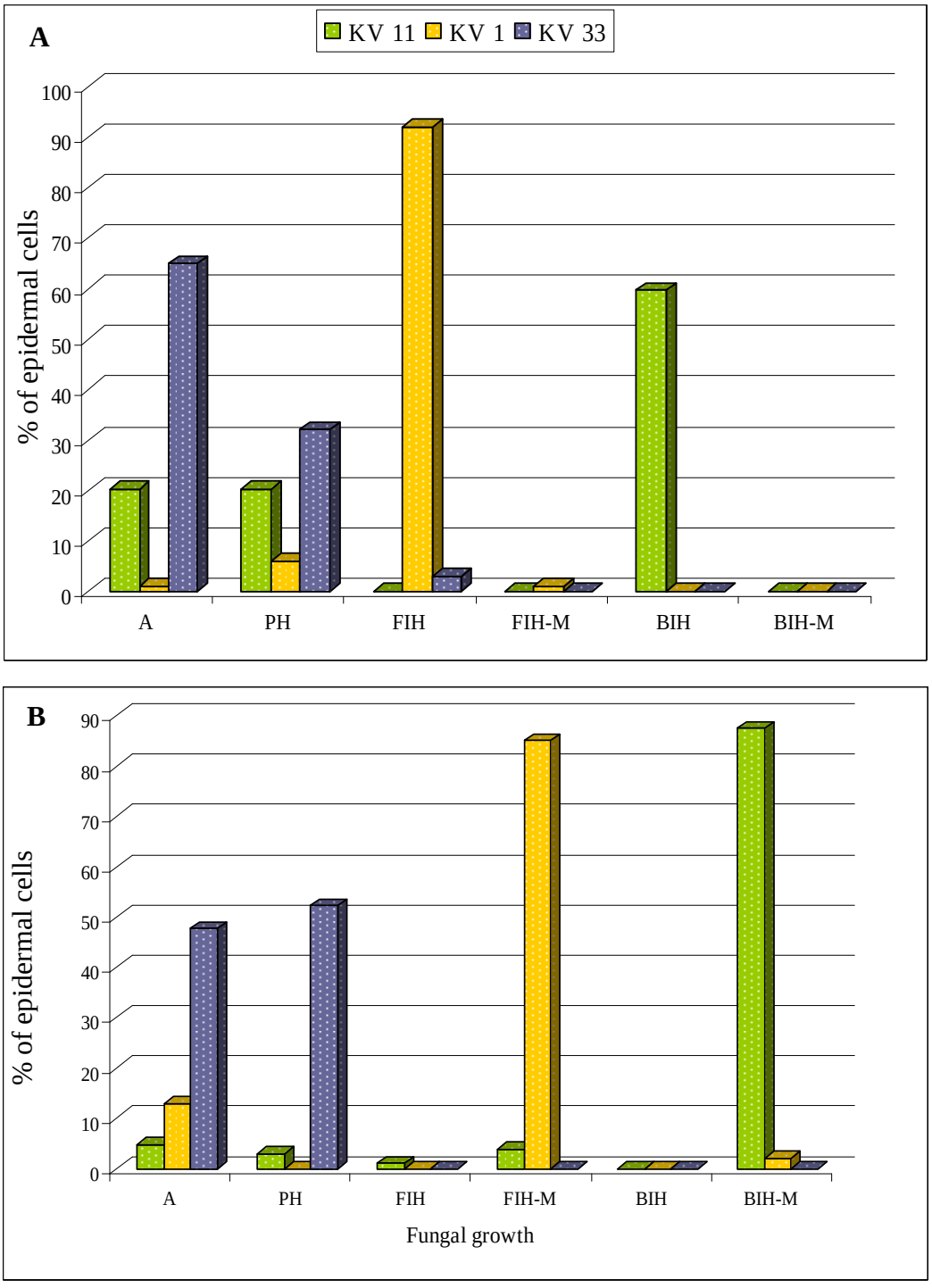

Figure 3-3. Percentage of epidermal cells showing fungal development in Yashiro-mochi excised leaf sheaths.

Panel A, 24-27 hai; Panel B, 36-39 hai. A, appressorium; PH, primary hypha; FIH, filamentous invasive hypha; FIH-M, filamentous invasive hypha moving to next cell; BIH, bulbous invasive hypha; BIH-M, bulbous invasive hypha moving to next cell.

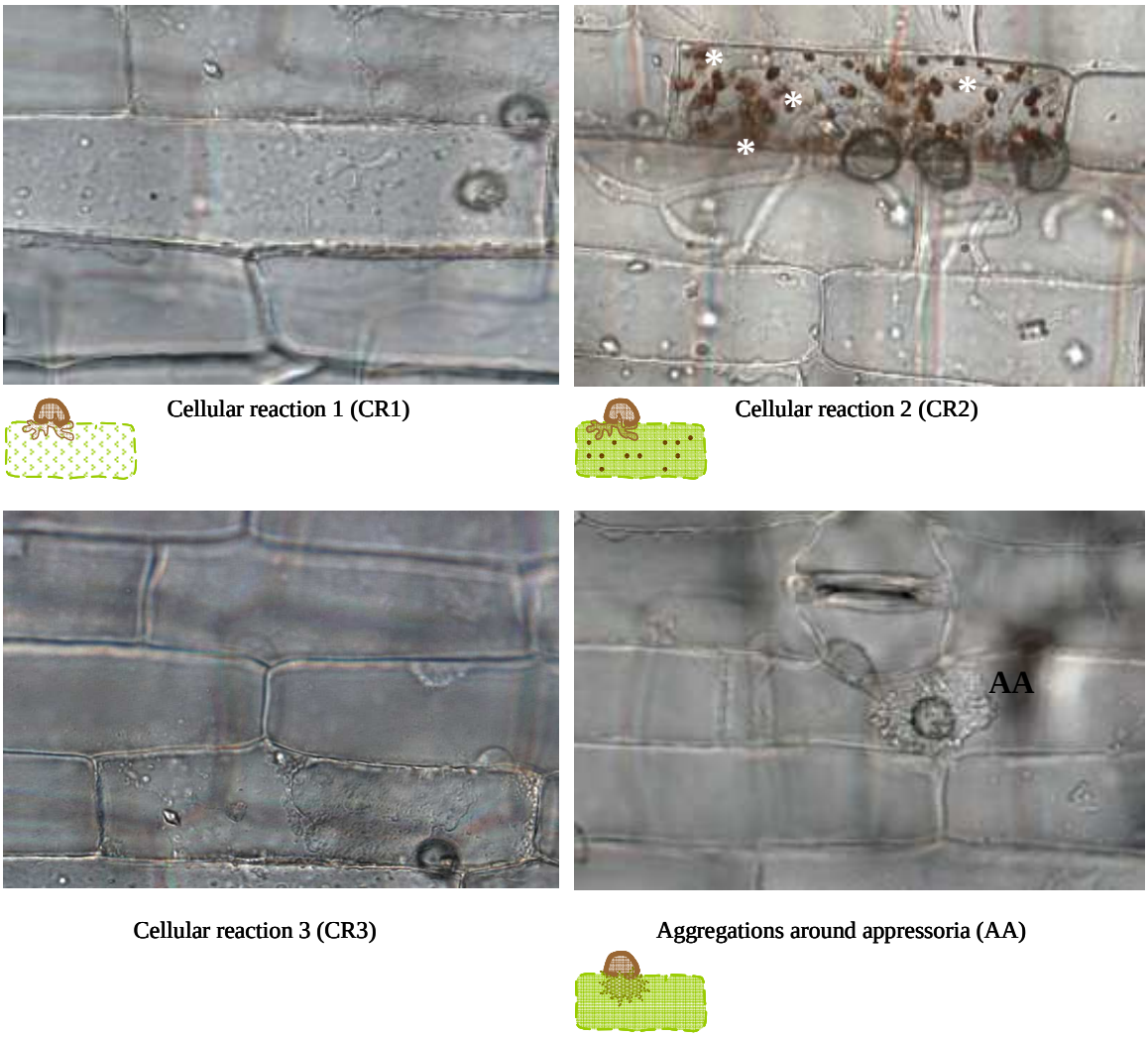

Figure 3-4. Epidermal cell responses in Yashiro-mochi leaf sheaths inoculated with KV11, KV1, and KV33 fungal strains.
The most common plant cell response observed in this study was cytoplasmic disorganization. Aggregations around the appressoria (AA) were highly induced in the non-host system treated with excised leaf sheath inoculation method. Cytoplasmic disorganization was divided into three groups: CR1, characterized by fine and irregular granular material in the cytoplasm; CR2, characterized by coarse cytoplasmic granulation and brown spherical globules (*); and CR3, characterized by fragmentation of the plasma membrane.

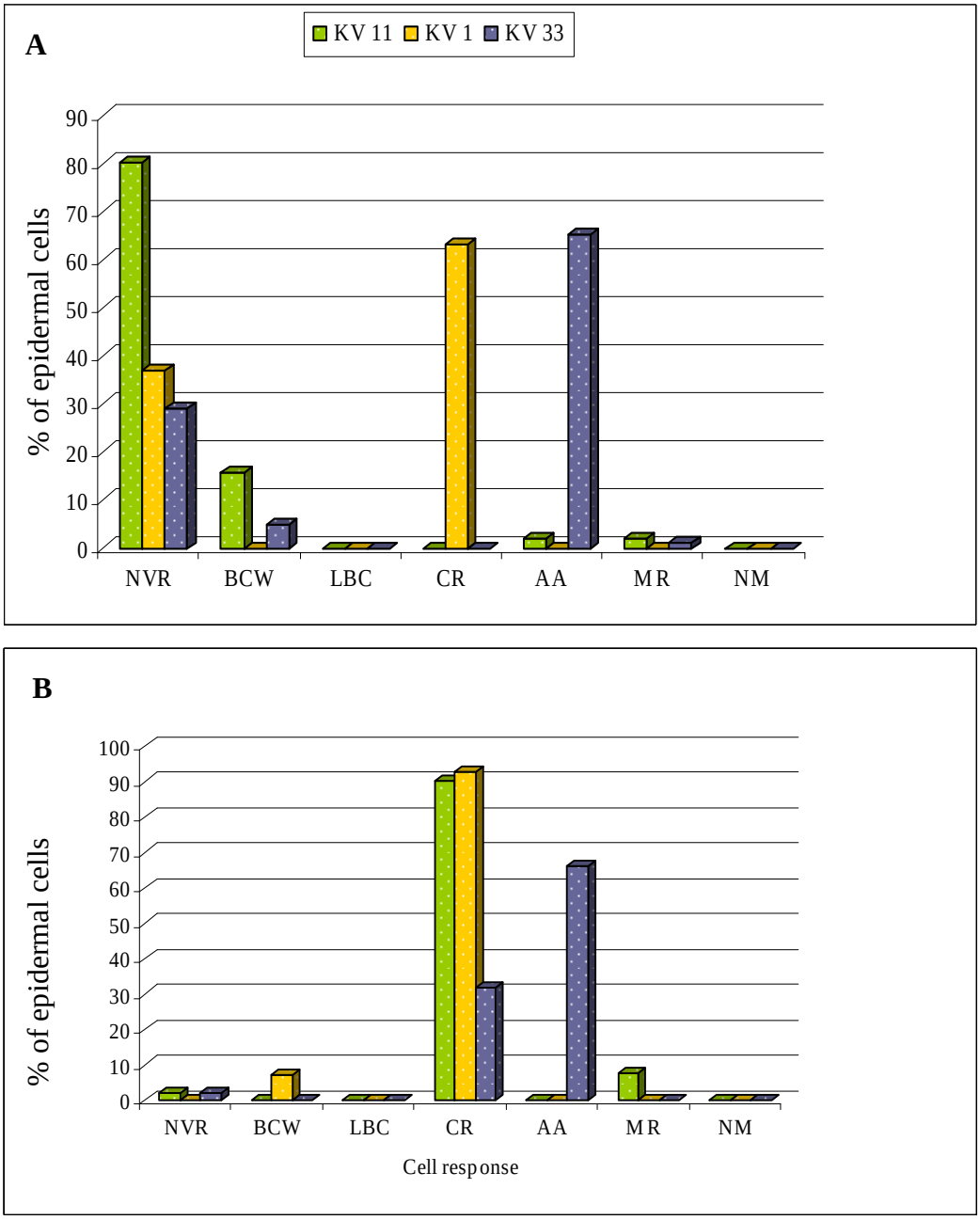

Figure 3-5. Percentage of epidermal cell responses in Yashiro-mochi excised leaf sheaths inoculated with KV11, KV1, and KV33 fungal strains.
Panel A, 24-27 hai; Panel B 36-39 hai. NVR, non-visible response; BCW, brown cell wall; LBC, light brown cytoplasm; CR, cytoplasmic reactions; AA, aggregations around appressorium; MR, mixed reactions; and NM, nucleus migration toward penetration site.

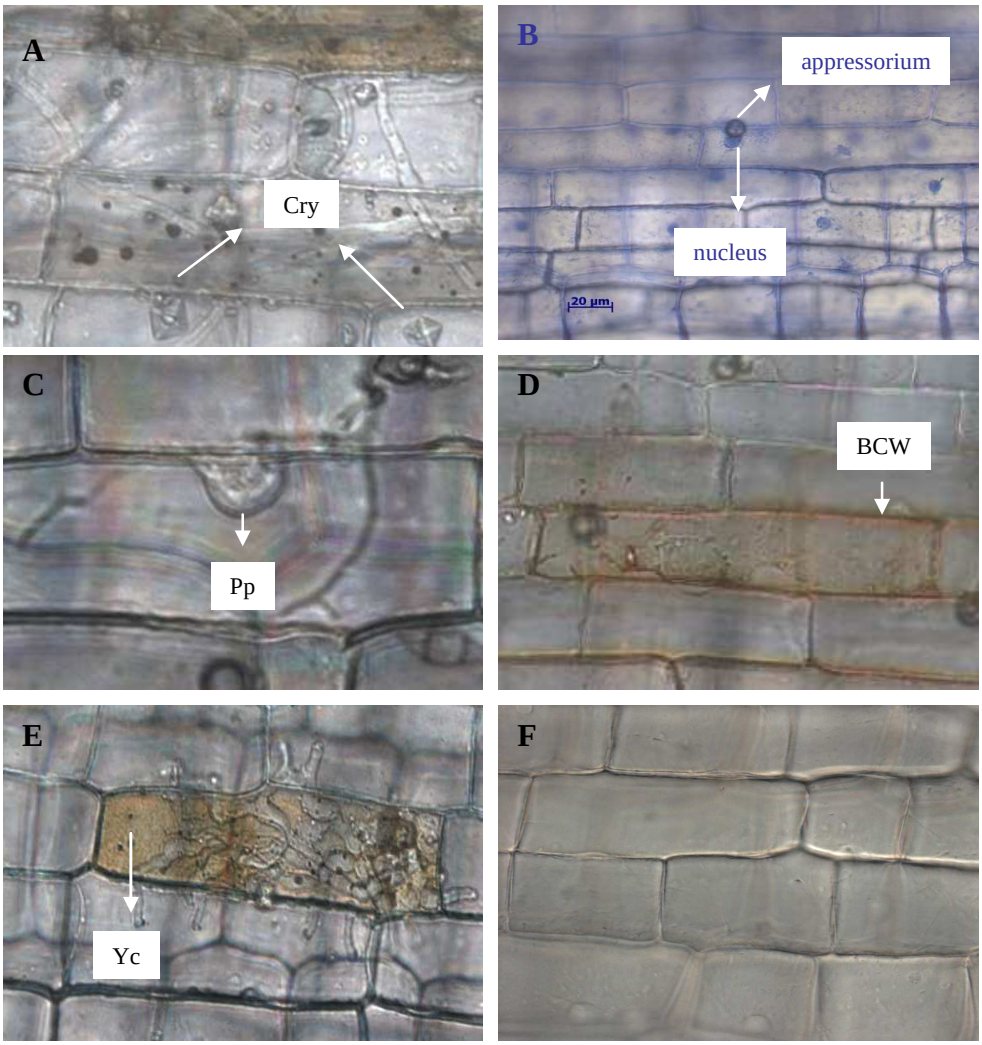

Figure 3-6. Epidermal cell responses in Yashiro-mochi sheaths inoculated with KV11, KV1, and KV33 fungal strains.
Additional responses observed in epidermal leaf sheath cells were the induction of crystal-like bodies (A), nuclear migration toward penetration sites (B), papilla formation (C), browning cell wall (D), and cytoplasmic discoloration (E). Mock inoculated leaf sheaths were sprayed with distilled water (F). BCW, brown cell wall; Cry, crystal-like bodies; Pp, papilla; Yc, yellowish cytoplasm

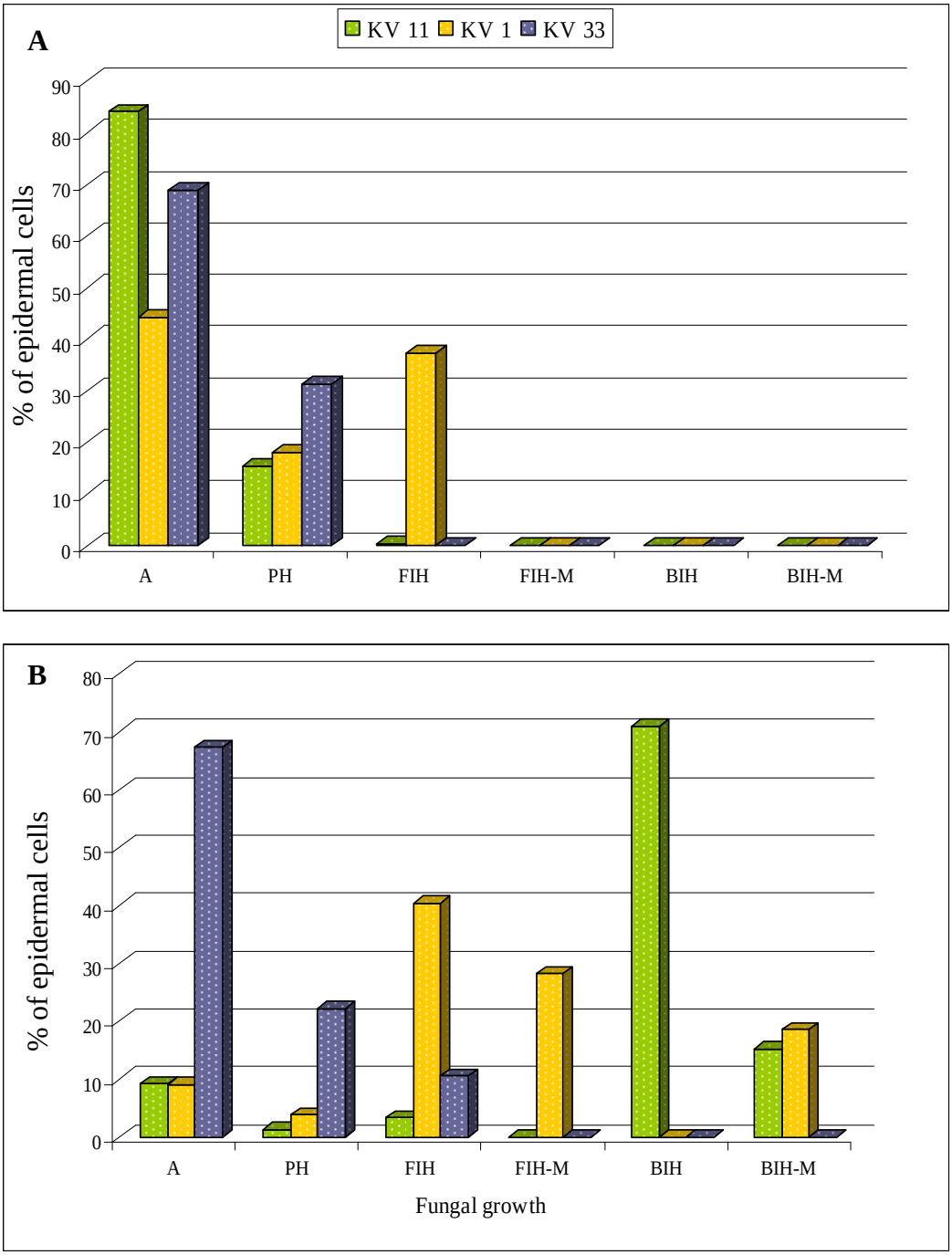

Figure 3-7. Percentage of epidermal cells showing fungal development in Yashiro-mochi intact leaf sheaths.

24-27 hai (Panel A) and 36-39 hai (Panel B). A, appressorium; PP, penetration peg; PH, primary hypha; FIH, filamentous invasive hypha; FIH-M, filamentous invasive hypha moving to next cell; BIH, bulbous invasive hypha; BIH-M, bulbous invasive hypha moving to next cell.

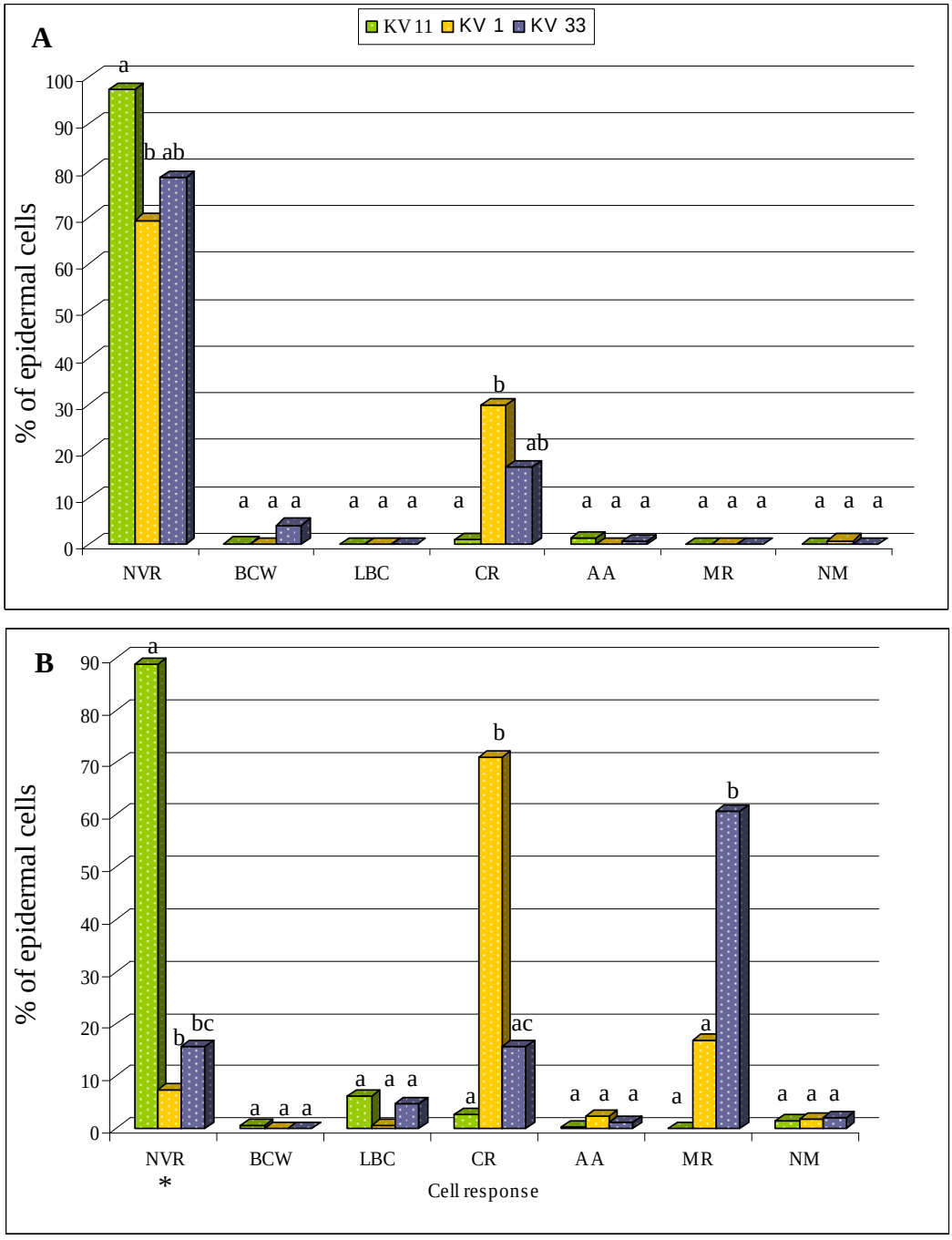

Figure 3-8. Percentage of epidermal cell responses in Yashiro-mochi intact leaf sheaths inoculated with KV11, KV1, and KV33 fungal strains.

Panel A, 24-27 hai; Panel B, 36-39 hai. NBR, non-visible response; BCW, brown cell wall; LBC, light brown cytoplasm; CR, cytoplasmic reactions; AA, aggregations around appressorium; MR, mixed reactions; and NM, nucleus migration toward penetration site.

* values in the same cell response with the same letter are not significantly different (*Pr>0.05*).

Table 3.1 Rice leaf epidermal cell reactions at the early stage of *Magnaporthe oryzae* disease cycle in compatible (susceptible) and incompatible (resistant) interactions.

Leaf blades Koga and Kobayashi (1982 a-b)[a]	Leaf blades Peng and Shishiyama (1988, 1989)[b]	Leaf blades Heath M. C. *et al*, (1990a)[b]	Sliced leaf sheaths Tomita and Yamanaka (1983)[b]	Leaf sheaths Koga H. (1994)[c]
No penetration without any host reaction	No visible changes	Papilla formation	Fine and coarse cytoplasmic granulation	Cytoplasmic streaming around nucleus
No penetration with cytoplasmic granules	Light brown and aniline blue staining of cell walls	Browning and/or autofluorescence of cell walls		Fine cytoplasmic granulation
Poorly-developed invasive hypha with cytoplasmic granules	Fine cytoplasmic granulation	Cytoplasmic granulation		Separation of plasma membrane from cell wall
Well-developed invasive hypha without cytoplasmic granules	Cell necrosis	Cell necrosis		Fragmentation of plasma membrane and cell organelles collapse
Well-developed invasive hypha with cytoplasmic granules	Coarse cytoplasmic granulation			Papilla formation
Deep browning of host cell				

a Reactions at 72 hours after inoculation (hai)
b Reactions at 24 to 48 hai
c Reactions at 17 to 25 hai
All plant responses were observed in both compatible and incompatible interactions. The difference between them depended on time and frequency of the cell response.

Table 3.2 *Magnaporthe oryzae* strain 4091-5-8 and the *Oryza sativa* cultivar Yashiro-mochi: a non- host system

	KV11 [Guy11 (0-391)] *avr1-co39, avr-pita*	KV1 (O-137) *AVR-Pita, AVR-Pita*^{2}	KV33 (4091-5-8) *AVR-M201, AVR-CO39, AVR1-YAMO**
Yashiro-mochi *Pi-ta*	Susceptible	Resistant	Non-host
YT16 *pi-ta*	Susceptible	Susceptible	Resistant

* These uncharacterized genes were identified by genetic studies. It has not been shown whether *AVR1-YAMO* corresponds to *Pi-ta* or to another resistance gene in Yashiro-mochi.

REFERENCES

Agrios, G.N. (1997). Plant Pathology. Fourth Edition. Harcourt/Academic Press. USA. 635p.

Ayliffe, M.A., and Lagudah, E.S. (2004). Molecular genetics of disease resistance in cereals. Annals of Botany **94,** 765-773.

Bell, A.A., and Wheeler, M.H. (1986). Biosynthesis and functions of fungal melanins. Annual Review of Phytopathology **24,** 411-451.

Bent, A.F. (1996). Plant disease resistance genes: Function meets structure. The Plant Cell **8,** 1757-1771.

Berruyer, R., Poussier, S., Kankanala, P., Mosquera, G., and Valent, B. (2006). Quantitative and qualitative influence of inoculation methods on in palnta growth of rice balst fungus. Phytopathology **96,** 346-355.

Bourett, T.M., and Howard, R.J. (1990). *In vitro* development of penetration structures in the rice blast fungus *Magnaporthe grisea*. Canadian Journal of Botany **68,** 329-342.

Butler, M.J., and Day, A.W. (1998). Fungal melanins: a review. Canadian Journal of Microbiology **44,** 1115-1136.

Calvo, A.M., Wilson, R.A., Bok, J.B., and Keller, N.P. (2002). Relationship between secondary metabolism and fungal development. Microbiology and Molecular Biology Reviews **66,** 447-459.

Chumley, F.G., and Valent, B. (1990). Genetic analysis of melanin-deficient, nonpathogenic mutants of *Magnaporthe grisea*. Molecular Plant-Microbe Interactions **3,** 135-143.

Couch, B.C., and Kohn, L.M. (2002). A multilocus gene genealogy concordant with host preference indicates segregation of a new species, *Magnaporthe oryzae*, from *M. grisea*. Mycologia **94,** 683-693.

Dean, R. A., Talbot, N. J., Ebbole, D. J., Farman, M. L., Mitchell, T. K., Orbach, M. J., Thon, M., Kulkarni, R., Xu, J-R, Pan, H., Read, N. D., Lee, Y-H, Carbone, I., Brown, D., OH, Y. Y., Donofrio, N., Jeong, J. S., Soanes, D. M., Djonovic, S., Kolomiets, E., Rehmeyer, C., Li, W., Harding, M., Kim, S., Lebrun, M-H., Bohnert, H., Coughlan, S., Butler, J., Calvo, S., Ma, L-J., Nicol, R., Purcell, S., Nusbaum, C., Galagan, J. E., and Birren, B. W. (2005). The genome sequence of the rice blast fungus Magnaporthe grisea. Nature **434**, 980-986.

Dangl, J.F., and Jones, J.D.G. (2001). Plant pathogens and integrated defense responses to infection. Nature **411,** 826-833.

de Jong, C.J., McCormack, B.J., Smirnoff, N., and Talbot, N.J. (1997). Glycerol generates turgor in rice blast. Nature **389,** 244-245.

DeZwaan, T.M., Carroll, A.M., Valent, B., and Sweigard, J.A. (1999). *Magnaporthe grisea* Pth11p is a novel plasma membrane protein that mediates appressorium differentiation in esponse to inductive substrate cues. The Plant Cell **11,** 2013-2030.

Dufresne, M. and Osbourn, A. E. (2001). Definition of tissue-speific and general requirements for plant infection in a phytopathogenic fungus. Molecular Plant-Microbe Interactions **14**, 300-307.

Eliahu, N., Igbaria, A., Rose, M.S., Horwitz, B.A., and Lev, S. (2007). Melanin biosynthesis in the Maize Pathogen *Cochliobolus heterostrophus* depends on two mitogen-activated protein kinases Chk1 and Mps1, and the transcription factor Cmr1. Eukaryotic Cell **6,** 421-429.

Flor, H.H. (1971). Current status of the gene-for-gene concept. Annual Review of Phytopathology **9,** 275-297.

Hamer, J.E., Howard, R.J., Chumley, F.G., and Valent, B. (1988). A mechanism for surface attachment in spores of a plant pathogenic fungus. Science **239,** 288-290.

Hammond-Kosack, K.E., and Jones, J.D.G. (1996). Resistance gene-dependent plant defense responses. The Plant Cell **8,** 1773-1791.

Heath, M. C. (1981). A generalized concept of host-parasite specificity. Phytopathology **71**:1121-1123.

Heath, M. C. (2001). Non-host resistance to plant pathogens: nonspecific defense or the result of specific recognition events? Physiological and molecular Plant Pathology **58,** 53-54.

Heath, M.C., Valent, B., Howard, R.J., and Chumley, F.G. (1990b). Correlations between cytologically detected plant-fungal interactions and pathogenicity of *Magnaporthe grisea* toward weeping lovegrass. Phytopathology **80,** 1382-1386.

Heath, M.C., Valent, B., Howard, R.J., and Chumley, F.G. (1990a). Interactions of two strains of *Magnaporthe grisea* with rice, goosegrass, and weeping lovegrass. Canadian Journal of Botany **68,** 1627-1637.

Heath, M.C., Howard, R. J., Valent, B., and Chumley, F. G. (1992). Ultrastructural interactions of one strain of *Magnaporthe grisea* with goosegrass and weeping lovegrass. Canadian Journal of Botany **70,** 779-787.

Heath, M.C., Nimchuk, Z. L., and Xu, H. (1997). Plant nuclear migrations as indicators of critical interactions between resistant or susceptible cowpea epidermal cells and invasion hyphae of the cowpea rust fungus. New Phytologist **135,** 689-700.

Hebert, T.T. (1971). The perfect stage of *Pyricularia grisea* Phytopathology **61,** 83-87.

Henson, J.M., Butler, M.J., and Day, A.W. (1999). The dark side of the mycelium: Melanins of phytopathogenic fungi. Annual Review of Phytopathology **37,** 447-471.

Holub, E.B., and Cooper, A. (2004). Matrix, reinvention in plants: how genetics is unveiling secrets of non-host disease resistance. Trends in Plant Science **9,** 211-214.

Howard, R.J. and Valent, B. (1996). Breaking and entering: host penetration by the fungal rice blast pathogen *Magnaporthe grisea*. Annual Review of Microbiology **50,** 491-512.

Howard, R.J., Ferrari, M.A., Roach, D.H., and Money, N.P. (1991). Penetration of hard substrates by a fungus employing enormous turgor pressures. Proc. Natl. Acad. Sci. USA **88**.

Hückelhoven, R. (2007). Cell wall-associated mechanisms of disease resistance and susceptibility. Annual Review of Phytopathology **45,** 2.1-2.27.

Huitema, E., Vleeshouwers, V.G.A.A., Francis, D.M., and Kamoun, S. (2003). Active defence responses associated with non-host resistance of *Arabidopsis thaliana* to the oomycete pathogen *Phytiphthora infestans*. Molecular Plant Pathology **4,** 487-500.

Jarosh, B., Kogel, K-H., and Schaffrath, U. (1999). The ambivalence of the barley *Mlo* locus: Mutations conferring resistance against powdery mildew (*Blumeria graminis* f. sp. *hordei*) enhance susceptibility to the rice blast fungus *Magnaporthe grisea*. Molecular Plant-Microbe Interactions **12**, 508-514.

Jia, Y., McAdams, S. A., Bryan, G. T., Hershey, H. P., and Valent, B. (2000). Direct interaction of resistance gene and avirulence gene products confers rice blast resistance. EMBO J **19**: 4004-4014.

Jones, J.D.G.a., and Dangl, J.L. (2006). The plant immune system. Nature **444,** 323-329.

Kankanala, P., Czymmek, K., and Valent, B. (2007). Roles for rice membrane dynamics and plasmodesmata during biotrophic invasion by the blast fungus. The Plant Cell **19,** 706-724.

Kawamura, C., Moriwaki, J., Kimura, N., Fujita, Y., Fuji, S., Hirano, T., Koizumi, S., and Tsuge, T. (1997). The melanin biosynthesis genes of *Alternaria alternata* can restore pathogenecity of the melanin deficient mutants of *Magnaporthe grisea*. Molecular Plant-Microbe Interactions **10,** 446-453.

Keller, N.P., and Hohn, T.M. (1997). Metabolic pathway gene clusters in filamentous fungi. Fungal Genetic and Biology**,** 17-29.

Khang, C.H., Park, S., Lee, Y., and Kang, S. (2005). A dual selection based, targeted gene replacement tool for *Magnaporthe grisea* and *Fusarium oxysporum*. Fungal Genetics and Biology **42,** 483-492.

Kimura, N., and Tsuge, T. (1993). Gene cluster involved in melanin biosynthesis of the filamentous fungus *Alternaria alternata*. Journal of Bacteriology **175,** 4427-4435.

Koga, H. (1994). Hypersensitive death, autofluorescence, and ultratructural changes in cells of leaf sheaths of susceptible and resistant near-isogenic lines of rice (*Pi-z*^{t}) in relation to penetration and growth of *Pyricularia oryzae*. Canadian Journal of Botany **72,** 1463-1477.

Koga, H., and Kobayashi, T. (1980). A whole-leaf clearing and staining technique to observe the invaded hyphae of blast fungus and host responses in rice leaves Ann. Phytopath. Soc. Japan **46,** 679-681.

Koga, H., and Kobayashi, T. (1982 b). Cytological reactions in leaves of the rice variety, Toride 1, to the incompatible race of *Pyricularia oryzae* Cav. Proceedings of the Association for Plant Protection of Hokuriku **30,** 12-18.

Koga, H., and Kobayashi, T. (1982a). Comparison of the early infection process of *Pyricularia oryzae* Cav. in rice leaves of compatible and incompatible combinations. Ann. Phytopath. Soc. Japan **48,** 506-513.

Koga, H., and Horino, O. (1984 b). Electron microscopical observation of rice leaves infected with *Pyricularia oryzae* Cav. in compatible and incompatible combinations. IV. The interface between invading hyphae and host cytoplasm in epidermal cells of leaf-sheath. Ann. Phytopath. Soc. Japan **50,** 375-378.

Koga, H., and Horino, O. (1984a). Electron microscopical observation of rice leaves infected with *Pyricularia oryzae* Cav. in compatible and incompatible combinations. III. Resistance expression and loss of capability for plasmolysis in inner epidermal cells of leaf-sheath. Ann. Phytopath. Soc. Japan **50,** 353-360.

Koga, H., Dohi, K., Kakayachi, O., and Mori, M. (2004). A novel inoculation method of *Magnaporthe grisea* for cytological observation of the infection process using intact leaf sheaths of rice plants. Physiological and molecular Plant Pathology **64,** 67-72.

Kubo, Y., Tsuda, M., Furusawa, I., and Shishiyama, J. (1989). Genetic analysis of genes involved in mealnin biosynthesis of *Cochliobolus miyabeanus*. Experimental Mycology **13,** 77-84.

Kubo, Y., Nakamura, H., Kobayashi, K., Okuno, T., and Furusawa, I. (1991). Cloning of a melanin biosynthetic gene essential for appressorial penetration of *Colletotrichum lagenarium*. Molecular Plant-Microbe Interactions **4,** 440-445.

Kubo, Y., Takano, Y., Endo, N., Yasuda, N., Tajima, S., and Furusawa, I. (1996). Cloning and structural analysis of the melanin biosynthesis gene *SCD1* encoding scytalone dehydratase in *Colletotrichum lagenarium*. Applied and Environmental Microbiology **62,** 4340-4344.

Kurahashi, Y. (2001). Melanin biosynthesis inhibitors (MBIs) for control of rice blast. Pesticide Outlook, 32-35.

Langfelder, K., Jahn, B., Gehringer, H., Schmidt, A., Wanner, G., and Brakhage, A. A. (1998). Identification of a polyketide synthase gene (*pksP*) of *Aspergillus fumigatus* involved in conidial pigment biosynthesis and virulence. Med. Microbiol. Immunol. **187**:79-89.

Langfelder, K., Streibel, M., and B., H., G., and Brakhage, A. A. (2003). Biosynthesis of fungal melanins and their importance for human pathogenic fungi. Fungal Genetics and Biology **38,** 143-158.

Laugé, R., Goodwin, P.H., de Wit, P.J.G.M., and Joosten, M.H.A.H. (2000). Specific HR-associated recognition of secreted proteins from *Cladosporium fulvum* occurs in both host and non-host plants. The Plant Journal **23,** 735-745.

Lodish, H., Berk, A., Zipursky, S. L., Matsudaira, P., Baltimore, D., and Darnell, J. (1999). Molecular Cell Biology. Fourth Edition. Freeman and Company. USA. 1084p.

Lu, J., Liu, T., and Lin, F. (2005). Identification of mature appressorium-enriched transcripts in *Magnaporthe grisea*, the rice blast fungus, using suppression substractive hybridization. Microbiology Letters **245,** 131-137.

Lu, M., Tang, X., and Zhou, J.-M. (2001). Arabidopsis *NHO1* is required for general resistance against *Pseudomonas* bacteria. The Plant Cell **13,** 437-447.

Mayorga, M. E. and Timberlake, W. E. (1992). The developmentally regulated *Aspergillus nidulans wA* gene encodes a polypeptide homologous to polyketide and fatty acid synthases. Mol. Gen. Genet. **235**:205-212.

Mellersh, D.G., and Heath, M.C. (2003). An investigation into the involvement of defense signaling pathways in components of the nothost resistance af *Arabidopsis thaliana* to rust fungi also reveals a model system for studying rust fungalcompatibility. Molecular Plant-Microbe Interaction **16,** 398-404.

Mellersh, D.G., Foulds, I.V., Higgins, V.J., and Heath, M.C. (2002). H2O2 plays different roles in determining penetration failure in three diverse plan-fungal interactions. The Plant Journal **29,** 257-268.

Mendgen, K., Hahn, M., and Deising, H. (1996). Morphogenesis and Mechanisms of penetration by plant pathogenic fungi. Ann. Rev. Phytopathol. **34,** 367-386.

Mysore, K.S., and Ryu, C.-M. (2004). Nonhost resistance: how much do we know? Trends in Plant Science **9,** 97-104.

Neu, C., Keller, B., and Feuillet, C. (2003). Cytological and molecular analysis of the *Hordeum vulgare-Puccinia triticina* nonhost interaction. Molecular Plant-Microbe Interaction **16,** 626-633.

Nürnberger, T., Brunner, F., Kemmerling., and Piater, L. (2004). Innate immunity in plants and animals:striking similarities and obvious differences. Immunological Reviews **198,** 249-266.

Oh, S.K., Lee, S., Chung, E., Park, J.M., Yu, S.H., Ryu, C.-M., and Chio, D. (2006). Insight into Types I and II nonhost resistance using expression patterns on defense-related genes in tobacco. Planta **223,** 1101-1107.

Osiewacz, H.D. (2002). Molecular biology of fungal development. (New York: M. Dekker).

Pappelis, A.J., Pappelis, G.A., and Kulfinski, F.B. (1974). Nuclear orientation in onion epidermal cells in relation to wounding and infection. Phytopathology **64,** 1010-1012.

Peng, Y.L., and Shishiyama, J. (1988). Temporal sequence of cytological events in rice leaves infected with *Pyricularia oryzae*. Canadian Journal of Botany **66,** 730-735.

Peng, Y.L., and Shishiyama, J. (1989). Timing of a cellular reaction in rice cultivars associated with differing degress of resistance to Pyricularia oryzae. Canadian Journal of Botany **67,** 2704-2710.

Perpetua, N.S., Kubo, Y., Yasuda, N., Takano, Y., and Furusawa, I. (1996). Cloning and characterization of a melanin biosynthetic *THR1* reductase gene essential for appressorial penetration of *Colltotrichum lagenarium*. Molecular Plant-Microbe Interactions **9,** 323-329.

Plonka, P. M. and Grabacka, M. (2006). melanin synthesis in microorganisms - biotechnological and medical aspects. Acta Bioquimica Polonica 53, 3:429-443.

Sesma, A., and Osbourn, A.E. (2004). The rice leaf blast pathogen undergoes developmental processes typical of root-infecting fungi. Nature **431,** 582-586.

Shigyo, T., Kuchii, Y., Araki, Y., and Sawada, H. (2004). Efficacy of carpropamid against mutants of *Magnaporthe grisea* at codon 75 on scytalone dehydratase. S. Kawasaki (ed.), Rice Blast: Interaction with Rice and Control. Kluwer Academic Publishers, Netherlands 281-287.

Snyder, L. and Champness, W. (2003). Molecular genetics of bacteria. Second Edition. ASM Press. USA. 566p.

Spieth, J., and Lawson, D. (2006). Overview of gene structure. (2006). WormBook, ed. The C. elegans Research community, WormBook,doi/1895/wormbook.1.65.1, http://wormbook. org.

Sweigard, J.A., Chumley, F.G., and Valent, B. (1992). Cloning and analysis of CUT1, a cutinase gene from *Magnaporthe grisea*. Mol Gen Genet **232,** 174-182.

Sweigard, J. A., Carroll, A. M., Kang, S., Farrall, L., Chumley, F. G., and Valent, B. (1995). Identification, cloning, and characterization of PWL2, a gene for host species specificity in the rice blast fungus. Plant Cell **7**:1221-1233.

Takano, Y., Kubo, K., Shimizu, K., Mise, T., Okuno, and Furusawa, I. (1995). Structural analysis of *PKS1*, a polyketide synthase gene induced in melanin biosynthesis of Colletotrichum lagenarium. Mol. Gen. Genet. 249, 162-167.

Takano, Y., Kubo, Y., Kuroda, I., and Furusawa, I. (1997). Temporal transcription pattern of three melanin biosynthesis genes, *PKS1*, *SCD1*, and *THR1*, in appressorium differentiating and nondifferentiating conidia of *Colletotrichum lagenarium*. Applied and Environmental Microbiology **63,** 351-354.

Talbot, N.J. (2003). On the trail of a cereal killer: exploring the biology of *Magnaporthe grisea*. Annual Review of Microbiology **57,** 177-202.

Tanaka, C., Kubo, Y., and Tsuda, M. (1991). Genetic analysis and characterization of *Cochliobolus heterostrophus* colour mutants. Mycological Research **95,** 49-56.

Tao, Y., Xie, Z., Chen, W., Glazebrook, J., H-S., C., Han, B., Zhu, T., Zou, G., and Katagiri, F. (2003). Quantitative nature of *Arabidopsis* responses during compatible and incompatible interactions with the bacterial pathogen *Pseudomonas syringae*. The Plant Cell **15,** 317-330.

Thomma, B.P.H.J. (2003). *Alternaria* spp.: from general saprophyte to specific parasite. Molecular Plant Pathology **4,** 225-236.

Thompson, J.E., Fahnestock, S., Farrall, L., Liao, D., Valent, B., and Jordan, D.B. (2000). The second naphthol reductase of fungal melanin biosynthesis in *Magnaporthe grisea*. The Journal of Biological Chemistry **275,** 34867-34872.

Thordal-Christensen, H. (2003). Fresh insights into processes of nonhost resistance. Current Opinion in Plant Biology **6,** 351-357.

Tomita, H., and Yamanaka, S. (1983a). A sliced-sheath inoculation method for continuous observation of tissue cells of rice infected with *Pyricularia oryzae* Cavara. Ann. Phytopath. Soc. Japan **49,** 256-258.

Tomita, H., and Yamanaka, S. (1983b). Studies on the resistance reaction in the rice blast disease caused by *Pyricularia oryzae* Cavara I. The pathological changes in the early infection stage of the inner epidermal cells of leaf sheath. Ann. Phytopath. Soc. Japan **49,** 514-521.

Tsuji, G., Kenmochi, Y., Takano, Y., Sweigard, J., Farrall, L., Furusawa, I., Horino, O., and Kubo, Y. (2000). Novel fungal transcriptional activators, Cmr1p of *Colletotrichum lagenarium* and Pig1p of *Magnaporthe grisea*, contain Cys2His2 zinc finger and Zn(II)2Cys6 binuclear cluster DNA-binding motifs and regulate transcription of melanin biosynthesis genes in a developmentally specific manner. Molecular Microbiology **38,** 940-954.

Valent, B. (1997). The rice blast fungus, *Magnaporthe grisea*. The Mycota V Part B. Plant Relationships. Carroll/Tudzynski (Eds.). Berlin Heidelberg: Springer-Verlag. 37-54.

Valent, B., Farrall, L., and Chumley, F.G. (1991). Magnaporthe grisea genes for pathogenicity and virulence identified through a series of backcrosses. Genetics **127,** 87-101.

van Wees, S.C.M., and Glazebrook, J. (2003). Loss of non-host resistance of *Arabidopsis* NahG to *Pseudomonas syringae* pv. *phaseolicola* is due to degradation products of salicylic acid. The Plant Journal **33,** 733-742.

Yaegashi, H. (1988). Inheritance of blast resistance in two-rowed barley. Plant Disease **72**:608-610.

Yaegashi, H., and Udagawa, S. (1978). The taxonomical identity of the perfect state of *Pyricularia grisea* and its allies. Canadian Journal of Botany **55**, 180-183.

Yamaguchi, T., Yamada, A., Hong, N., Ogawa, T., Ishii, T., and Shibuya, N. (2000). Differences in the recognition of glucan elicitor signals between rice and soybean: β-glucan fragments from the rice blast disease fungus *Pyricularia oryzae* that elicit phytoalexin biosynthesis in suspension-cultured rice cells. The Plant Cell **12**:817-826.

Yu, J.-H., and Keller, N. (2005). Regulation of secondary metabolism in filamentous fungi. Annual Review of Phytopathology **43,** 437-458.

Zellerhoff, N., Jarosch, B., Groenewald, J.Z., Crous, P.W., and Schaffrath, U. (2006). Nonhost resistance of Barley is successfully manifested against *Magnaporthe grisea* and a closely related *Pennisetum*-infecting lineage but is overcome by *Magnaporthe oryzae*. Molecular Plant-Microbe Interaction **19,** 1014-1022.

Zhang, A., Lu, P., Dahl-Roshak, A.M., Paress, P.S., Kennedy, S., Tkacz, J.S., and An, Z. (2003). Efficient disruption of a polyketide synthase gene (pks1) required for melanin synthesis through *Agrobacterium*-mediated transformation of *Glarea lozoyensis*. Mol. Gen. Genomics **268,** 645-655.

Appendix A -

Table A-1. Primers used in this study

	Forward primer name	Sequence	Tm °C	Reverse primer name	Sequence	Tm °C
HTF: PCR RT-PCR probe	HTF-F	CGGCAAACGACA TTTCGGGTCTTT	60.3	HTF-R	TCCCATCCTCGGC GTTTACTTGAT	60.2
Target coding region: RT-PCR	Exon 1F	TTGAGCTTGAAA TATTGGCGCG	60.3	Exon 1R	CGCAATCCTTGCCA ATAGCGACAT	60.1
cDNA synthesis for 3'RACE-PCR	3'-CDS primer A	aagcagtggtatcaacgcaga gtac$(t)_{30}$gc	63.6			
3'RACE-PCR	Gene specific primer (GSP)	CGCCTCGTCGCCG TCATCCCCACC				
First fusion PCR 5'flanking region	Eco5'-F	acggaattcTCCTCGT CTCGCGAGCAAGT	66	HYG5'-R	ttgacctccactagctccagccaa gccGTTGGTGATGTC TTGGCAGG	72.1
First fusion PCR 3'flanking region	HYG3'-F	gaatagagtagatgccgacc CACACGGCTGCAA TGCTCAT	68.3	Xba3'-R	agctctagaCAGCGTCCC TTTCACAACCAG	64.3
First fusion PCR Hygromycin	HYG-F	ggcttggctggagctagtgga gg	63.8	HYG-2R	aacccgcggtcggcatctactcta	63.6
Third fusion PCR	Nested Kpn5'-F	ggggtaccGCAGCACC AGGGT TGCCTACC	70.5	Nested Xba3'-R	agctctagaCGGGTTGCG GCAGGACAGAAC	67.5
Actin: PCR RT-PCR	MgActin 328-F	tcccatgtcaccactttcaa		MgActin3 28-R	Ttcgagatccacatctgctg	
Hygromycin Probe	HYG probe-F2	tgtttatcggcactttgcatcggc	60.4	HYG probe-F2	agctgcatcatcgaaattgccgtc	60.4

Capital letters represent sequences with homology to the HTF DNA template.

Table A-2. Growing conditions for YT16 and Yashiro-mochi rice plants

Time	Temperature (°C)	Humidity	Incandescent Light	Halogen light	Automatic watering (seconds)
00	24	80	0	0	0
6:30	24	80	1	1	120
7:00	26	80	2	2	0
7:30	28	80	3	3	0
11:30	28	80	3	3	180
16:30	28	80	3	3	180
18:30	28	80	2	2	0
19:00	26	80	1	1	0
19:30	24	80	0	0	0
22:00	24	80	0	0	60
23:59	24	80	0	0	0

Table A-3 Expression profile of *Magnaporthe oryzae* at 36 hours after inoculation of YT16 rice plants.

Expression profile of the *Magnaporthe oryzae* melanin biosynthetic gene cluster comparing YT16 leaf sheaths inoculated with 0.25% gelatin, KV1 mycelia grown in liquid culture, and 36 hour infected leaf sheaths (Mosquera *et al*, submitted).

Melanin gene	GeneBank accession number	MGOS* name	Encoded protein	Fold change	p-value
PIG1	AF230811.1	AMGO1941	Pig1p	- 1.03	0.85109
4HNR	AF290182.2	AMGO1944	1,3,6,8-Tetrahydroxynaphthalene reductase	-28.10	0.0
HTFG	XM_367293.2	AMGO1948	Hypothetical transcription factor	-4.96	$1.39E^{-12}$
ALB1	XM_367294.2	AMGO1949	Polyketide synthase	-8.30	$1.18E^{-17}$
RSY1	AB004741.1 XM_359718.1	AMGO6064	Scytalone dehydratase	-24.63	$1.39E^{-37}$
BUF1	AY846878.1	AMGO2948	1,3,8-Trihydroxynaphthalene reductase	-24.90	$1.19E^{-21}$

* *Magnaporthe Grisea Oryza Sativa Interaction Database*

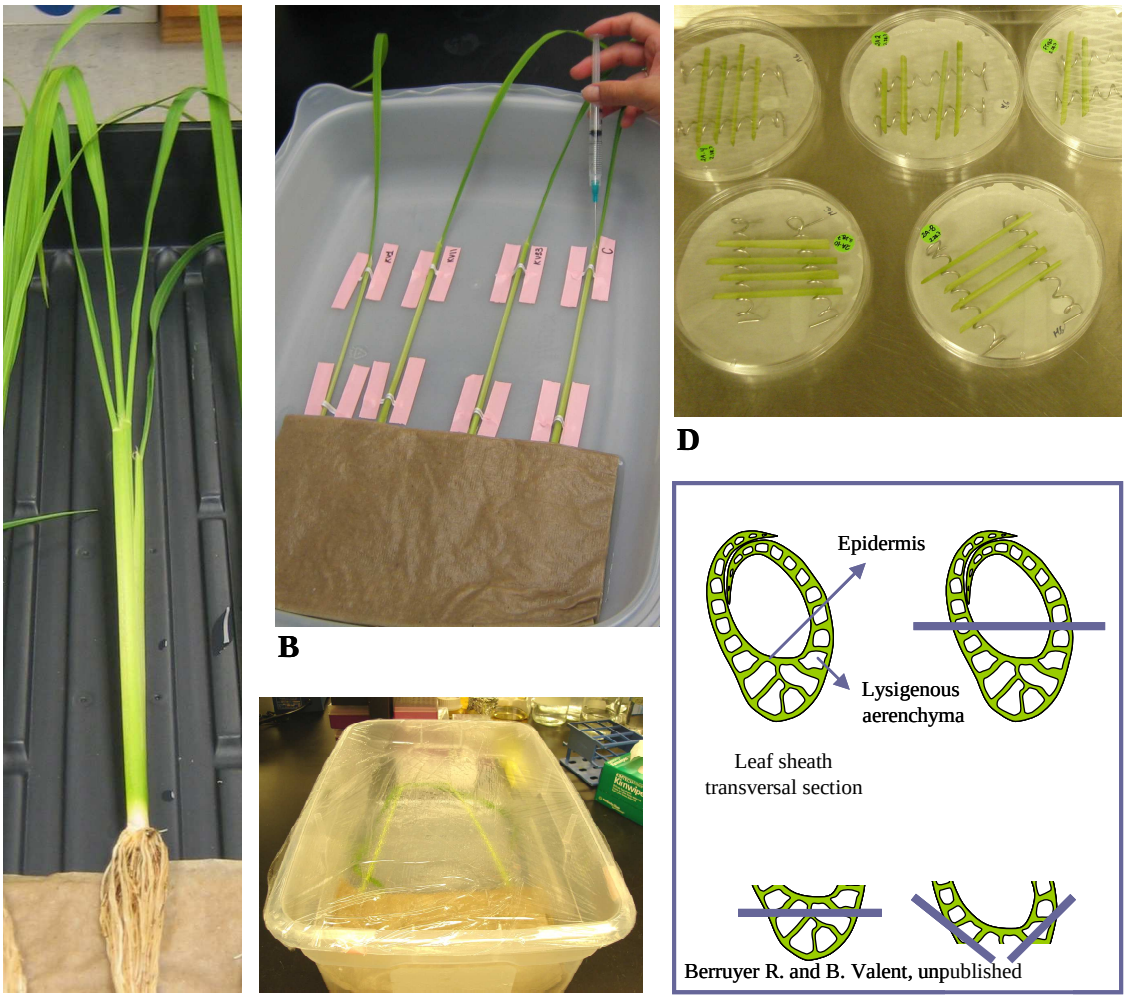

Figure A-1. 1. Inoculation methods.
Intact method (A-C). A, Leaf sheaths were removed with the leaf blades and roots intact. B, Leaf sheaths were laid horizontally in a plastic tray and inoculated by injecting the spore suspension. C, Roots were covered with wet paper towels and the try covered with clear plastic wrap to maintain humidity. **Excised method (D).** Leaf sheaths were dissected into 6 to 7 cm length segments. Four to five segments were laid horizontally over plastic or metallic spiral-shaped supports to hold them in Petri dishes containing wet paper towels for humidity. E, Diagrammatic representation of dissected-sheath tissues for microscopic analysis of fungal growth and plant cell responses.

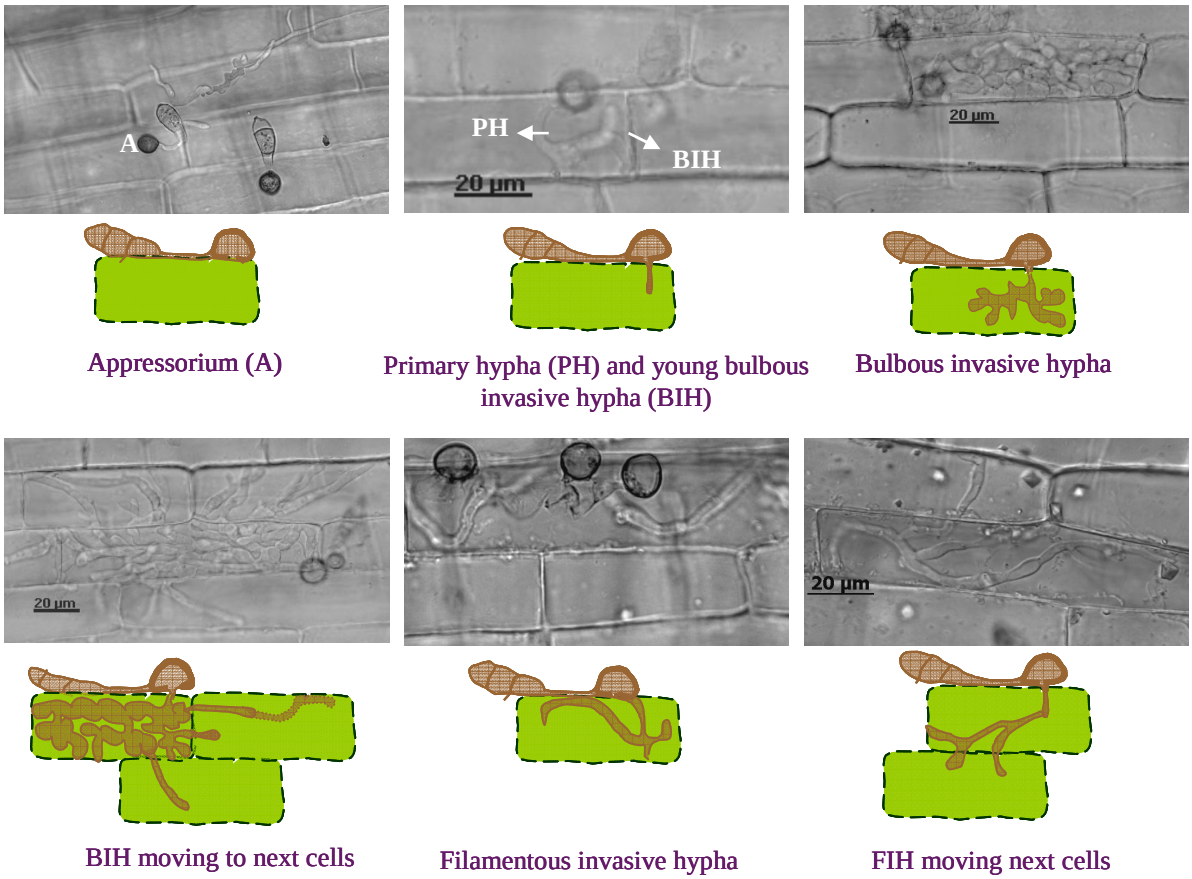

Figure A-1. 2. Fungal development.
Fungal development on Yashiro-mochi leaf sheath epidermal cells. Epidermal samples were dissected at 24 and 36 hours after inoculation and examined by DIC and fluorescent microscopy. Images were acquired using a Zeiss AxioCam HRc camera and analyzed with Zeiss Axiovision digital software.